



**NTNU – Trondheim**  
Norwegian University of  
Science and Technology

# Gel Evolution in Oil Based Drilling Fluids

**Ida Sandvold**

Earth Sciences and Petroleum Engineering

Submission date: June 2012

Supervisor: Pål Skalle, IPT

Co-supervisor: Arild Saasen, Det norske oljeselskap ASA

Norwegian University of Science and Technology

Department of Petroleum Engineering and Applied Geophysics



## **PREFACE**

This paper is written as the final product of the course TPG 4910 Petroleum Engineering – Drilling Engineering, Master’s Thesis at the Norwegian University of Science and Technology (NTNU), at the Department of Petroleum Engineering and Applied Geophysics. TPG 4910 counts for 30 credits in the European Credit Transfer System. The objective is that the student by specializing within a topic related to drilling technology performs an independent project work and presents the work as a scientific report according to accepted standards.

The title of this report is “Gel evolution in oil based drilling fluids”. The thesis is a continuation of the report with the same name “Gel evolution in oil based drilling fluids”, written for the course TPG 4520 Drilling Engineering, Specialization Project fall 2011. The project report contains theoretical background for the topic, and is an introduction to the work that will be performed in the Master’s Thesis. The Master’s Thesis becomes more holistic, and in this way easier to understand without requiring additional technical knowledge.

The thesis is prepared in cooperation between the Norwegian University of Science and Technology (NTNU), Det norske oljeselskap ASA and the student. A series of experiments is performed on the rheological properties of oil and water based drilling fluids to learn more and further understand the topic of gel evolution in oil based drilling fluids. The experiments are performed in a laboratory using a Fann viscometer and a Physica rheometer.

I would like to thank my supervisor Pål Skalle at NTNU for giving helpful feedback and guidance during the writing of this project. I would like to thank Halliburton for providing me with chemicals needed to perform the laboratory investigations. Additionally, I would like to thank Roger Overå at the Petroleum Laboratory for help and guidance of equipment used in the experimental investigations. Carl Christian Thodesen at SINTEF Byggforsk has been an invaluable help in completing my laboratory investigations. I would like to thank Jan David Ytrehus at SINTEF Petroleum for an educational and generous cooperation. The same goes for Binh Bui at the University of Tulsa, for helpful and relevant discussions of the topic. I would like to direct special thanks to Arild Saasen, Professor at the University of Stavanger and Technology Advisor in Det norske oljeselskap ASA for enthusiastic help in finding an interesting and relevant topic, and facilitating this project. Finally, I would like to thank Det norske oljeselskap ASA for

providing me with prime working facilities, and for continuously offering support, help and guidance.

## ABSTRACT

Drilling fluids make up an essential part of the drilling operation. Successful drilling operations rely on adequate drilling fluid quality. With the development of new drilling techniques such as long deviated sections and drilling in ultra-deep waters, the standard of required performance of the drilling fluids continue to increase. Narrow pressure margins and low tolerance for barite sag requires accurate prediction of the gel evolution in drilling fluids. Increased knowledge of how drilling fluids behave during low shear rates can lead to better design of drilling fluids to avoid settling of heavy particles at the wellbore. Settling of heavy particles at the wellbore can lead to serious incidents such as stuck pipe, lost circulation, poor cement jobs and well control difficulties. Studies on the gel evolution of oil based drilling fluids could be used to optimize hydraulic modelling and evaluate phenomena such as fluid loss, barite sag and cuttings transport.

The objective of this report was to investigate the gel evolution, low shear viscosity and viscoelastic properties of oil based drilling fluids. Literature study and experimental investigations were performed on water based and oil based drilling fluids to extend the understanding of low shear viscosity of oil based drilling fluids.

Literature study performed on low shear viscosity of drilling fluids confirmed that there is a need for improved models for describing dynamic yield point and low shear behaviour. A case study performed illustrates the relevance of the topic, and the consequences unexpected gel effects could have when drilling a well.

Two water based drilling fluid samples and one oil based drilling fluid sample were prepared and tested. Quantitative information about the dynamic properties of drilling fluids was found. Flow curves and gel strength were measured using a Fann viscometer. Four different drilling fluid samples were investigated using an Anton Paar Physica rheometer. Oscillatory tests such as amplitude sweeps determined linear viscoelastic range (LVE). Determination of the linear viscoelastic range was necessary to further investigate viscoelastic properties by performing frequency sweeps within the LVE range. Both amplitude sweeps and frequency sweeps were performed at different frequencies and strains. The viscoelastic properties investigated were structure formation, structure breakage and low shear viscosity. The effect of variables such as temperature, frequency, time of rest on dynamic yield point and viscous and elastic modulus was investigated by varying these variables in series of experiments.

Experiments performed conclude that there is little correlation between the dynamic yield point found from extrapolation of flow curves using the Herschel Bulkley model and the Bingham plastic model, and the dynamic yield point found from amplitude sweeps. Amplitude sweeps showed that the three samples of drilling fluids exhibit viscoelastic behaviour, and that the linear viscoelastic range in strain rate was approximately 1 % at a temperature of 20 °C and a frequency of 1 s<sup>-1</sup> for all tested samples. Frequency sweeps showed that the elastic modulus dominates the viscous modulus within the LVE range for all three samples. Linear viscoelastic range and dynamic yield point were found to be temperature and frequency dependent. The properties of the different samples were found to not change monotonically with frequency or temperature. Results of experiments performed on a model water based drilling fluid conclude that time of rest had little influence on the properties even for longer period of rest. A slight increase in viscosity was observed for longer rest periods.

## SAMMENDRAG

Formålet med denne masteroppgaven har vært å studere gel utvikling, lavskjær reologi og viskoelastiske egenskaper for oljebaserte borevæsker. Et litteraturstudie samt eksperimentelle undersøkelser har blitt utført på både vannbaserte og oljebaserte borevæsker for å øke forståelsen av oljebaserte borevæskers adferd for lave skjærrater. Oppgaven inneholder kvantitative data om borevæsker som kan brukes til å optimalisere hydrauliske modeller og evaluere transport av kaks og tyngre partikler i borehullet.

Borevæsker utgjør en fundamental del av enhver boreoperasjon. Vellykkede boreoperasjoner avhenger av god borevæske kvalitet. Med utviklingen av nye boreteknikker som lange vinklede seksjoner og boring på ekstreme havdyp øker stadig kravet til kvalitet på borevæsker. Økt kunnskap om borevæskers oppførsel for lave skjærrater kan føre til bedre design på borevæskene, og muligens føre til mindre avsetting av tunge partikler i borehullet. Konsekvensene av slik avsetting kan være tap av sirkulasjon, fastsatt borestreng, dårlig sementering av fôringsrør og brønnkontrollproblemer.

En litteraturstudie vedrørende lavskjær viskositet av borevæsker bekrefter behovet for forbedring av hydrauliske modeller som beskriver borevæskers oppførsel for lave skjærrater. En casestudie av en brønn boret på norsk sokkel understreker aktualiteten og viktigheten av slike studier, og illustrerer potensielle problemer relatert til gelutvikling i oljebaserte borevæsker.

Denne masteroppgaven har sett nærmere på oljebaserte borevæskers viskoelastiske egenskaper. To vannbaserte borevæsker og en oljebasert borevæske har blitt fremstilt og studert. Viskositetskurver og gelstyrke har blitt målt og funnet ved hjelp av et Fann viskosimeter. Fire ulike borevæsker har blitt testet med et Anton Paar reometer. Oscillerende tester der frekvens er konstant og amplitude varieres har blitt utført for å finne det lineære viskoelastiske området for de ulike prøvene. Det lineære viskoelastiske området har deretter blitt brukt til å utføre oscillerende tester der frekvens varierer mens amplitude er konstant. Tester med konstant amplitude og varierende frekvens har blitt utført for å studere de viskoelastiske egenskapene for de ulike prøvene. De viskoelastiske egenskapene som har blitt studert er dannelsen av gel, brytning av gel og lavskjærviskositet. Effekten av varierende temperatur, frekvens og hviletid på egenskaper som flytgrense og den viskøse og elastiske andelen av borevæskene har blitt studert ved å utføre forsøk der disse variablene endres.

De utførte forsøkene konkluderer med at det er lite sammenheng mellom verdien for flytgrense som finnes ved forlengelse av viskositetskurver ved bruk av Herschel Bulkley og Bingham modellene, og flytgrense funnet ved dynamiske tester. Oscillerende forsøk med varierende amplitude og konstant frekvens har bekreftet at borevæsker oppfører seg viskoelastisk under visse betingelser, og at dette området er rundt 1 % tøyning for en temperatur på 20 °C og en frekvens lik  $1\text{s}^{-1}$ . Oscillerende tester med varierende frekvens og konstant amplitude har vist at den elastiske andelen dominerer den viskøse innenfor det lineære viskoelastiske området. Det lineære viskoelastiske området og flytgrensen varierte med temperatur og frekvens. De ulike borevæskene endret seg ulikt for endring i frekvens og temperatur. Forsøk utført på en fjerde vannbasert borevæske har vist at hviletid ikke har særlig innvirkning på viskoelastiske egenskaper. En liten økning i viskositet har ble dog observert.



## TABLE OF CONTENTS

<b>PREFACE</b> .....	<b>IV</b>
<b>ABSTRACT</b> .....	<b>VI</b>
<b>SAMMENDRAG</b> .....	<b>VIII</b>
<b>TABLE OF CONTENTS</b> .....	<b>X</b>
<b>LIST OF FIGURES</b> .....	<b>XIV</b>
<b>LIST OF TABLES</b> .....	<b>XX</b>
<b>1 INTRODUCTION</b> .....	<b>1</b>
<b>2 BACKGROUND</b> .....	<b>3</b>
2.1 BASIC PRINCIPLES OF RHEOLOGY .....	3
2.1.1 SHEAR RATE.....	4
2.1.2 VISCOSITY.....	5
2.1.3 EXTENSIONAL VISCOSITY .....	7
2.1.4 YIELD STRESS .....	8
2.1.5 VISCOELASTICITY .....	8
2.2 RHEOLOGICAL MODELLING.....	9
2.2.1 NEWTONIAN MODEL.....	9
2.2.2 BINGHAM PLASTIC MODEL .....	10
2.2.3 POWER LAW MODEL .....	10
2.2.4 HERSCHEL AND BULKLEY MODEL .....	11
2.2.5 RHEOLOGICAL MODELLING IN THE DRILLING INDUSTRY	
11	
2.3 OIL BASED DRILLING FLUIDS.....	13
2.3.1 APPLICATION OF OIL BASED DRILLING FLUIDS.....	13
2.3.2 RHEOLOGY OF OIL BASED DRILLING FLUIDS .....	14
2.4 DYNAMIC MEASUREMENTS OF DRILLING FLUIDS .....	17
2.4.1 VISCOELASTIC MEASUREMENTS .....	18
2.4.2 CREEP TEST .....	20
2.4.3 RELAXATION TEST .....	20
2.4.4 OSCILLATORY TEST .....	21
2.4.5 AMPLITUDE SWEEP TEST .....	23

2.4.6	FREQUENCY SWEEP TEST.....	24
2.4.7	TIME-DEPENDANT BEHAVIOUR AT CONSTANT DYNAMIC MECHANICAL AND ISOTHERMAL CONDITIONS.....	24
2.4.8	TEMPERATURE-DEPENDANT BEHAVIOUR AT CONSTANT DYNAMICAL CONDITIONS.....	25
2.4.9	CLASSIFYING MATERIALS ON THE BASIS OF OSCILLATORY TESTS.....	25
2.5	DOWNHOLE EFFECTS OF VISCOELASTIC PROPERTIES.....	26
2.5.1	GEL BREAKAGE WHEN RESUMING CIRCULATION.....	26
2.5.2	BARITE SAG .....	27
<b>3</b>	<b>GEL EVOLUTION .....</b>	<b>29</b>
<b>4</b>	<b>CASE: THE IMPACT OF GEL EVOLUTION.....</b>	<b>39</b>
<b>5</b>	<b>EXPERIMENTAL STUDIES .....</b>	<b>41</b>
5.1	INVESTIGATIONS IN ACCORDANCE WITH API .....	42
5.1.1	EXPERIMENTAL SET UP - PREPARING SAMPLES .....	42
5.1.2	EXPERIMENTAL SET UP - FANN VISCOMETER.....	43
5.2	RESULTS OF INVESTIGATIONS IN ACCORDANCE WITH API 44	
5.2.1	FLOW CURVES - FANN VISCOMETER.....	44
5.2.2	GEL STRENGTH - FANN VISCOMETER.....	45
<b>6</b>	<b>DYNAMIC EXPERIMENTAL INVESTIGATIONS.....</b>	<b>47</b>
6.1	EXPERIMENTAL SET UP - ANTON PAAR RHEOMETER.....	47
6.2	RESULTS OF DYNAMICAL INVESTIGATIONS .....	48
6.2.1	OSCILLATORY AMPLITUDE SWEEP TEST .....	48
6.2.2	OSCILLATORY FREQUENCY SWEEP TEST.....	56
6.2.3	COMPARISON OF DYNAMIC YIELD POINT .....	58
6.3	A SPECIAL STUDY OF A WATER BASED DRILLING FLUID ..	61
6.3.1	EXPERIMENTAL SET UP – ANTON PAAR RHEOMETER	61
6.3.2	EFFECT OF TIME OF REST.....	63
6.3.3	EFFECT OF TIME CIRCULATED.....	66
<b>7</b>	<b>DISCUSSION .....</b>	<b>71</b>
7.1	WEAKNESSES AND LIMITATIONS.....	71
7.2	POTENTIAL IMPROVEMENTS AND FURTHER WORK.....	74
<b>8</b>	<b>CONCLUSION.....</b>	<b>75</b>

<b>NOMENCLATURE</b> .....	<b>77</b>
<b>BIBLIOGRAPHY</b> .....	<b>79</b>
<b>APPENDICES</b> .....	<b>83</b>
APPENDIX A – CONTENTS DRILLING FLUID SAMPLES .....	85
APPENDIX A.1 - BENTONITE DRILLING FLUID .....	85
APPENDIX A.2 - KCL/POLYMER DRILLING FLUID.....	86
APPENDIX A.3 - OIL BASED DRILLING FLUID.....	87
APPENDIX C – MEASUREMENTS ANTON PAAR RHEOMETER .....	89
APPENDIX C.1 – AMPLITUDE SWEEPS .....	89
APPENDIX C.2 – FREQUENCY SWEEPS .....	93
APPENDIX C.3– FLOW CURVES ANTON PAAR RHEOMETER.....	96
APPENDIX D –MODEL WATER BASED DRILLING FLUID .....	97
APPENDIX D.1 – TIME OF REST AS VARIABLE.....	97
APPENDIX D.2 – TIME CIRCULATED AS VARIABLE .....	100
APPENDIX E – ARTICLE PUBLISHED ON SINTEF PROJECT .....	103



## LIST OF FIGURES

Figure 1: Flow between two parallel plates illustrating shear stress (Wikipedia, n.d.).	3
Figure 2: Fann VG 35 viscometer (Anon., 2011).	6
Figure 3: The three different types of extensional flow. From left to right; uniaxial, biaxial and planar flow (Barnes et al., 1989).	7
Figure 4: Contraction flow for a viscoelastic fluid (Barnes et al., 1989).	7
Figure 5: Plot showing the most common rheological models used today (Skalle, 2012).	9
Figure 6: Picture showing a poorly sheared emulsion, where the size of the water droplets is larger than 100 $\mu$ m (Omland, 2009).	16
Figure 7: Vector diagram showing $G'$ , $G''$ and $G^*$ (Mezger, 2011).	18
Figure 8: Deformation behavior of a viscoelastic liquid (Mezger, 2011).	19
Figure 9: Deformation behaviour of a viscoelastic solid (Mezger, 2011).	19
Figure 10: Creep and recovery curve (Mezger, 2011).	20
Figure 11: Stress relaxation curve (Mezger, 2011).	21
Figure 12: The two plate model illustrating periodic oscillations (Mezger, 2011).	21
Figure 13: Viscoelastic behavior according to oscillatory tests (Mezger, 2011).	22

Figure 14: The graph to the left illustrates a strain amplitude sweep showing a gel-like character in the LVE range. The graph to the right illustrates a strain amplitude sweep of a sample showing the character of a viscoelastic liquid in the LVE range (Mezger, 2011).----- 23

Figure 15: Stress amplitude sweep showing the yield point at the limit of the LVE range and the flow point when  $G'=G''$  (Mezger, 2011).---- 24

Figure 16: Typical flow curve of a thixotropic yielding fluid predicted by the model of Coussot et al compared to the usual presentation of the flow curve for an ideal yield stress fluid (Coussot et al., 2002). -- 30

Figure 17: Shear localization for fluid showing unstable flow for low shear rates (Hertzhaf et al., 2006).----- 32

Figure 18: Plot showing the structural recovery for three different barite loaded slurries according to the Nguyen-Boger model (Yap et al., 2011).----- 34

Figure 19: Plot showing the structural recovery for three different barite loaded slurries according to the Leong model (Yap et al., 2011).----- 34

Figure 20: Figure showing a comparison of the gel strength evolution of the same type of drilling fluid used on three different wells (Det norske oljeselskap ASA, 2012).----- 39

Figure 21: Plot showing the correlation between gel strength and O/W ratio at 4°C (Det norske oljeselskap ASA, 2012).----- 40

Figure 22: Waring commercial blender (left) and Waring commercial blade (Kitchens, 2012). ----- 42

Figure 23: Flow curves for all three samples measured with Fann viscometer at  $T=20^{\circ}\text{C}$ .----- 44

Figure 24: Ten second and ten minute gel strength measured on all three samples according to API at  $20^{\circ}\text{C}$ .----- 45

Figure 25: Structural breakdown development after 10 and 30 seconds of shearing at 3 RPM, for all three samples after 10 seconds and 10 minute rest at  $T=20^{\circ}\text{C}$ .----- 45

Figure 26: Anton Paar: Physica Smart Pave Plus rheometer (Anon., 2012) and the parallel plate geometry (Bui et al., 2012).----- 47

Figure 27: Plot showing amplitude sweep for all three samples at 10°C with a frequency of 1s<sup>-1</sup>. Storage modulus (G') and loss modulus (G'') are plotted. Red arrows indicate the limit value of the LVE range. The black arrows point to the dynamic yield point.----- 48

Figure 28: Plot showing amplitude sweep for all three samples at 20°C with a frequency of 1s<sup>-1</sup>. Storage modulus (G') and loss modulus (G'') are plotted. Red arrows indicate the limit value of the LVE range. The black arrows point to the dynamic yield point.----- 50

Figure 29: Change in dynamic yield point for all three samples for an increase in temperature from 10°C to 20°C, frequency of 1 s<sup>-1</sup>. ----- 51

Figure 30: Time sweep with constant shear of 50 s<sup>-1</sup> performed on the oil based sample with a temperature of 10 °C and 20 °C.----- 53

Figure 31: Plot showing amplitude sweep for all three samples at 10°C with a frequency of 10s<sup>-1</sup>.The storage modulus (G') and loss modulus (G'') is plotted. ----- 54

Figure 32: Comparison of dynamic yield point of amplitude sweep performed at 10 °C with a frequency of 1 s<sup>-1</sup> and 10 s<sup>-1</sup>. ----- 54

Figure 33: Frequency sweeps for all three samples at 10 °C and strain of 1 %.----- 56

Figure 34: Frequency sweep for all three samples at 20 °C with a strain of 1 %.----- 57

Figure 35: Comparison of flow curves for KCl/Polymer sample and oil based sample measured with Fann viscometer and Anton Paar rheometer. ----- 59

Figure 36: Low shear viscosity curves for all three samples measured with Anton Paar rheometer at T=10°C. ----- 59

Figure 37: Low shear viscosity curves for all three samples measured with Anton Paar rheometer at T=10°C. ----- 60

Figure 38: Storage modulus of two tests performed consecutively on WBM 3 at 30 °C and a strain of 1 %.	63
Figure 39: Loss modulus of two tests performed consecutively on WBM 3 at 30 °C and a strain of 1 %.	63
Figure 40: Storage modulus of two tests performed consecutively on WBM 4 at 30 °C and a strain of 1 %.	64
Figure 41: Loss modulus of two tests performed consecutively on WBM 4 at 30 °C and a strain of 1 %.	64
Figure 42: Frequency sweep performed on WBM 1 measured with a two week interval.	65
Figure 43: Frequency sweep performed on WBM 2 measured with a two week interval.	65
Figure 44: Plot showing amplitude sweep of sample WBM 1 and WBM 2 and the effect time of circulation have on the viscous and elastic modulus.	66
Figure 45: Difference in dynamic yield point between WBM 1 (circulated one week) and WBM 2 (circulated two weeks).	67
Figure 46: Flow curve for both WBM 1 (circulated one week) and WBM 2 (circulated two weeks) to illustrate the effect time of circulation have on the viscosity curve.	67
Figure 47: Amplitude sweep for WBM 3 (circulated two hours) and WBM 4 (circulated two days) illustrating the effect of two days longer circulation on the viscous and elastic modulus.	68
Figure 48: Flow curve for both WBM 3(circulated two hours) and WBM 4 (circulated two days) to illustrate the effect time of circulation have on the viscosity curve.	68
Figure 49: Difference in dynamic yield point between WBM 3 (circulated two hours) and WBM 4 (circulated two days).	69



Figure 50: Plot showing amplitude sweep for all three samples at 10°C with a frequency of 1s <sup>-1</sup> . -----	89
Figure 51: Plot showing amplitude sweep for all three samples at 20°C with a frequency of 1s <sup>-1</sup> . -----	89
Figure 52: Plot showing amplitude sweep for all three samples at 10°C with a frequency of 10s <sup>-1</sup> .-----	90
Figure 53: Plot showing amplitude sweep for all three samples at 20°C with a frequency of 10s <sup>-1</sup> .-----	90
Figure 54: Plot showing amplitude sweep for all three samples at 10°C with a frequency of 100s <sup>-1</sup> . -----	91
Figure 55: Plot showing amplitude sweep for all three samples at 20°C with a frequency of 100s <sup>-1</sup> . -----	91
Figure 56: Plot showing frequency sweep for the Bentonite and KCl/Polymer sample at 50°C at a frequency of 1s <sup>-1</sup> . -----	92
Figure 57: Plot showing frequency sweep for all three samples at 10°C with a strain of 1%. -----	93
Figure 58: Plot showing frequency sweep for all three samples at 20°C with a strain of 1%. -----	93
Figure 59: Plot showing frequency sweep for all three samples at 10°C with a strain of 5%. -----	94
Figure 60: Plot showing frequency sweep for all three samples at 20°C with a strain of 5%. -----	94
Figure 61: Plot showing frequency sweep for all three samples at 10°C with a strain of 10%. -----	95
Figure 62: Plot showing frequency sweep for all three samples at 20°C with a strain of 10%. -----	95

Figure 63: Plot showing flow curves for all three samples at T=10°C performed measured with the Anton Paar rheometer. ----- 96

Figure 64: Plot showing flow curves for all three samples at T=20°C performed measured with the Anton Paar rheometer. ----- 96

Figure 65: Frequency sweep performed on WBM 1 measured with a two week interval. ----- 97

Figure 66: Frequency sweep performed on WBM 2 measured with a two week interval. ----- 97

Figure 67: Frequency sweep performed consecutively on sample WBM 3. ----- 98

Figure 68: Frequency sweep performed consecutively on sample WBM 4. ----- 98

Figure 69: Flow curves of WBM1 before and after a two week period of rest. ----- 99

Figure 70: Flow curves for sample WBM 3 before and after one week rest. ----- 99

Figure 71: Amplitude sweep of sample WBM 1 and WBM 2 and the effect time of circulation have on the viscous and elastic modulus. -100

Figure 72: Amplitude sweep of sample WBM 3 and WBM 4 illustrating the effect of two days longer circulation on the viscous and elastic modulus. -----100

Figure 73: Flow curve for WBM 1 and WBM 2 to illustrate the effect time of circulation have on the viscosity curve. -----101

Figure 74: Flow curve for both WBM 3 and WBM 4 to illustrate the effect time of circulation have on the viscosity curve -----101

## LIST OF TABLES

Table 1: Classifying a materials viscoelasticity using  $G'$ ,  $G''$  and the damping factor (Mezger, 2011). ..... 25

Table 2: Comparison of dynamic yield point found from amplitude sweeps performed at 10°C and 20°C, frequency of 1s<sup>-1</sup>. ..... 51

Table 3: Comparison of yield point found from extrapolation of flow curve with the Herschel Bulkley model and the value of dynamic yield point found by amplitude sweep for all three samples at 20°C. .... 58

Table 4: Comparison of yield point found from extrapolation of flow curve with the Bingham plastic model and the value of dynamic yield point found by amplitude sweep for all three samples at 20°C. .... 58



# 1 INTRODUCTION

Optimizing drilling fluid parameters is important to achieve a successful drilling process. Rheological properties of the drilling fluid such as density and viscosity are designed to give the best pressure control and hole cleaning possible. The drilling fluid is a part of a system that alternately changes between a dynamic and a steady state, and the challenge is to design a drilling fluid that exhibits adequate qualities both at rest and in motion. When the pumps are shut off or running at low speed the drilling fluid will take on a gel-like state. The gelling of the drilling fluid helps keep cuttings and barite suspended in the drilling fluid instead of allow for settling at the wellbore. To hinder the settling of heavy particles out of suspension, it is desirable that the drilling fluid quickly develops relatively high gel strength. It is advantageous that when the gel strength has reached the required strength the strength stays at this level as time goes, and that it does not continue to grow further. When resuming circulation, the gel strength has to be broken. This requires increased energy from the pumps. This leads to a pressure peak in the borehole, and it is important that this peak do not exceed the fracturing pressure of the formation.

Drilling fluids are divided into two different categories depending on their content. Water based drilling fluids consist mainly of water and clay and are considered a suspension. Oil based drilling fluids consist mainly of a base oil and water emulsion. A range of additives are also added to influence properties such as density, viscosity and wettability. The drilling fluid experience an extreme range of different external conditions such different temperatures, different pressures and different shear rates. Extensive testing is therefore required for prediction of behaviour and to generate accurate models.

The phenomenon called “sagging” came to the industry’s attention in the 1980’s. “Sag” is the settling of heavy particles out of suspension, causing the particles to settle at the wellbore wall. The sag tendency is significantly higher in deviated wellbores than in vertical wellbores. Barite is added to the drilling fluid to create the appropriate density of the drilling fluid to control the subsurface pressures. Sagging of the barite particles can lead to hole problems such as lost circulation, well control difficulties, poor cement jobs and stuck pipe incidents.

Rheology of drilling fluids is a complex subject. Several papers have been written and published on the topic of rheology of drilling fluids. However, low shear rheology is a subject that still needs attention. Previously, drilling fluids have been viewed as purely viscous materials. Current work suggests that drilling fluids are viscoelastic

materials. This means that drilling fluids exhibit both viscous and elastic behaviour. Viscoelastic properties will tell much about the gel evolution of drilling fluids. Properties such as structural stability, dynamic yield point and loss and storage modulus is related to the gel evolution. The experiments described in this thesis study the viscoelastic properties of drilling fluids. The objective is to extend the understanding of gel evolution in oil based drilling fluids. Comparing the viscoelastic behaviour of oil based and water based drilling fluids might lead to a better understanding of why drilling with oil based drilling fluids leads to better hole cleaning. Identifying the differences in viscoelastic behaviour could lead to an understanding of what creates a drilling fluid that give good hole cleaning as well as accurate pressure control.

## 2 BACKGROUND

This chapter contains theoretical background and insight relevant for the experiments performed in the master thesis. An introduction to rheology and the properties and terms needed to understand the content of the report will be presented (Sandvold, 2011).

### 2.1 BASIC PRINCIPLES OF RHEOLOGY

Rheology is defined as the science of deformation and flow of matter. Rheology as a theoretical subject is a branch of physics and physical chemistry. Numerous industries rely on extended knowledge of this subject in their daily operations. Industries such as the food industry, chemical processing and the oil industry face challenges that involve rheology science every day. Furthermore, the subject has since the beginning of the 20<sup>th</sup> century been acknowledged as a scientific discipline in itself, and both physicists, chemists, biologists and engineers are working on advancing the understanding and the appliance of rheology (Mezger, 2011).

In any flow there are different layers of fluid that move at different velocities. This implies that molecules are moving relative to one another when the fluid is in motion. In a system that consists of two plates with fluid flowing in between the plates where one plate is moving in one direction while the other is stationary, the fluid will shear because of the friction between the fluid and the moving plate. The viscosity of the fluid is found by measuring the amount of force required for the plate to start moving. Fig. 1 illustrates how the plate with velocity  $\mu$  causes the fluid to shear.

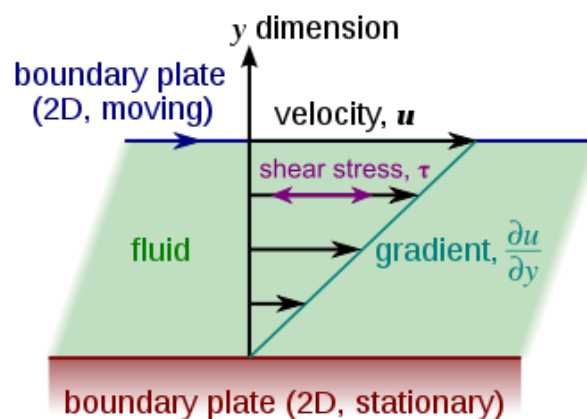


Figure 1: Flow between two parallel plates illustrating shear stress (Wikipedia, n.d.).

If assuming that the distance between the plates and the plates themselves to be very large, then the entrance effects can be ignored. If the force moving the upper plate is called  $F$  and  $F$  is moving with a velocity  $u$ , then the force  $F$  can be defined as:

$$F = \mu A \frac{u}{y} \quad [1]$$

The shear stress  $\tau$  is defined as force divided by area and can be written as a product of the viscosity and the velocity gradient in the direction perpendicular to the layers:

$$\tau = \mu \frac{\partial u}{\partial y} \quad [2]$$

The shear rate is written as  $\dot{\gamma}$ , and is found by dividing the velocity  $v$  by the distance  $h$  between the plates. Eq. 2 is crucial for understanding and describing how different types of fluids behave. The shear stress is often expressed in Pascal and the shear stress in  $s^{-1}$ . The viscosity is given in Pas. A more common unit used is centi Poise (cP) which is found by Pas times 1000 (Wikipedia, n.d.).

### 2.1.1 SHEAR RATE

Shear rate is the velocity gradient of a fluid. It is the rate of which the shear is applied. Shear rate is expressed as the velocity of the fixed plate divided by the distance between the two plates, as defined in chapter 2.1. All non-Newtonian fluids change viscosity when exposed to different shear rates. The vorticity of a flow is expressed as  $\omega = 1/t$ , the same unit as shear rate. Shear rate can be expressed as the fluid vorticity of the flow along the shear layer. Shear causes the particles to rotate, and the vorticity is equal to twice the rotation rate of any fluid element along the shear. A factor that complicates the understanding of the behaviour of the fluid is that many fluids exhibit time dependant behaviour. This means that the fluid will behave differently under same shear rate, depending on the shear rate the regime the fluid previously has experienced. This will be discussed further in chapter 2.3



### 2.1.2 VISCOSITY

The most elementary property dealt with in rheology is viscosity. Viscosity is the measure of a fluid's resistance to deform when undergoing stress. Viscosity describes the thickness of a fluid, and the thicker the fluid is the larger the internal friction in the fluid. Newton was the first to introduce the relationship between shear rate, shear stress and shear viscosity.

$$\tau = \mu * \dot{\gamma} \quad [3]$$

$\tau$  = Shear stress

$\dot{\gamma}$  = Shear rate

$\mu$  = Viscosity

The viscosity can for some Newtonian liquids be a coefficient, but for most fluids the viscosity is a function of shear rate. It is important to emphasize that this function is not a law of nature, but a constitutive equation. Viscosity is a property that varies with several external factors. Variables such as shear rate, temperature, pressure, time of shearing and chemical or physical nature affect the apparent viscosity. In order to predict the behaviour of a fluid and determine its properties correctly, it is important to have a thorough knowledge of how fluids change under different conditions .

Viscosity can be measured using special rheometers called viscometers. A viscometer can only perform measurements under one flow condition. There are several types of viscometers and one category of viscometers is rotational viscometers. A rotational viscometer consists of a cup and a bob. The Fann VG 35 rheometer is depicted in Fig. 2. The fluid is poured into the cup and the bob is placed concentrically into the cup so that the bob is completely immersed in the fluid. The bob is attached to a small motor, and when switched on the cup will start rotating. The fluid's resistance to flow is transmitted to the bob as torque. This torque is measured through a measuring instrument connected to the bob. The cup can be rotated with different speeds and the result is a set of measured stress for different angular speeds. This data can be transformed through the following equations:

Shear stress:

$$\sigma = \frac{F}{A} \quad [4]$$

Shear rate:

$$\dot{\gamma} = \frac{R\Omega}{R-r} \quad [5]$$

This will eventually result in a set of data with the shear stress as a function of shear rate. These data can further be used for determining what kind of rheological model that best describe the fluid in question (Anon., 2010).



**Figure 2: Fann VG 35 viscometer (Anon., 2011).**

Temperature and pressure are as mentioned two external factors that can influence the way which a fluid behaves. Viscosity is strongly dependent on temperature, and for Newtonian fluids the viscosity decrease with increasing temperature. The pressure dependence is also important, and a fluid's viscosity increases exponentially with isotropic pressure. When performing experiments in the lab, a slight change in temperature can have a significant influence on the measurements. A change in pressure of approximately one bar from atmospheric pressure has a negligible effect on the viscosity. Therefore the effect of pressure is ignored when performing experiments using a viscometer. Outside the lab on the other hand, fluids may experience large differences in pressures, especially in the oil industry. Both pressure and temperature can vary significantly in wellbores, and this demands a basic understanding of how the drilling fluid behaves under different conditions.

### 2.1.3 EXTENSIONAL VISCOSITY

The study of extensional flow is more complicated than studies of shear flow. There are three types of extensional flows. The different flows are shown in Fig. 3.

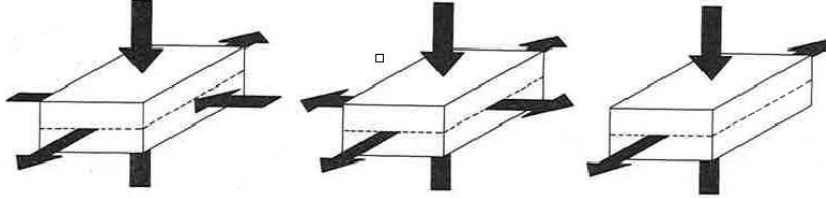


Figure 3: The three different types of extensional flow. From left to right; uniaxial, biaxial and planar flow (Barnes et al., 1989).

Extensional flows can occur when a fluid is flowing through a sudden contraction or out of an orifice. The values for extensional viscosity are larger than the values of viscosity measured under shear. Extensional flow leads to a stretching of the molecules. This results in a greater resistance to flow, leading to an increase in viscosity. It is possible to compare the extensional and shear viscosity through the Truton ratio.

$$T_R = \frac{\eta_E(\dot{\epsilon})}{\eta(\dot{\gamma})} \quad [6]$$

In Eq. 6  $\eta_E$  is the extensional viscosity and  $\eta$  is the shear viscosity at the corresponding shear rate. For non-Newtonian fluids the value of the Truton value can be high (Barnes et al., 1989). Determination of extensional properties can be done by contraction flow. Contraction flow can be induced using capillary rheometry, allowing the fluid to flow from a barrel into a capillary of a much smaller radius. When a viscoelastic fluid flows through the contraction, there will be a vortex enhancement as shown in Fig. 4.

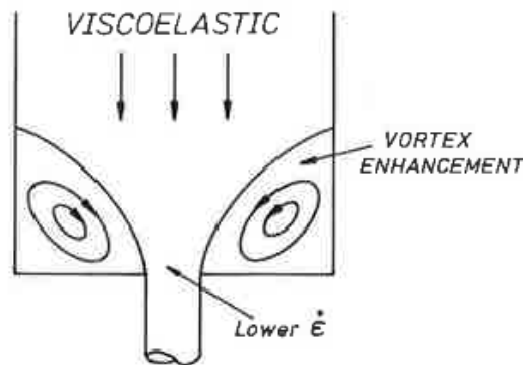


Figure 4: Contraction flow for a viscoelastic fluid (Barnes et al., 1989).

The central core flow will have a lower strain rate. This leads to shear flow near the walls and extensional flow in the centre flow. The Mars funnel has a contracted geometry. The viscosity found when performing experiments with a Marsh funnel is called funnel viscosity. The viscosity is found by measuring the time it takes for a known volume of fluid to flow through the funnel. Funnel viscosity is therefore a type of extensional viscosity.

#### 2.1.4 YIELD STRESS

The yield point of a fluid is the point at which the fluid will start to flow. The flow starts because the external forces acting on the material are larger than the internal structural forces. When exhibiting a stress on the material with a stress smaller than the yield stress, the fluid will behave elastically and any deformation will recover completely. When the stress exhibited is equal to the yield point or larger, viscous or viscoelastic flow will start. Therefore it is sometimes better to speak of a yield zone. The yield stress is also time dependant. This means that the yield stress that is measured depends on whether the fluid has been at rest or whether it has been agitated. The transition from elastic behaviour to viscous behaviour is often not a clear bend (Barnes et al., 1989). There are many methods for measuring yield stress, however the methods for finding the yield stress is a subject that is under discussion and this will be further studied in Chapter 3.

#### 2.1.5 VISCOELASTICITY

Viscoelasticity is the property of materials that exhibit both viscous and elastic characteristics when undergoing deformation. The elastic portion of a viscoelastic material stores energy when deformed and do not dissipate energy. The viscous portion will when deformed dissipate energy as heat. Creep, relaxation and periodic oscillations are different test to investigate viscoelastic properties. Viscoelastic materials display time-dependent behaviour when a stress or a strain is applied. Viscoelastic properties are temperature dependant. Viscoelasticity and how to measure different viscoelastic properties will be further elaborated in Chapter 2.4.

## 2.2 RHEOLOGICAL MODELLING

Rheological modelling is to mathematically describe the rheology of a drilling fluid. A constitutive equation has to be chosen and empirical constants have to be determined experimentally. Experiments are typically performed using a rheometer with a coquette, parallel late or cone and plate geometry. The data set from the measurements performed is plotted in a rheogram. The shear rate make up the horizontal axis and the shear stress make up the vertical axis. The data points will result in a flow curve. By comparing the shape of the flow curve to the shape of the curve for the different rheological models it is possible to determine which rheological model best describes the fluid the measurements have been performed on. The most important property found from these measurements is the viscosity. The viscosity will be the slope of the curve, and is found through the shear stress divided by the shear rate. Fig. 5 shows a plot with the most commonly used rheological models. The following subchapters will give a more detailed description the different rheological models.

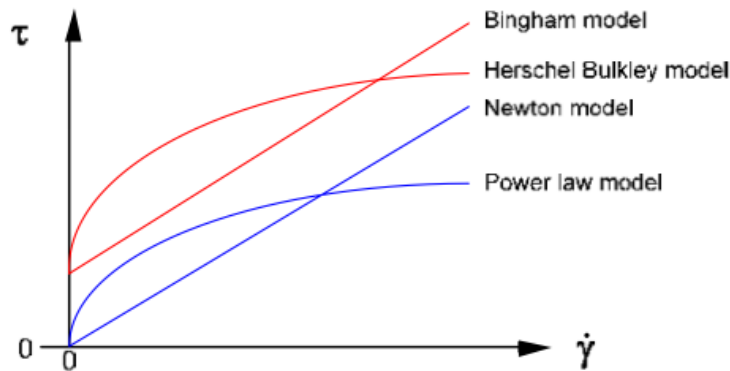


Figure 5: Plot showing the most common rheological models used today (Skalle, 2012).

### 2.2.1 NEWTONIAN MODEL

$$\tau = \mu * \dot{\gamma} \quad [7]$$

The Newtonian model describes Newtonian fluids. Newtonian fluids have a viscosity that is independent of shear rate and the time of shearing. A familiar example of a Newtonian fluid is water. The fluid will behave the same way regardless of shearing and history of shearing. A flow curve of a Newtonian fluid will therefore be a linearly increasing curve where the slope of the line is the viscosity.

## 2.2.2 BINGHAM PLASTIC MODEL

$$\tau = \tau_y + \mu_{pl} * \dot{\gamma} \quad [8]$$

The Bingham plastic model is designed to describe fluids with a yield stress. Bingham plastic fluids will not flow until a critical yield stress is exceeded. After this critical yield point is exceeded the fluid will behave like a Newtonian fluid when increasing shear rate, meaning that the viscosity will be constant. The Bingham model has been found to be accurate in describing fluids that contain suspension of solids. The Bingham model is therefore very often applied when describing drilling fluids. The model is best suited for calculating the state of the drilling fluid, but is poorly fitted for calculating viscosity and pressure loss.

## 2.2.3 POWER LAW MODEL

$$\tau = K\dot{\gamma}^n \quad [9]$$

The power law model gives good description of how pseudoplastic fluids behave for a big span of different shear rates. The model gives especially good description of how pseudoplastic fluids behave at low shear rates. The shear thinning behaviour occurs for different reasons. If the particles in a colloidal system aggregate, then an increase in shear rate will break the aggregates down, and reduce the amount of immobilized solvent. To describe the fluid properly the parameters K and n need to be defined. The parameter K is the consistency index and is expressed as:

$$K = \frac{\tau}{\dot{\gamma}^n} \quad [10]$$

The parameter n is the power law index. It is expressed as:

$$n = \frac{\log \tau_1 / \tau_2}{\log \dot{\gamma}_1 / \dot{\gamma}_2} \quad [11]$$

Depending on the value of n, the model describes three types of different fluids:

- n=1 Newtonian fluid
- n>1 dilatant fluid
- n<1 pseudoplastic fluid

The pseudoplastic fluid is shear thinning, whereas the dilatant fluid is shear thickening.

## 2.2.4 HERSCHEL AND BULKLEY MODEL

$$\tau = \tau_y + K\dot{\gamma}^n \quad [12]$$

The Herschel and Bulkley model also describes pseudoplastic fluids. The Herschel Bulkley model takes yield point into consideration and is therefore the model that often describes measured data the best for drilling fluids. The constants  $n$  and  $K$  are the same as for the Power law model, but in addition the yield point,  $\tau_y$ , is included. This model gives a better result for lower shear rates. For low shear rates  $K$  is related to the viscosity of the fluid. For higher shear rates  $K$  is a measure of the solid content of the fluid. The lower the value of  $n$ , the more shear thinning the fluid is (Skalle, 2012).

## 2.2.5 RHEOLOGICAL MODELLING IN THE DRILLING INDUSTRY

The Herschel Bulkley model is the model most used in the oil industry today. In the oil industry the drilling fluid will experience a range of different shear rates, and the Herschel Bulkley model has been found to be the most accurate rheological model for the whole range of shear rates. When designing the viscosity curve of the drilling fluid, the range of shear rate the drilling fluid will experience in the different sections must be considered. In the 12-1/4" section there will be a big difference in the shear rate inside the pipe and in the annulus. Inside the pipe, the fluid will experience high shear rates, and the behaviour of the drilling fluid in the range of  $511\text{s}^{-1}$  to  $1022\text{s}^{-1}$  is most relevant. Assuming that a Newtonian fluid is being pumped through the drill pipe, then the shear rate inside the drill pipe will be:

$$\dot{\gamma}_{pipe,Newtonian} = \frac{8v}{d} \quad [13]$$

If the drilling fluid is being pumped at 3000 LPM and the inner diameter of the drill pipe is 4,125 inches then the shear rate will be:

$$\dot{\gamma}_{pipe,Newtonian} = \frac{8 * 5,8\text{m/s}}{0,1047\text{m}} = 443 \text{ 1/s}$$

In the annulus the shear rate for a Newtonian fluid will be found by:

$$\dot{\gamma}_{annulus,Newtonian} = \frac{12v}{d_o - d_i} \quad [14]$$

For the 12-1/4" section the shear rate in the annulus will be:

$$\dot{\gamma}_{annulus,Newtonian} = \frac{12v}{d_o - d_i} = \frac{12 * 1,88 \text{ m/s}}{0,311\text{m} - 0,127\text{m}} = 122 \text{ 1/s}$$

For the 8-1/2" section the shear rate in the annulus will be:

$$\dot{\gamma}_{annulus,Newtonian} = \frac{12v}{d_o - d_i} = \frac{12 \cdot 8,1 \text{ m/s}}{0,216\text{m} - 0,127\text{m}} = 1087 \text{ 1/s}$$

When the drilling fluid is pumped put into the annulus the large area of the annulus results in a reduction of the fluid velocity and the shear rate. In the annulus the lower range of shear rate is relevant. When wanting to design a drilling fluid that reduces the Equivalent Circulation Density (ECD) effects, it is important to know which region of shear rate is relevant. In the 8-1/2" section annulus, the drilling fluid will experience higher shear rates than in the 12-1/4" section because the area of the annulus is reduced. When wanting to design a proper drilling fluid for this section, the viscosity curve for shear rates around  $170\text{s}^{-1}$  to  $511\text{s}^{-1}$  might be more relevant (Bourgoyne et al., 1984).



## 2.3 OIL BASED DRILLING FLUIDS

The drilling fluid is an essential part of the drilling process. Drilling fluids have several important tasks:

- Maintain pressure control in the well, keep formation fluids from leaking uncontrolled into the well
- Clean the borehole and transport cuttings to the surface
- Keep cuttings and barite suspended
- Lubricate the drill and cool the bit
- Stabilize borehole wall

### 2.3.1 APPLICATION OF OIL BASED DRILLING FLUIDS

In order for the drilling fluid to be able to perform these tasks combined, the drilling fluid has to be carefully designed. Designing the proper drilling fluid is a complex matter. Oil based drilling fluids are complex and can consist of up to ten different components. Oil based drilling fluids are often called inhibitive drilling fluids. The benefit of drilling with oil based drilling fluids is that the oil based drilling fluids suppress the hydration of clay, which can occur when drilling through shale sections of a well. The use of oil based drilling fluids is still restricted in many areas, and oil based drilling fluid is often considered more environmentally harmful compared to water based drilling fluid, even though the oil based drilling fluids used on the Norwegian Continental Shelf only contain food grade oils.

The water that is dispersed in the oil is given a salinity to match the formation to hinder water influx from or to the formation. The droplets are dispersed in oil, and create a filter cake in permeable formations. The water is given the same salinity as the formation to prevent osmosis. In addition to being an inhibitive drilling fluid, oil based drilling fluids also provides good lubrication of the drill. Drilling with oil based drilling fluids reduce the friction in the well, which reduce the ECD effects. This is particularly an advantage when drilling highly deviated sections. The oil base of the oil based drilling fluid can be diesel oils or less harmful mineral oils. Regulations regarding emissions sometimes exclude the possibility of drilling with oil based drilling fluids (Skalle, 2012).

### 2.3.2 RHEOLOGY OF OIL BASED DRILLING FLUIDS

Fluids that have a viscosity that is time dependant are called rheopectic or thixotropic. Thixotropy is related to shear thinning fluids, this means fluids that exhibit a behaviour where the viscosity decrease when exposed to shear over time. The longer the period of shear, the lower the viscosity. Rheopexy is related to shear thickening fluids, this means fluids where the viscosity increase when exposed to shear stress over time. Most drilling fluids are thixotropic fluids. This implies that drilling fluids are time dependant and exhibit a shear thinning behaviour. When drilling a well this means that during low shear rates, or at quiescence the viscosity is higher, and has a higher ability to keep heavy particles suspended. When the drilling fluid is pumped at high shear rate, the viscosity decreases so that the drilling fluid flows easier and there is no need for high viscosity because the velocity of the drilling fluid transports the heavy particles. Thixotropic fluids can also have a yield point. Thixotropy is a time-dependant decrease of viscosity in a fluid due to a change of the fluid microstructure during shear. This change is reversible. When at quiescence rebuilding of the structure starts. This process is called aging. Colloidal particles in a liquid will always strive to achieve a maximum degree of entropy. The entropy reaches its maximum when the molecules are statistically distributed in the available volume. As the particles move, they occasionally collide and change direction. This will lead to a complicated and random pattern that is called Brownian movements. Brownian movements are what cause the aging and rebuilding of structure in a fluid. Brownian movements increase with increasing temperature, because the velocity of the molecules is proportional to the square root of temperature.

Drilling fluids are often described as colloidal suspensions. Colloidal suspensions consist of a dispersed phase that is insoluble in another medium. Colloids have a high surface to volume ratio. Colloidal dispersions are defined as systems that consist of solid, liquid or gaseous colloidal particles dispersed in a continuous phase that have a different chemical composition. Colloidal dispersions can be both lyophobic and lyophilic. In lyophobic systems there are repulsive forces between the dispersed particles. In lyophilic systems there are attractive forces between the dispersed particles (Mørk, 1997).

For oil based drilling fluids, oil is the continuous phase, and water is the dispersed phase. When both the continuous phase and the dispersed phase are liquid the system is called an emulsion. It is important to keep the emulsion stable, and hinder the droplets from gravity separating due to gravity and from merging and forming a continuous phase. There are two methods for creating a stable

emulsion. The first is called electrostatic stabilization, and the basic principle is that the dispersed phase is given an electrical charge that makes them repel each other. Steric stabilization is the method most often used for oil based drilling fluids. The droplets are coated with an emulsifier that will surround the water droplets. This will prevent aggregation and help keep the emulsion stable, assuming that they will not gravity separate. Emulsions can also be stabilized by particle addition. Adding clay particles that are adsorbed on the droplet surface keep the droplets from coalescing.

Dispersed systems can take on different states. Flocculation is a reversible formation of an open matrix of particles. Flocculation occurs due to attractive forces between the dispersed units. If the attractive forces are larger than the repulsive forces than the particles will flocculate. There are different types of forces that can lead to flocculation. Van der Waal forces, ionic forces and hydrogen bindings and chemical bindings are all forces that can lead to flocculation. In a flocculated system there is a distance between the particles, and the attractive forces between the particles are quite small. Flocculated particles are often easy to redisperse. If there is a large amount of flocculation in a system, then the system can turn into continuous network. This network will lead to a gelling of the system. The three-dimensional structure that is formed is capable of immobilising large amount of liquid. If two particles collide and the attractive Van der Waals forces are larger than the repulsive forces, then the particles will lose their kinetic identity and remain attached. These two particles are aggregated.

The shape, size and surface of the dispersed phase have great influence on the system's properties. The amount of water emulsified in the oil can vary from 5-50 % (UiS, 2011). For oil based drilling fluids where water is the dispersed phase, the size and the amount of water droplets influence on the viscosity. The smaller and the more monodispersed the water droplets are, the more viscous the fluid becomes. The type of emulsifying agent, salt type and concentration and the O/W ratio will influence on the stability of the emulsion. The droplet size and specific surface area are affected by emulsifier concentration. Increasing emulsifier concentration leads to a decrease in the average droplet size. The specific surface area of the droplets increases when increasing concentration of emulsifier (Al-Mutairi et al., 2009). The preparation and mixing of the drilling fluid will also influence on the stability of the emulsion. The shear stress increase when the emulsion experiences an increase in shear energy. This is due to the increase of the surface area of the internal water droplets that occurs when the shear energy increase. A poorly prepared drilling fluid will have larger water droplets than a properly sheared

fluid. An example of a poorly sheared fluid is shown in Fig. 6. Dispersion by mechanical grinding is the most common way to prepare drilling fluid emulsions. A stable emulsion is produced by the use of high pressure pumps and turbulent mixing. The process splits the water droplets into smaller units creating a more stable emulsion (Omland, 2009).

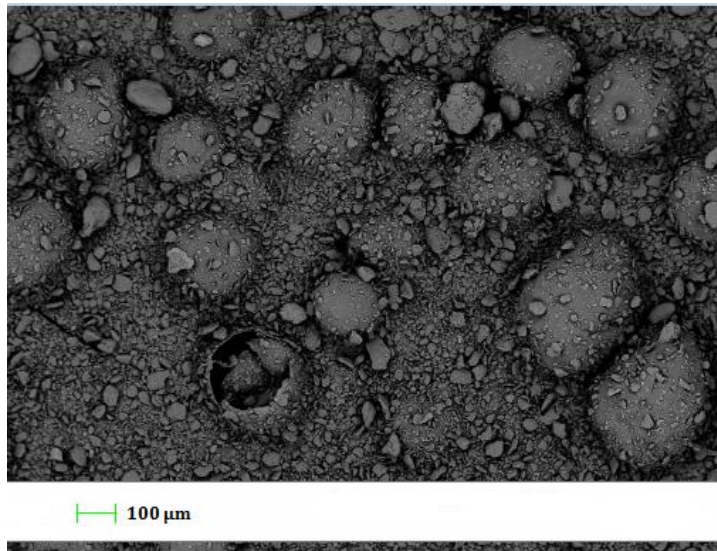


Figure 6: Picture showing a poorly sheared emulsion, where the size of the water droplets is larger than 100μm (Omland, 2009).

The viscosity of a simple oil water emulsion can be found by extending Einstein's formula assuming the motion is sufficiently slow to prevent droplet-droplet interaction.

$$\mu = \mu_{bo}(1 + 2,5\varphi + b\varphi^2) \quad [15]$$

In Eq. 15, the viscosity of the based oil is represented by  $\mu_{bo}$ , and  $\varphi$  is the volume fraction of water. If the shear rate is increased, Brownian motion no longer dominates the movements in the fluid. A chaotic pattern of motions occurs, and this leads to an increase in the viscosity of the emulsion. Saasen showed that this only happens for a short range of shear rates, but the increase in viscosity is dramatic for these shear rates (Saasen, 2002). Continuing to increase the shear rate will lead to formation of clusters of water droplets, allowing larger volume of free oil. This leads to a decrease in viscosity.

## 2.4 DYNAMIC MEASUREMENTS OF DRILLING FLUIDS

Viscoelasticity is a merger of viscosity and elasticity. Viscosity is a property used when describing liquids, and elasticity is a property used when describing solids. Drilling fluids can exhibit both these properties at the same time and is therefore a complex material to describe. Predicting the behaviour of drilling fluids is essential in drilling operations. Extended knowledge can lead to better modelling and more accurate prediction of drilling fluid behaviour. Viscoelasticity is a subject essential to understand especially low shear viscosity, structure formation and structure breakage.

Viscoelastic liquids and solids display time-dependant behaviour when undergoing deformation. The storage modulus  $G'$  and the loss modulus  $G''$  are two parameters that describe the viscoelastic behaviour of a fluid. Both  $G'$  and  $G''$  are measured in shear, and represent the relationship between stress and strain. The storage modulus,  $G'$ , represents the elastic behaviour of the material. The storage modulus is a measure of the deformation energy stored by the material during a shear process. If this energy is fully stored in the sample, then the sample will reclaim its original structure. This indicates that the sample display a reversible deformation behaviour. The loss modulus,  $G''$ , is a measure of the deformation energy lost by the sample during the shear process. The loss modulus represents the energy lost when the material changes its structure. The friction between the components is a process called viscous heating. This is irreversible deformation behaviour. The damping factor,  $\tan \delta$ , describes the ratio between the elastic and the viscous deformation illustrated in Eq. 16.

$$\tan \delta = G''/G' \quad [16]$$

For ideally elastic behaviour the storage modulus completely dominates the loss modulus so that the damping factor equals 0. For ideally viscous behaviour the loss modulus completely dominates the storage modulus so that the damping factor equals to  $\infty$ . When the damping factor reaches 1, the sol/gel transition point is reached. This is an important criterion for gel formation and the curing process.

$\tan \delta > 1$ :	Fluid or liquid state
$\tan \delta < 1$ :	Solid or gel like state
$\tan \delta = 1$ :	The sol/gel transition points

$G^*$  is the complex shear modulus and  $G^*$  can be imagined as the rigidity of the material.  $G^*$  is a measure of the materials overall resistance to deformation. The correlation between  $G'$ ,  $G''$  and  $G^*$  are shown in Fig. 7.

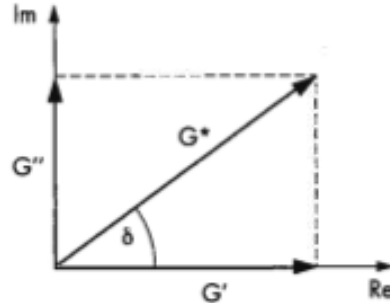
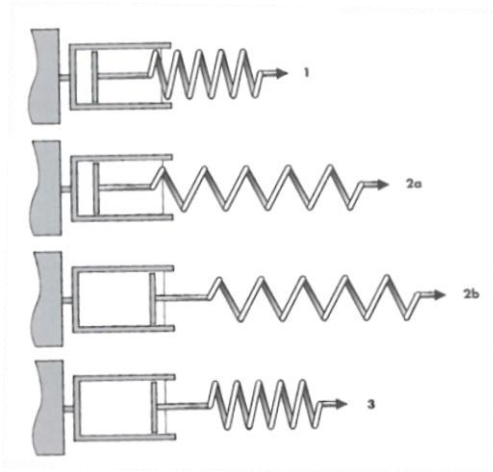


Figure 7: Vector diagram showing  $G'$ ,  $G''$  and  $G^*$  (Mezger, 2011).

Complex viscosity is noted as  $\eta^*$  and is a frequency dependant viscosity function determined during harmonic oscillation of shear stress. The complex viscosity is the vector sum of the dynamic viscosity  $\eta'$  and the out-of-phase viscosity  $\eta''$ . The dynamic viscosity  $\eta'$  is the ratio of the loss modulus  $G''$  to the angular frequency. The out-of-phase viscosity  $\eta''$  is the ratio of storage modulus  $G'$  to angular frequency.

#### 2.4.1 VISCOELASTIC MEASUREMENTS

The Maxwell model uses a spring and a dashpot to illustrate the behaviour of viscoelastic liquids. A load is applied to the system. The spring displays immediate deformation, which is proportional to the load. After some time the piston of the dashpot will begin to move. The piston will continue to move as long as the load is applied. When releasing the load, the spring recoils elastically and completely. The spring represents the elastic portion, and the piston corresponds to the viscous portion. The viscous portion is the permanently remaining deformed. The irreversible deformation that occurs makes the sample a viscoelastic liquid. The Maxwell model is illustrated in Fig. 8.



**Figure 8: Deformation behavior of a viscoelastic liquid (Mezger, 2011).**

The Kelvin/Voigt model uses a spring and a dashpot in parallel connection to illustrate viscoelastic solid behaviour. When the load is applied, the two components deform together because of the rigid frame that connects them. The motion of the spring is slowed down by the dashpot. When the load is removed, the spring elastically recoils back to its initial position. Since the piston and the spring are connected, the piston will also reach its initial position. The process will be delayed, but the reformation will be complete. The Kelvin Voigt model is illustrated in Fig. 9.

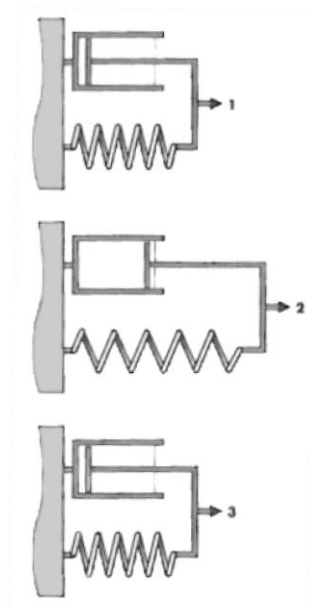


**Figure 9: Deformation behaviour of a viscoelastic solid (Mezger, 2011).**

There are three main types of tests that can be conducted to examine viscoelastic behaviour. The tests will be described in the following subchapters (Mezger, 2011).

## 2.4.2 CREEP TEST

The creep test is performed using two shear stress steps. The creep test enables an examination of the samples behaviour under very low shear rates. The first step of the creep test is to increase the stress to a value  $\tau_0$  that is kept constant for a certain time interval. The second step is to reduce the stress back to the initial level and keep it constant for a time interval. The change in stress should be performed as quickly as possible, and this requires a highly dynamic rheometer drive. This is illustrated in the top plot in Fig. 10. The first step is called the creep curve and the second step is called the creep recovery curve. This test will give three different results for ideally elastic, ideally viscous and viscoelastic samples (Mezger, 2011).

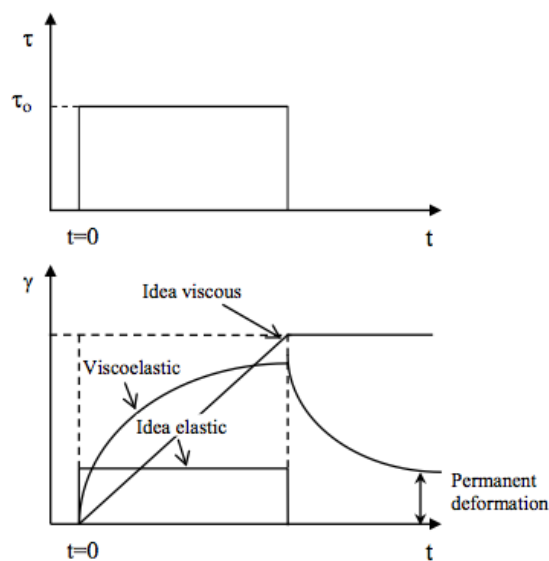


Figure 10: Creep and recovery curve (Mezger, 2011).

Viscoelastic materials under constant stress will display one immediate deformation and one delayed. The deformation that remains permanently after the load is released and after a rest phase is the viscous portion of the sample. This is shown in the lower plot in Fig. 10. The ideally viscous material remains deformed. The ideally elastic material goes back to its original state.

## 2.4.3 RELAXATION TEST

The relaxation test is performed by doing a strain step. The test is performed by applying a fixed strain to the sample, and the shear stress is monitored. This step should be performed as quickly as possible. This test will give three different results for ideally elastic, ideally viscous and viscoelastic samples. For an ideally elastic solid, there will be no stress relaxation. For an ideally viscous liquid complete stress relaxation occurs, this is shown in Fig. 11.



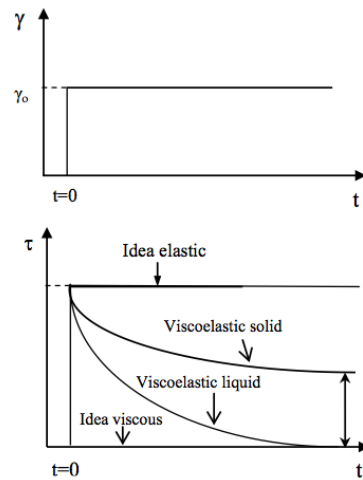


Figure 11: Stress relaxation curve (Mezger, 2011).

#### 2.4.4 OSCILLATORY TEST

Oscillatory tests are also called dynamic mechanical analysis (DMA) and the tests are used to determine viscoelastic properties of materials. The basic principle is that the fluid is exposed to periodic oscillations. The two plate model can be used to illustrate the model and Fig. 12 illustrates the principle. The sample is placed between a stationary plate and an oscillating plate. The oscillating plate is dynamically moving back and forth, causing shearing of the sample. The dynamic plate has an area  $A$  and is being pushed back and forth with the force  $\pm F$ .

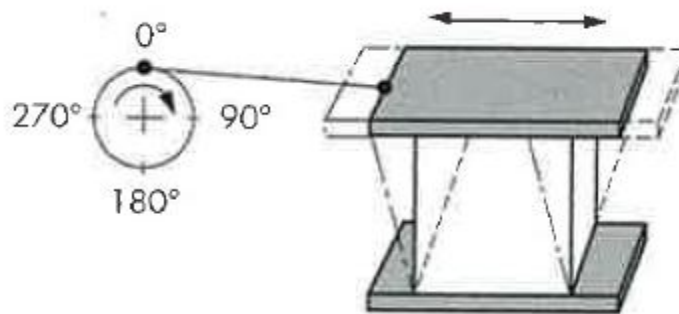


Figure 12: The two plate model illustrating periodic oscillations (Mezger, 2011).

Dynamic mechanical analysis applies a sinusoidal force, and the storage modulus can be described as an in-phase component, and the loss modulus as an out of phase component. A phase shift angle  $\delta$  between deformation and response is shown in Fig. 13. The phase shift angle is a measure of the energy dissipation of a material.

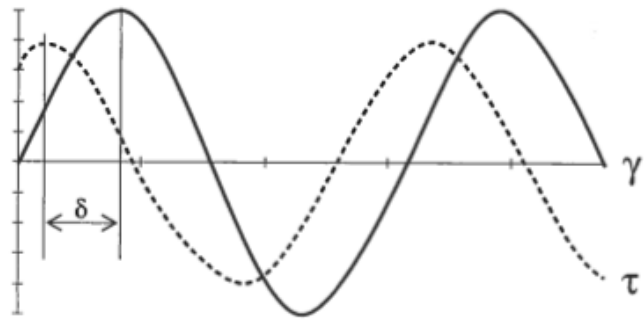
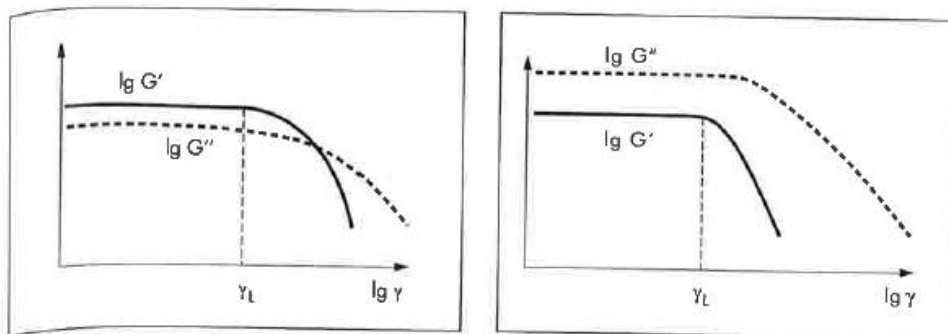


Figure 13: Viscoelastic behavior according to oscillatory tests (Mezger, 2011).

## 2.4.5 AMPLITUDE SWEEP TEST

Amplitude sweeps are oscillatory tests used to determine the linear viscoelastic (LVE) range of a material. The amplitude sweep test is performed at variable amplitudes while the frequency is kept constant. The test is also called strain sweeps. The linear viscoelastic range is found where the values of  $G'$  and  $G''$  are constant for an interval of strains. This is the range where the material functions such as dynamic modulus, viscosity and creep function do not depend on the level of deformation. The difference in value between the two parameters will tell whether the viscous or the elastic behaviour dominates the other. If  $G' > G''$  then the elastic behaviour dominates, and the material has the character of a gel or a solid. However, many materials can show low-viscosity behaviour at higher shear rates. If  $G'' > G'$  then the viscous behaviour is the dominating portion, and the material has the character of a sol or liquid. The different behaviours are illustrated in Fig. 14. The purpose of finding the LVE range is to detect for which strains the sample remains intact and the structure remains unchanged. The range outside the LVE range is where irreversible deformation occurs.



**Figure 14:** The graph to the left illustrates a strain amplitude sweep showing a gel-like character in the LVE range. The graph to the right illustrates a strain amplitude sweep of a sample showing the character of a viscoelastic liquid in the LVE range (Mezger, 2011).

It is possible to determine the yield point  $\tau_y$  and the flow point  $\tau_f$  by analyzing the amplitude sweep plot. The flow point is found where the storage modulus is equal to the loss modulus. The yield point is found at the limit of the LVE range. This is illustrated in Fig. 15.

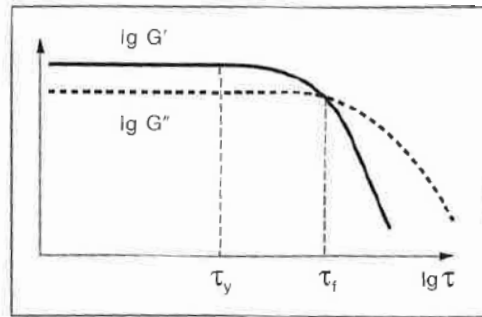


Figure 15: Stress amplitude sweep showing the yield point at the limit of the LVE range and the flow point when  $G'=G''$  (Mezger, 2011).

#### 2.4.6 FREQUENCY SWEEP TEST

Frequency sweeps are oscillatory tests where the amplitude is kept constant and the frequency is varied. Frequency sweeps are performed to investigate the time-dependent deformation of the material since the frequency is the inverse value of time. At high frequencies the short-term behaviour is simulated, and at low frequencies the long-term is simulated. It is only useful to do frequency sweeps within the LVE range. It is therefore important to find the LVE range before performing frequency sweeps.

For dispersions and gels the value of  $G'$  is higher than the value for  $G''$  for the whole frequency range. This means that the elastic portion dominates the viscous portion. Dispersions and gels are built up by a physical network of intermolecular forces. The structural strength of this network can be analyzed. Within the LVE range this structural strength will remain relatively constant. Frequency sweeps are used to evaluate viscoelastic properties such as long-term storage stability.

#### 2.4.7 TIME-DEPENDANT BEHAVIOUR AT CONSTANT DYNAMIC MECHANICAL AND ISOTHERMAL CONDITIONS

When testing the time-dependent behaviour of a material using oscillatory tests, both the amplitude and the frequency is kept constant. The temperature is also kept constant throughout the experiment. Testing called time-dependent behaviour of samples showing no hardening will tell whether the structural strength remain the same, decrease or increase over time. Increase in the structural strength might occur for dispersions or gels. The increase in structural strength is caused by an increased number of physical interactions leading to the formation of gel. Decrease in structural strength in a dispersion or gel is caused by a softening or a decreasing number of physical interactions.

#### 2.4.8 TEMPERATURE-DEPENDANT BEHAVIOUR AT CONSTANT DYNAMICAL CONDITIONS

Temperature-dependant behaviour is investigated by keeping the amplitude and frequency constant, and performing experiments at different temperatures. Temperature can either be increased linearly or stepwise.

#### 2.4.9 CLASSIFYING MATERIALS ON THE BASIS OF OSCILLATORY TESTS

The raw data that is measured during oscillatory tests are used to calculate the storage and loss modulus that are discussed in chapter 2.4. These are the only two parameters that are needed to present the results.  $G'$  and  $G''$  should be plotted in a log-log diagram. How these parameters can be used to classify the materials which the tests are performed on is presented in Table 1.

Ideally viscous flow behaviour	Behaviour of a viscoelastic liquid	Viscoelastic behaviour showing 50/50 ratio of the viscous and elastic portions	Behaviour of a viscoelastic gel or solid	Ideally elastic deformation behaviour
$\delta = 90^\circ$	$0^\circ > \delta > 45^\circ$	$\delta = 45^\circ$	$0^\circ > \delta > 45^\circ$	$\delta = 0^\circ$
$\tan\delta \rightarrow \infty$	$\tan\delta > 1$	$\tan\delta = 1$	$\tan\delta < 1$	$\tan\delta \rightarrow 0$
$(G' \rightarrow 0)$	$G'' > G'$	$G' = G''$	$G' > G''$	$(G'' \rightarrow 0)$

Table 1: Classifying a materials viscoelasticity using  $G'$ ,  $G''$  and the damping factor (Mezger, 2011).

## 2.5 DOWNHOLE EFFECTS OF VISCOELASTIC PROPERTIES

The viscoelasticity of the drilling fluid is related to the important task of holding cuttings and weighting particles suspended in the drilling fluid. A gel like structure forms when the drilling fluid is not submitted to shear stress. This gel structure holds heavy particles suspended, and prevent cuttings from precipitating and settle at the wellbore wall. The gel structure is created by the rebuild of structure because viscoelastic fluids have the ability to store energy. The time it takes for the drilling fluid to build up a gel structure is one of the most important ways to classify the drilling fluid.

### 2.5.1 GEL BREAKAGE WHEN RESUMING CIRCULATION

When drilling vertical sections, it is desirable to drill with a drilling fluid that quickly build up high gel strength to hinder the heavy particles from sinking far before the gel forms and keep the particles suspended. As time goes the drilling fluid should have a small increase in gel strength to avoid an increase in pump pressure needed to break the gel strength and risk possible damage to the formation. A drilling fluid that continue to build up gel strength as time goes by is called a progressive drilling fluid and is not desirable to drill with because the amount of pump pressure needed to break the gel strength could be too high (Saasen, 2002). In deviated sections gelling of the drilling fluid is unwanted. In deviated sections the gel works as glue that sticks the particles that have settled at the wellbore together. This hinders transport of the cuttings to the surface. It is therefore difficult to say what a good drilling fluid is and what a poor drilling fluid is with respect to gel strength in wells that have deviated sections.

A way of classifying a drilling fluid is through 10 second and 10 minute gel strength. The 10 second gel test is performed using a Fann viscometer, and allowing the drilling fluid to rest for 10 seconds before measuring the peak shear stress at 3 RPM. The 10 minute gel test is performed using a Fann viscometer, and allowing the drilling fluid to rest for 10 minute before measuring the peak shear stress at 3 RPM. This gives a good characterisation of the drilling fluids ability to keep cuttings suspended at the same time it tells something about the amount of pressure needed to break the gel structure.

When the circulation of the drilling fluid is resumed after a period of quiescence, the pump pressure has to be increased above the regular circulation pressure to break the gel structure that has formed during still stand. This will lead to a pulse of increased pressure called a

pressure peak. Pressure peak is a phenomenon that is important to predict accurately, since an increase in pump pressure results in an increase in wellbore pressure that in worst case can cause fracturing of the formation. This is particularly important in deep-water wells and in wells with a narrow pressure window (Saasen, 2002). If the pressure peak exceeds the formation pressure, the formation will fracture and the drilling fluid will be lost to the formation. This leads to a decrease in hydrostatic column, and the pore pressure might exceed the wellbore pressure causing kicks or uncontrolled blow outs.

## 2.5.2 BARITE SAG

Barite sag is the settling of particles out of suspension. This phenomenon came to the industry's attention in the 1980s, and is still a problem today. Barite sag occurs when the drilling fluid is unable to keep the weighting particles suspended, both during circulation of the well and during quiescence. The result is settling of particles at the wellbore wall, which can lead to incidents such as fluid loss, stuck pipe, casing or liner running problems. The gel properties of the drilling fluid reduce the static sag effects. Static sag is partially related to dynamic sag (Saasen, 2002). Sagging that occurs during circulation is dynamic sag, and sagging that occurs when the pumps are shut off is static sag. Better knowledge of low shear rheology and gel formation and breakage is therefore important when trying to reduce the incidents of barite sag.

Particles that are kept suspended in the drilling fluid are influenced by two forces; gravity and buoyancy. When gel is formed, the gravity force has to overcome the gel strength in order for sag to occur. The force that has to be overcome in order for sagging to occur is

$$F = \tau_g * A_p \quad [17]$$

In Eq. 17  $\tau_g$  is the gel strength and  $A_p$  is the surface area of the particle. When buoyancy and gravity are the two forces that act on the particle, the gel strength needed to keep the particles suspended is equal to

$$\tau_g = \frac{\Delta\rho}{6} gD \quad [18]$$

The maximum size for self-suspension is one micron. In order to reduce the amount of sag in emulsions, the viscosity of the continuous phase must be increased. If the viscosity within the continuous phase is increased, then both dynamic and static sag will be reduced (Saasen, 2002).

The parameters that influence barite sag are many. Wellbore angle influence the settling rate, and barite sag occurs more often in inclined wells. This is called the Boycott effect, and was discovered in 1920 by A.E. Boycott. In non-Newtonian fluids the shape and particle distribution has a significant impact on settling rate. Viscosity has an impact on the dynamic sag and a certain viscosity is required in order for the drilling fluid to be able to carry the weighting particles. However, a continuous increase in viscosity does not necessary lead to less dynamic sag. An increase in viscosity will also lead to increased ECD effects that are unwanted. Experiments performed show that the preparation of oil based drilling fluid also influence on settling rate (Omland, 2009). A study performed in 2009 demonstrated how pipe rotation during quiescence could reduce barite sag (Nguyen et al., 2011). Placement of the pipe also had an impact on the reduction of sag. When the pipe was placed eccentric in the borehole the reduction of sag was larger.

Both dynamic and static barite sag are influenced by low shear viscosity and gel formation. This supports the argumentation for why more accurate knowledge of viscoelastic properties is important in achieving a more successful drilling process.



### 3 GEL EVOLUTION

Determination of yield stress for a fluid has been a subject of discussion for more than 20 years. There have been proposed several different ways to measure this property. In 2002, Coussot et al concluded that even though there have been developed more methods than for any other parameter, there still is not a standard procedure for determining yield stress (Coussot et al., 2002). Finding the yield stress value by extrapolation of the flow curve obtained from measurements is the dynamic method for determining yield stress. The points are extrapolated from a low shear rate value to zero shear rate. This method has been found to be inaccurate, and with great variations. Numerous papers have recently been written about low shear viscosity and determination of true yield stress value, attempting to try to increase the knowledge of this subject. Different models for how to determine static yield stress have been proposed, and some of them will be discussed in the following section.

Barnes and Walters claimed that true yield stress does not exist (Barnes & Walters, 1987). Experiments showed that the Bingham plastic model and the Hershel Bulkley model was inadequate in describing how drilling fluids behave under low shear rates. Barnes and Walters concluded that there is a need for a model that accurately described the behaviour of drilling fluids under low shear rates in order to predict the behaviour of the drilling fluid during quiescence. In 1987, Speers et al examined the shear stress overshoot behaviour of drilling fluids, on fourteen different samples using two different rheometers (Speers et al., 1987). The objective was to measure and model the change in gel strength over time, and to determine the effect of temperature on gel strength. The measurements were performed based on requests from several oil companies. Gel strength measurements results using Fann 35 A viscometer and Weissenberg Rheogonimeter was compared. The measurements were performed according to the API procedure. Speers et al found that drilling fluid shear history and chemical composition influenced gel strength values (Speers et al., 1987). The paper concluded that there was little information about gel formation in drilling fluids. There had only been written one paper upon the effect of gelation time on low shear behaviour of bentonite dispersions previous to this paper. The result from the measurements was that the API gel strength increase could be predicted by first order kinetic theory. The increase in temperature led to reduction in initial and equilibrium gel strength. The gelation rate coefficient increased with increasing temperature.

Fifteen years after the work of Speers, Coussot et al did a complete set of rheometrical tests on a bentonite suspension (Coussot et al., 2002).

Experiments such as inclined plane test showed that drilling fluids stopped flowing abruptly below a critical stress, and started flowing at a high velocity above a critical stress. The conclusion was that no steady state flow could be obtained at shear rates below a critical value. Coussot et al found that the viscosity is at all time the result of the competition between aging and shear rejuvenation, and that aging occurs due to the thixotropic property of the drilling fluid (Coussot et al., 2002). When at rest, the drilling fluid will rebuild structure and gel. The value of gel strength depended on the time the drilling fluid had been at rest. During shear, a reversible change of the fluid microstructure occurred, and the viscosity decreased. The yielding character and the thixotropic character of the fluid were found to be closely related. Coussot et al discovered that under low stresses the fluid would abruptly stop flowing and become solidified. This was not the result of the equilibrium state where the rates of structural breakdown and structural recovery were equal, but it was caused by viscosity bifurcation. Viscosity bifurcation is the abrupt transition towards complete stoppage or rapid shear. For a critical value of stress the viscosity will increase continuously and eventually stop flowing (Cruz et al., 2002). Under low stress the fluid will show an anti-thixotropic behaviour and not a stable flow. This behaviour is shown in Fig. 16, and compared to ideal yield stress behaviour.

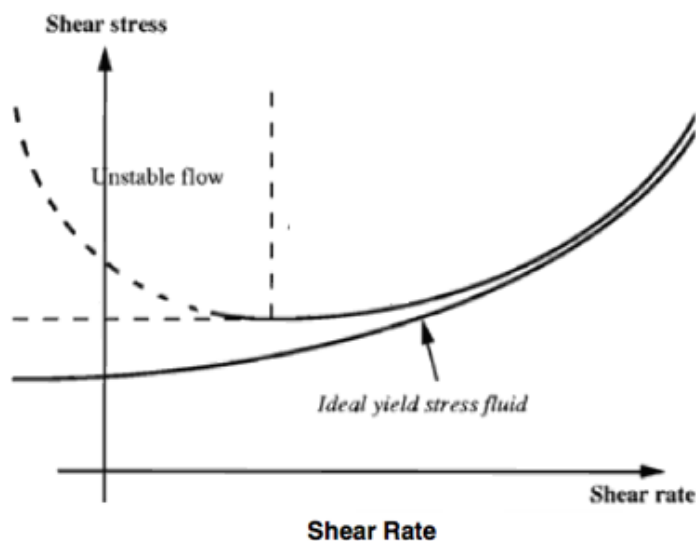


Figure 16: Typical flow curve of a thixotropic yielding fluid predicted by the model of Coussot et al compared to the usual presentation of the flow curve for an ideal yield stress fluid (Coussot et al., 2002).

The existence of a viscosity bifurcation effect in a drilling fluid has been shown using magnetic resonance imaging (MRI) (Ragouilliaux et al., 2006). The test was performed with a water in oil emulsion in a suspension of solid particles with a range of different additives. The droplet size was evenly distributed and with an average diameter of 1

micrometer. Experiments showed that below a critical stress the fluids stopped flowing. The study also showed that the material developed transient shear localization along the outer cylinder. This might have been caused by the formation of solid network of droplets linked by clay particles. The experiments showed that the simple thixotropic model was capable of predicting the steady state properties of the fluid used in the experiment.

Herzhaft et al presented a thixotropic model they claimed could completely describe all the features of the rheological behaviour of drilling fluids (Hertzhaft et al., 2006). The parameters needed in the model could be found using a Fann 35 rheometer. Herzhaft et al showed that drilling fluid viscosity was the result of the competition between aging and shear rejuvenation (Hertzhaft et al., 2006). Shear thinning properties could be characterized by using a Couette viscometer, however the yield stress value was more difficult to quantify. Different measuring procedures gave different results. Models that existed such as the Herschel Bulkley model failed to describe the low shear rheology because the model did not take the thixotropic effect into consideration. The models did not take the shear history of the fluid into consideration, but tried to describe the characteristics of the fluid in steady state. It was desirable to design a model that described both the shear thinning properties and the low shear viscosity. The model Hertzhaft et al presented is shown in Eq. 19:

$$\frac{\sigma}{\gamma} = \mu_0(1 + \lambda^n) \quad [19]$$

The state of structure “ $\lambda$ ” was a single variable that is a function of flow history. It was related to the number of links between the particles in a flocculating system or to the average depth of the potential wells of particles in non-flocculating suspension. “ $\lambda$ ” accounted for the flow history. The apparent viscosity is calculated by  $\mu = \frac{\sigma}{\gamma}$ , where and  $\mu_0$  and  $n$  were fluid parameters. From Equation [19] it was evident that the viscosity increased with increasing structural parameter. This was logical when  $\lambda$  represented the number of links between the particles. The next step was to derive the time dependence of  $\lambda$ , demonstrated in Eq. 20:

$$\frac{d\lambda}{dt} = \frac{1}{\phi} - \alpha\lambda\gamma \quad [20]$$

The intrinsic characterisation of the material that represented the aging properties was represented by  $\frac{1}{\phi}$  which described the rate of

restructuring. The shear rejuvenation constantly competes with the aging. The second term represented the rate of destruction due to flow. Current work seeks to propose a more detailed description of the aging mechanism for oil based drilling fluids, as function of constituents of the fluid. The model also predicted unusual behaviour like shear localization under low for low shear rate. The shear localization is illustrated in Fig. 17.

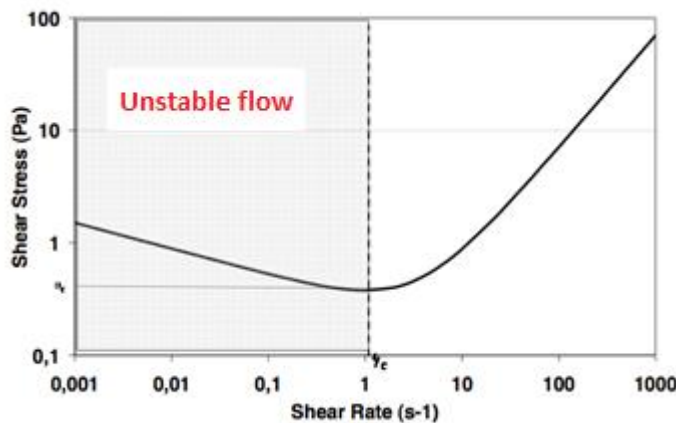


**Figure 17: Shear localization for fluid showing unstable flow for low shear rates (Hertzhaft et al., 2006).**

The effort to find new and better ways to determine yield stress continued when Masalova et al carried out experiments trying to determine the yield stress of emulsions (Masalova et al., 2008). Both oscillations and steady shearing of the samples were used to determine the yield stress. Amplitude sweep tests were performed at three different frequencies and plotted. The dynamic yield stress was determined as the stress where deviation from the linearity occurred. The dynamic yield stress found from the amplitude sweep test was found to be frequency dependant. The experiment also showed that there was no correlation between the dynamic yield stress found by performing amplitude sweep test, and the yield stress found from the flow curves. The same year, Maxey et al also concluded that the Bingham model was not accurate in predicting the yield stress of a fluid (Maxey et al., 2008). Maxey et al questioned the relevance of the measured yield stress values to drilling fluid performance in the field. The paper concluded that different measuring techniques resulted in different measured values, and that there was a need for further rheological characterization for strain rates below  $0,1s^{-1}$ . Jachnik discussed low shear rheology of drilling fluids (Jachnik, 2003). By performing experiments on several drilling fluids, the paper concluded that curve fits of conventional viscometer data often over or underestimated the upcurve apparent yield stress. Underestimates appeared to be associated with drilling fluids that have a high

concentration of fine drill solids. The paper concluded that far too much emphasis has been placed on the Bingham yield point, and that the viscosity in parts of the annulus was much greater than the models predicted due to the existence of a central plug where shear rates are less than  $0.01s^{-1}$ .

In 2010 Yap et al presented the structural recovery behaviour of barite-loaded bentonite drilling fluids (Yap et al., 2011). Yap et al found that the Nguyen-Boger model shown in Eq. 21 and the Leong model shown in Eq. 22 were accurate in predicting the structural recovery behaviour of these suspensions (Yap et al., 2011). The yield stress parameter measured the strength of the flocculated network structure and indirectly the strength of the interparticle force. The time dependent behaviour of the drilling fluid was reflected by the strength of the network structure changes with time of agitation and rest. In an agitating slurry yield stress would decrease with time and in undisturbed slurry the yield stress would increase with time. The Nguyen-Boger model for structural recovery is based on yield stress and not storage modulus. The Leong model was presented as:

$$\tau_y(t) = \tau_\infty \left( 1 - \frac{1 - \left( \frac{\tau_{y0}}{\tau_{y\infty}} \right)^{\frac{3}{2}}}{1 + K_r t} \right)^{\frac{3}{2}} \quad [21]$$

Whereas the Nguyen-Boger model was presented as:

$$\tau_y(t) = \tau_\infty - (\tau_\infty - \tau_{y0})e^{-Kt} \quad [22]$$

where

$\tau_{y0}$  = Yield stress at complete structural breakdown

$\tau_{y\infty}$  = Yield stress at complete structural recovery

In the tests performed on the barite loaded bentonite suspension performed by Yap et al the yield stress was measured directly using the vane technique. The yield stress was measured as a function of time. The tests were performed on three different slurries with different barite-bentonite concentration. Yap et al found that all three samples showed the largest decrease in yield stress during the first period of agitated aging time. All three samples also had significant increase in yield stress during the first period of aging. Yap et al found that the Long model and the Nguyen-Boger model provided good description for structural recovery behaviour, especially for short recovery times. For longer recovery time the models underestimated the yield stress. Fig. 18 shows the match between measured values

and the Nguyen-Boger model. Fig. 19 shows the match between measured values and the Leong model.

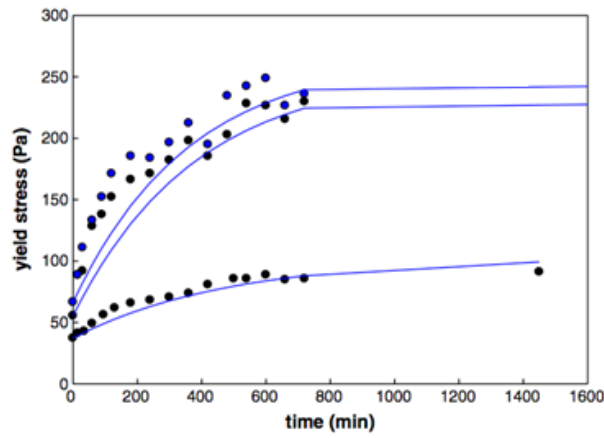


Figure 18: Plot showing the structural recovery for three different barite loaded slurries according to the Nguyen-Boger model (Yap et al., 2011).

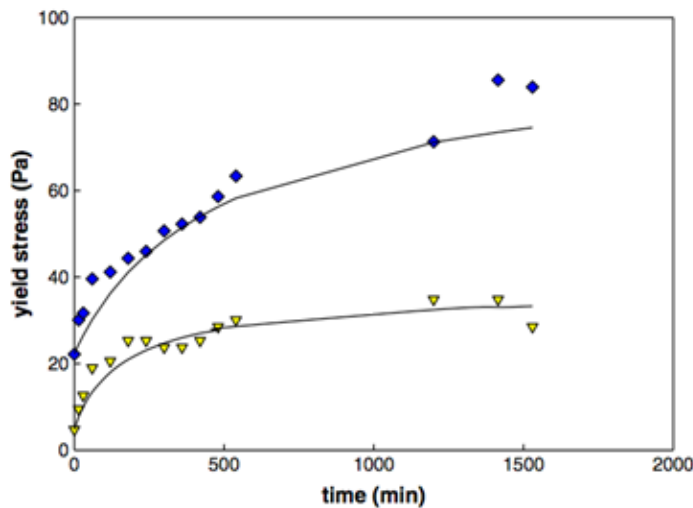


Figure 19: Plot showing the structural recovery for three different barite loaded slurries according to the Leong model (Yap et al., 2011).

Another rheological model that had been used to describe shear thinning fluids was the Quemada model (Hodne et al., 2007). The Quemada model tried to take into account the inter-particle forces in concentrated suspensions. The Quemada model is presented as:

$$\eta = \eta_{\infty} \left[ \frac{1 + \Gamma^P}{\chi + \Gamma^P} \right]^2 \quad [23]$$

The structural units that form due to interparticle forces lead to an increase in viscosity for low shear rates. The Quemada model

predicted this behaviour, and experiments performed on shear thinning cement showed that the model gives a good fit.

In 2011, Balhoff et al presented a model they claimed could be used for determining rheological properties of non-Newtonian fluids by measurements performed using a Marsh funnel (Balhoff et al., 2011). The results obtained for viscosity and shear-thinning index using a Mars funnel very much resembled the results obtained using a Fann 35 viscometer. The paper also presented a static method for determining yield stress. The measurements were performed on water based drilling fluids. The Marsh funnel used in the experiments is a device that measures the time it takes for a fluid to fill a set volume. The tests were performed on different fluids, first using the Fann 35 rheometer, and then the Marsh funnel. The equation for the static yield stress is found to be:

$$\tau_o = \tau_w = \frac{\rho g(h_{ss}+L)}{\frac{2L}{R} + \frac{2H_f}{R_f}} \quad [24]$$

The formula was built on the assumption that entrance effects were eliminated and that the elastic effects were negligible. The assumption to neglect elastic effects might have been questionable; when water based drilling fluids and some new oil based drilling fluids have been known to exhibit elastic behaviour. The entrance effect was dependent on the ratio between the capillary length and diameter. The L/D ratio of the tube used in the experiments was 10. Han and Charles discussed the problems that occurred under low shear rates when neglecting entrance effects (Han & Charles, 1971). When draining a fluid through a funnel, the flow became mixed because of the convergence of the flow close to the die. The convergence result was shear flow at the walls and strong extensional flows in the centre. When neglecting entrance effects, the effect of extensional flow was also neglected. The shear velocity varied from zero in the middle, to a max near the walls. The measurement would include particles with varying orientation. Measurements performed under low shear rates might have been inaccurate because of slip at the walls (Mørk, 1997).

The rate at which the funnel was being drained is equal to  $U=Q/A$ . The extension rate in the funnel would be  $dU/dx$ . This leads to the following expression for extension rate in the funnel:

$$\dot{\epsilon} = \frac{Q}{L} * \frac{A_{top\ of\ funnel} - A_{bottom\ of\ funnel}}{A_{bottom\ of\ funnel} * A_{top\ of\ funnel}} \quad [25]$$

The extension rate for this experiment is equal to  $\approx 0.1$  m/s. The extensional viscosity is a function of extensional rate, in the same way as the shear viscosity is a function of shear rate. The extensional flow that occurred when the fluid was drained through the funnel indicates that the viscosity measured was the extensional viscosity. This indicates that assuming that there was no viscous resistance to flow in the funnel might have been incorrect.

It is evident when reviewing papers written upon rheology of drilling fluids that increased attention has been brought the rheology of drilling fluids in recent years. Drilling fluids could experience a wide range of variables, such as temperature and pressure. Different papers have been published studying the effect of such variables on the properties of drilling fluids. In 2010, Maxey presented how to differentiate drilling fluids by gel structure (Maxey, 2010). Simple viscometry should not be used to differentiate between drilling fluids that have great rheological difference. Maxey listed the parameters that have the largest influence on the start-up circulation pressure, and temperature was number one. Large amplitude oscillatory shear tests were performed on different samples of drilling fluids using an Anton Paar rheometer. The results found was that the amount of low gravity solids in the drilling fluids affected the nature of the gel that is formed. When the amount exceeded a threshold concentration, the difference between the stress required to initiate flow and the stress required to maintain flow was always large. Maxey also found that the amount of organophilic clay had a great effect on the disassociation of microstructure. In drilling fluids where organophilic clay was not present, the microstructure would break more abruptly, and it would require less stress. This was found to be independent of the yield stress of the different fluids (Maxey, 2010).

Herzhaft et al published an article discussing the influence of temperature and clays microstructure on the rheology of oil based drilling fluids (Herzhaft, 2003). In deep water environments the temperature could go down to 0 °C and having thorough knowledge of the effect that temperature have on the gel evolution of the drilling fluids is important. A narrow pressure margin does not allow for much increase in pump pressure. Herzhaft et al found that temperature had an effect on the flow regimes of the fluids. An increase in temperature led to an increase in the critical shear that delimited the low shear quasi-Newtonian regime and the high shear-thinning regime. Oscillatory tests showed that a solid like structure develops at rest, and that the elastic portion of the samples was more affected by temperature and shear history than the viscous portion. Herzhaft et al found that the organophilic clays in interaction with the emulsion droplets create a solid like structure when the fluid is at rest



(Herzhaft, 2003). Tehrani further investigated the behaviour of suspensions and emulsions in drilling fluids (Tehrani, 2007). Tehrani mentioned high shear viscosity, yield stress and the gelling properties as the rheological parameters of significance. The paper concluded that more work needed to be performed on the complex subject of low shear rheology.

Experimental investigations recently performed on a series of oil based drilling fluids have concluded that oil based drilling exhibit time-dependent viscoelastic behaviour (Bui et al., 2012). Viscoelasticity was influenced by temperature and gelling time. Periodic oscillatory tests in linear viscoelastic range showed that it sometimes took more than 30 minutes for the sample to reach stable structure. The drilling fluid samples were found to thermorheologically complex, and that the time-temperature superposition principle was not applicable. The influence of temperature on gel evolution will be illustrated in the following chapter.



## 4 CASE: THE IMPACT OF GEL EVOLUTION

A recently drilled well on the Norwegian Continental Shelf experienced how important gel effects can be when drilling a well. The drilling fluid used was a linear paraffin based drilling fluid. At the temperature of 4 °C, it was evident that gelling occurred in the drilling fluid, although these effects were not expected with the drilling fluid that was used. When drilling the 8 $\frac{1}{2}$ " section, a zone with an abnormally high pore pressure was encountered. To avoid influx from the formation, the drilling fluid density was increased stepwise. During this process, something happened that completely changed the properties of the drilling fluid. Great losses to the formation occurred. The drilling fluid that was lost to the formation was tested. Gel strength of the drilling fluid measured with other samples of the drilling is shown in the Fig. 20. The curves that are named Well x and Well y are taken from two other wells that drilled with the same drilling fluid. The curve called Problem well is the sample taken from the well when the losses occurred.

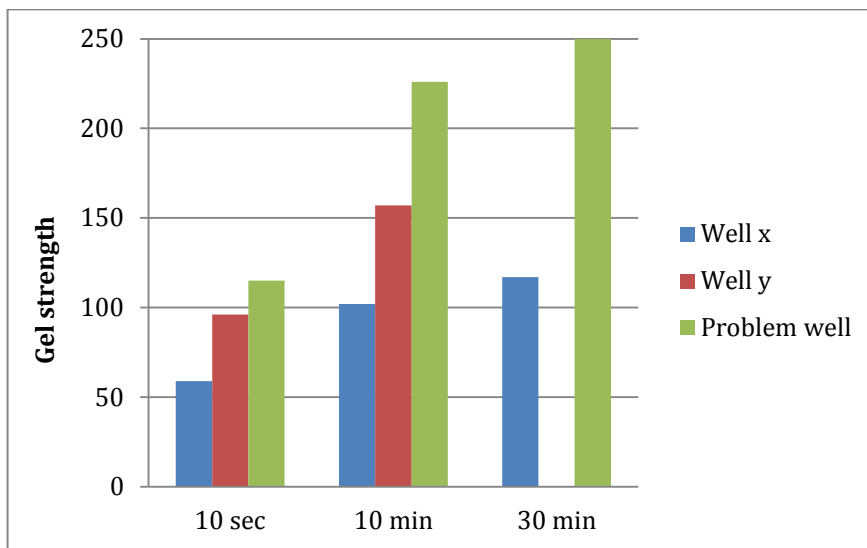


Figure 20: Figure showing a comparison of the gel strength evolution of the same type of drilling fluid used on three different wells (Det norske oljeselskap ASA, 2012).

From the plot it is evident that sample taken from the problem well was extremely progressive. A theory of what might have caused this change in gel strength is that the light components of the base oil of the fluid had evaporated, leaving only heavy components left causing the gel to become progressive at low temperatures.

To evaluate other reasons for what might have caused this change in the drilling fluids gel properties, the daily mud reports was investigated. Fig. 21 is a plot of the 10 second and 10 minute gel strength together with the oil water (O/W) ratio. When evaluating the plot, it is possible to identify peaks in the gel strength. Around the 50<sup>th</sup>

measurement the gel strength increase, as the oil water ratio decrease. An increase in the internal water phase can lead to an increase in viscosity and this might cause the increase in gel strength (Herzhaft, 2003). Around the 100<sup>th</sup> measurement another peak in gel strength occurs. When looking at the point where the gel strength peaked, an increase in the oil water ratio is also observed. This was at a time when the pore pressure increased, and the drilling fluid was weighed up. Here, the oil water ratio increases. At this point, a maximum gas peak of 37.3 % occurred. The increase in O/W ratio might be caused by solved gas in the drilling fluid. When the drilling fluid is circulated out of the well, most of the gas will dissolve out of the drilling fluid and the oil water ratio will again decrease. This might cause this increased gel strength.

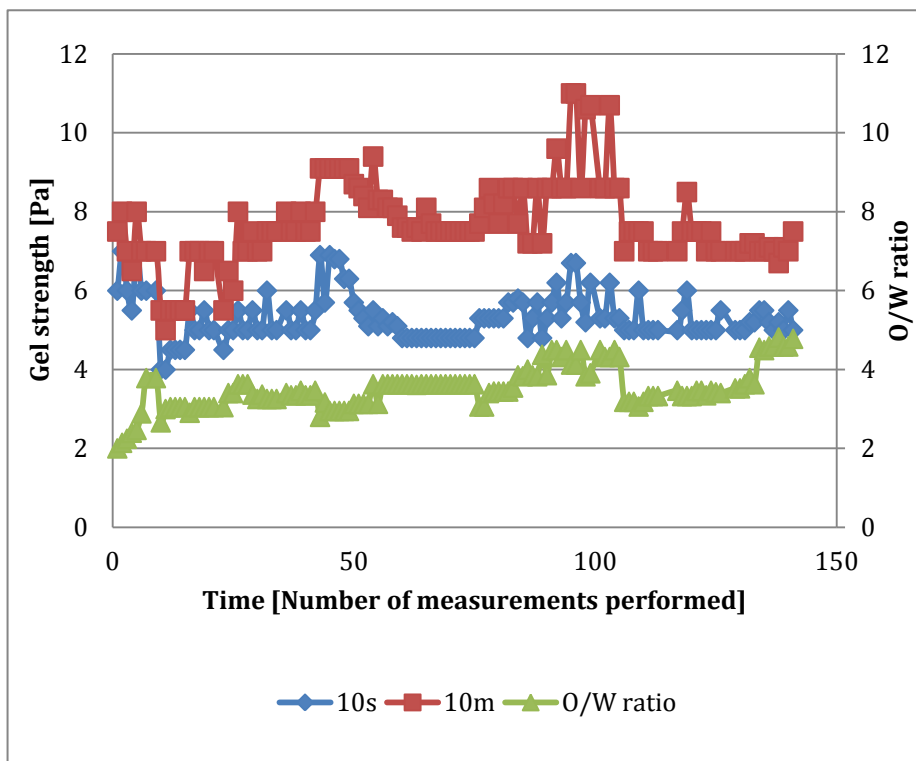


Figure 21: Plot showing the correlation between gel strength and O/W ratio at 4°C (Det norske oljeselskap ASA, 2012).

The consequences of this incident could have been severe, and great efforts were made to understand what happened to the quality of the drilling fluid. The incident led to a delay in the drilling operation. Luckily, the consequences were not more severe.

## 5 EXPERIMENTAL STUDIES

As previously mentioned drilling fluid operations are an essential part of any drilling operation, and continuing to improve the knowledge and understanding of the behaviour of drilling fluids can lead to an improved drilling operation. Better hole stability and increased rate of penetration are two factors related to drilling fluid performance that can lead to great cost savings and reduced risks during drilling operations. Studies show that the use of oil based drilling fluids in the field leads to 5- 30 % better hole cleaning than drilling with water based drilling fluids (Det norske oljeselskap ASA, 2012). However, when performing studies on water based and oil based drilling fluids in the laboratory, it is difficult to understand and explain why this difference occurs. Continuing to perform experiments on oil based and water based drilling fluids might help understand these differences and possibly lead to better design of both water based and oil based drilling fluids.

To further examine the gel evolution in oil based drilling fluids a series of experiments have been conducted on four different types of drilling fluids. The experiments performed focus on studying properties and behaviour of the drilling fluids that could help increase the understanding of gel evolution. The experimental investigations have been divided into three chapters. The first section will describe preliminary investigations such as mixing and preparing the drilling fluids. The second section will describe the main experimental investigations performed with the Anton Paar rheometer. The final section will contain tests of a special water based drilling fluid.

## 5.1 INVESTIGATIONS IN ACCORDANCE WITH API

The preliminary investigations involved preparing the three different drilling fluid samples, using a Fann viscometer. The preliminary experiments were performed to examine the basic properties such as viscosity and gel strength of the drilling fluids. Flow curves for the three different drilling fluids were found. Static yield strength was determined through performing API 10 second and 10 minute gel strength tests. The different drilling fluids were as follows:

Bentonite drilling fluid  
KCl/polymer drilling fluid  
Oil based drilling fluid

The contents of each of the different mixes and the mixing procedures can be found in attachments A1 – A3.

### 5.1.1 EXPERIMENTAL SET UP - PREPARING SAMPLES

All three mixes were prepared using a Waring commercial blender which is illustrated in Fig. 22. The drilling fluids were mixed on the low speed function. This equalled to an RPM of 19 000. The blade of the Waring commercial blender is also shown in Fig. 22. The geometry of the blade and the rotational speed regulates the amount of shear the fluid experiences during mixing, and can therefore to some degree influence on the properties of the drilling fluid.



**Figure 22: Waring commercial blender (left) and Waring commercial blade (Kitchens, 2012).**

Due to the high rotational speed the temperature increased significantly during mixing. The maximum recommended temperature for the oil based drilling fluid was 62 °C. In order to keep the mix from exceeding this temperature it was necessary to cool the fluid during mixing. This was done by placing the blender container in a cold water bath. The temperature was kept around 50 °C throughout the mixing period.

### 5.1.2 EXPERIMENTAL SET UP - FANN VISCOMETER

Before tested with the Fann viscometer the temperature and density of the mixes were measured. The flow curve was measured by starting to shear the drilling fluid with the maximum shear of 600 RPM. The shear was then stepwise decreased through six different speeds, before increased again. After this the mixes were sheared for two minutes on 600 RPM. The mixes then rested for ten seconds and the 10 second gel strength was measured with a shear rate of 3 RPM. The same was done for the 10 minute gel strength. Readings were also taken after 10 seconds and 30 seconds of shearing at 3 RPM after the peak shear stress was measured. This was done to investigate how the gel structure was broken down the first 30 seconds of shearing after the rest period where gel strength was build up.

## 5.2 RESULTS OF INVESTIGATIONS IN ACCORDANCE WITH API

The following subchapters contains the results of the experiments performed using the Fann viscometer. A discussion of the results follows the graphical representations of the results.

### 5.2.1 FLOW CURVES - FANN VISCOMETER

The flow curves showed that the viscosity curves of the three samples were different. The viscosity curve of the bentonite drilling fluid ended up shifted downwards compared to the other two. The original goal was to design three drilling fluids with similar viscosity curves to make it easier to compare the three. After several efforts to try to design similar viscosity curves, the result in Fig. 23 was the best outcome.

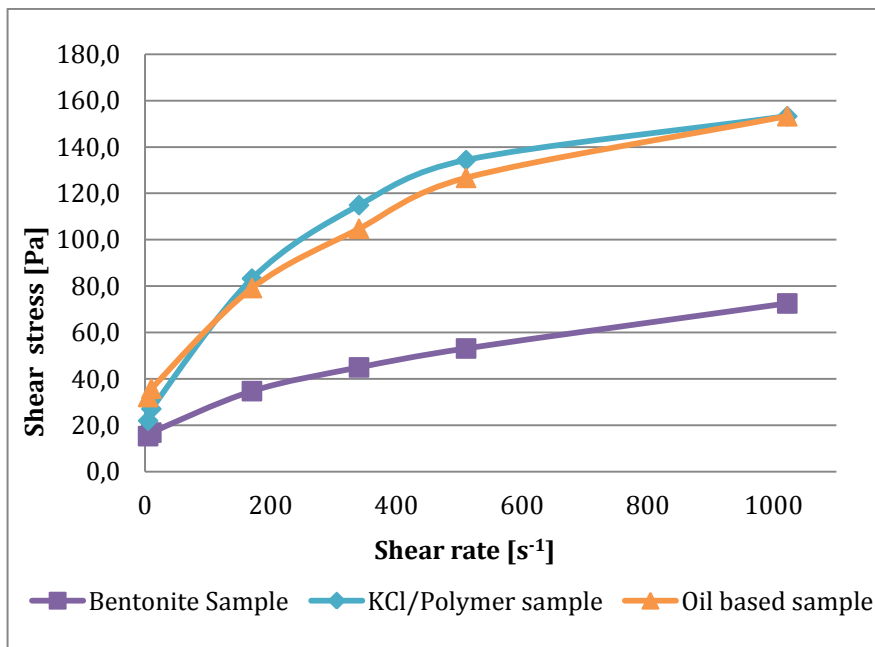


Figure 23: Flow curves for all three samples measured with Fann viscometer at T=20°C.

For the oil based sample, the Herschel Bulkley model was the best fit because the sample had a yield point and the shear stress increased exponentially with increasing shear rate. The Herschel Bulkley model also was the best fit for the KCl/polymer sample. The oil based drilling fluid had a higher yield point than the KCl/polymer sample, but for maximum shear rate the fluids had approximately the same viscosity. The viscosity curve of the bentonite drilling fluid sample resembled the Bingham model with near constant plastic viscosity. All three samples displayed pseudoplastic behaviour, because the samples' resistance to flow decreased with increasing shear rate.



## 5.2.2 GEL STRENGTH - FANN VISCOMETER

The 10 minute (10') and 10 second (10'') gel strength were measured according to API standard and the results are shown in Fig. 24.

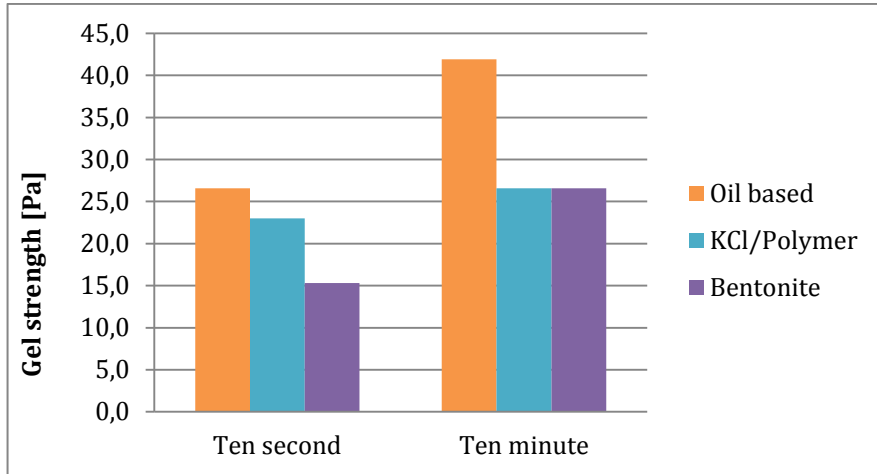


Figure 24: Ten second and ten minute gel strength measured on all three samples according to API at 20°C.

The oil based sample showed the largest increase in gel strength build up from the 10 second measurement to the 10 minute measurement. The bentonite sample also showed a significant increase from the 10'' to the 10' gel strength. The KCl/Polymer sample hardly showed any build up in gel strength compared to the other two samples. The development of how the gel structure broke down was studied by continuing to shear the samples at 3 RPM and perform readings 10 seconds and 30 seconds after peak. This is illustrated in Fig. 25.

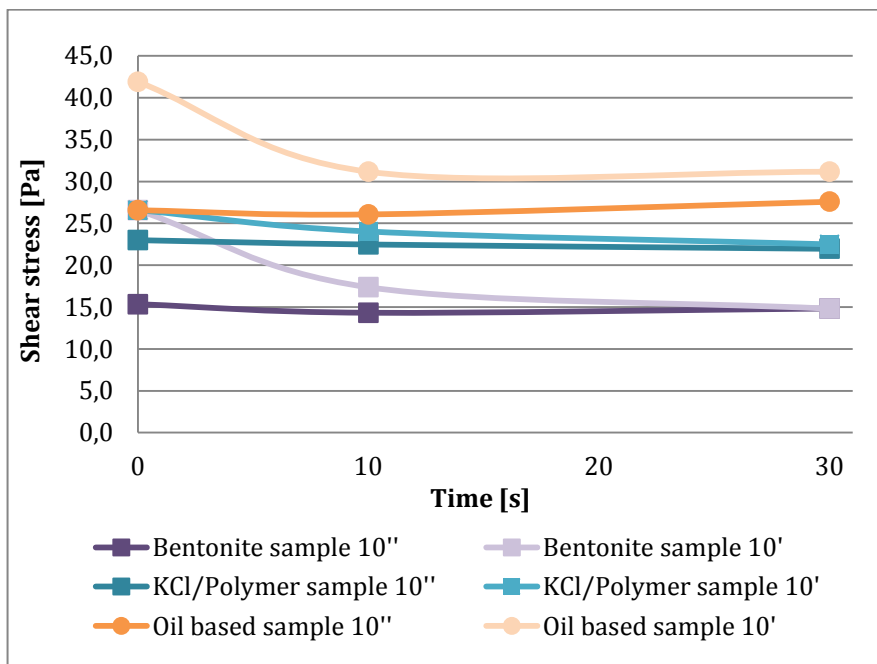


Figure 25: Structural breakdown development after 10 and 30 seconds of shearing at 3 RPM, for all three samples after 10 seconds and 10 minute rest at T=20°C.

For the oil based sample the gel was rapidly broken during the first 10 seconds of shearing. During the next 20 seconds the shear stress did not decrease further. The slight increase at the end of the shearing period could be indication of large particles or lumps of gel. The structure breakdown of the bentonite sample resembled that of the oil based sample, where the shear stress decreased most the first 10 seconds of shearing. For the bentonite sample the shear stress measured was the same after 30 seconds of shearing both after 10 minutes and 10 seconds of gel build up time. The little gel strength that was built up for the KCl/polymer sample was reduced the most in the first 10 seconds of shearing.

The gel strength measurements showed that the oil based drilling fluid has the highest 10' gel strength, and it was significantly higher than the 10' gel strength for the two other samples. The oil based sample and the bentonite sample had a resembling structure build up and breakdown, however the measured shear stress was higher for the oil based drilling fluid. The gel build up and breakdown for the KCl/polymer sample differed from the two other samples. The chemistry that created the gel strength was different for the three samples, and this might have been the reason for the differences that was found. For the bentonite drilling fluid there were electrostatic bindings that created the gel strength. For the KCl/polymer sample there were polymer chains that created the gel strength. For the oil based sample it was the structure of the water droplets that created the gel strength. The results showed that polymer chain structure was not as strong as the other two structures.

## 6 DYNAMIC EXPERIMENTAL INVESTIGATIONS

The main investigations were performed using an Anton Paar Physica rheometer. The tests performed were amplitude sweeps and frequency sweeps. The amplitude sweeps were performed at different frequencies. From the results of the amplitude sweeps the linear viscoelastic range was found. Frequency sweeps were then performed within the linear viscoelastic range. The tests were performed at two different temperatures to investigate the effect of temperature.

### 6.1 EXPERIMENTAL SET UP - ANTON PAAR RHEOMETER

The main experimental investigations were performed using an Anton Paar: Physica Smart Pave Plus rheometer which is depicted in Fig. 26. The rheometer is equipped with an electrically heated temperature chamber.

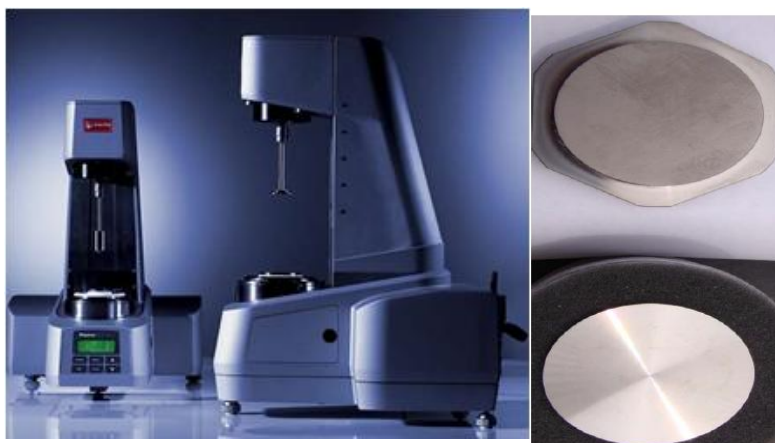


Figure 26: Anton Paar: Physica Smart Pave Plus rheometer (Anon., 2012) and the parallel plate geometry (Bui et al., 2012).

- The experiments were conducted using the smooth parallel geometry, with a 1 mm gap. The plates have a diameter of 25mm.
- The three mixes were prepared three days prior to testing. Before tested, the samples were mixed with the Waring blender for 3 minutes.
- The amplitude sweep tests were performed at a strain ramp from 0.01 to 1000 %. The tests were performed at a constant frequency of  $1 \text{ s}^{-1}$ ,  $10 \text{ s}^{-1}$  and  $100 \text{ s}^{-1}$ . The experiments were performed at a temperature of  $10 \text{ }^{\circ}\text{C}$  and  $20 \text{ }^{\circ}\text{C}$ .
- Frequency sweeps were performed with strains within the LVE range, and with a frequency ranging from  $0.1 \text{ s}^{-1}$  to  $100 \text{ s}^{-1}$ . The experiments were performed with temperatures of  $10 \text{ }^{\circ}\text{C}$  and  $20 \text{ }^{\circ}\text{C}$ .

## 6.2 RESULTS OF DYNAMICAL INVESTIGATIONS

The results of the main experimental investigations will be presented in the following chapter. To avoid too many confusing graphical presentations only the most important graphical representations have been included. Most of the results are presented in the appendices. The results are divided into different chapters for the different tests.

### 6.2.1 OSCILLATORY AMPLITUDE SWEEP TEST

Amplitude sweeps were performed on all three samples. The sweeps were performed with a strain ranging from 0.01-1000 % at frequencies of  $1 \text{ s}^{-1}$ ,  $10 \text{ s}^{-1}$  and  $100 \text{ s}^{-1}$ . These were performed at both a temperature of  $10 \text{ }^\circ\text{C}$  and  $20 \text{ }^\circ\text{C}$ . The amplitude sweep performed with a strain of 1 % is chosen to illustrate the result of the tests. The red arrows inserted in Fig. 27 point at the strain that limit the linear viscoelastic (LVE) range. This point is referred to as the yield point,  $\tau_y$ . The black arrows point at the strain where the loss and storage moduli cross. This point is referred to as the flow point,  $\tau_f$ . This thesis will define the point where the viscous and elastic moduli cross, pointed at by the black arrows, as the dynamic yield point

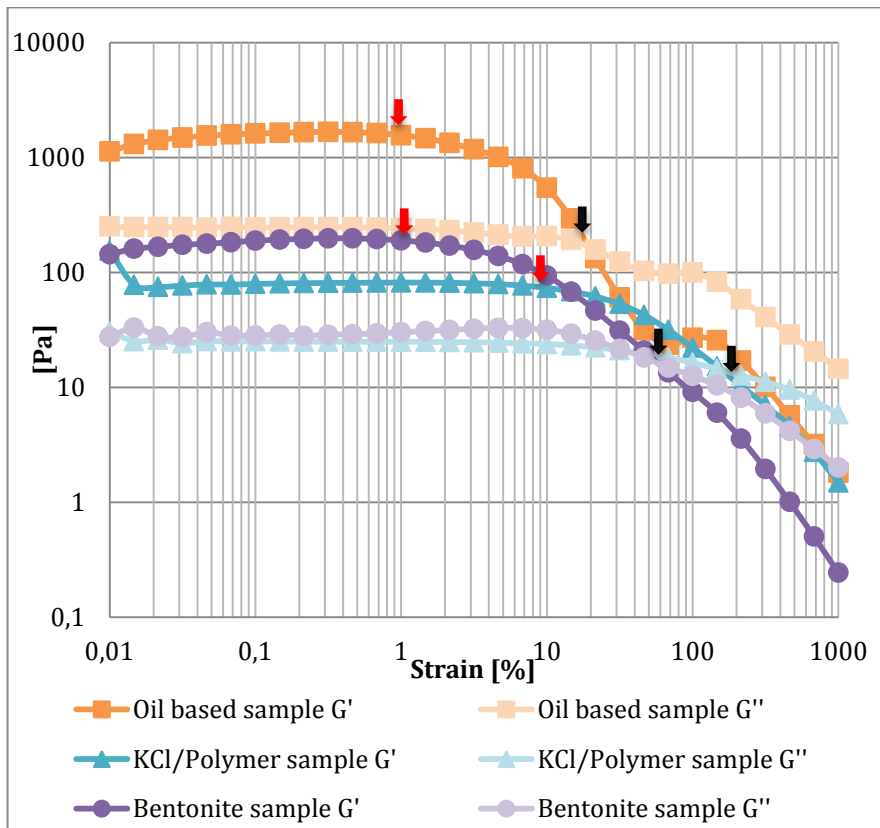


Figure 27: Plot showing amplitude sweep for all three samples at  $10^\circ\text{C}$  with a frequency of  $1 \text{ s}^{-1}$ . Storage modulus ( $G'$ ) and loss modulus ( $G''$ ) are plotted. Red arrows indicate the limit value of the LVE range. The black arrows point to the dynamic yield point.

The plot of the viscous and elastic modulus showed that there existed an LVE range, and that the limit of the LVE range was close to 1 % strain for the oil based sample and the bentonite sample. The value that limited the LVE range for the KCL/polymer sample was closer to 8 %. The relationship between strain amplitude and shear rate is described in Eq. 26:

$$\dot{\gamma} = \gamma_A * \omega \quad [26]$$

A strain of 1 % therefore equals to

$$\dot{\gamma} = \frac{1\%}{100\%} * 1s^{-1} = 0.01s^{-1}$$

The value where the LVE range ends is the value where the viscous modulus and elastic modulus are balanced. When exceeding this value the internal gel structure will break, and the viscous response will start to dominate. When this value is low, such as one percent this means that the transient viscoelastic response is short (Bui et al., 2012).

For all three samples the  $G'$  value was higher than the  $G''$  value and the samples therefore showed a gel like behaviour in the LVE range. This means that the elastic portion dominated the viscous portion within the LVE range. This indicates that in the low shear range the samples displayed a firmness or stability.

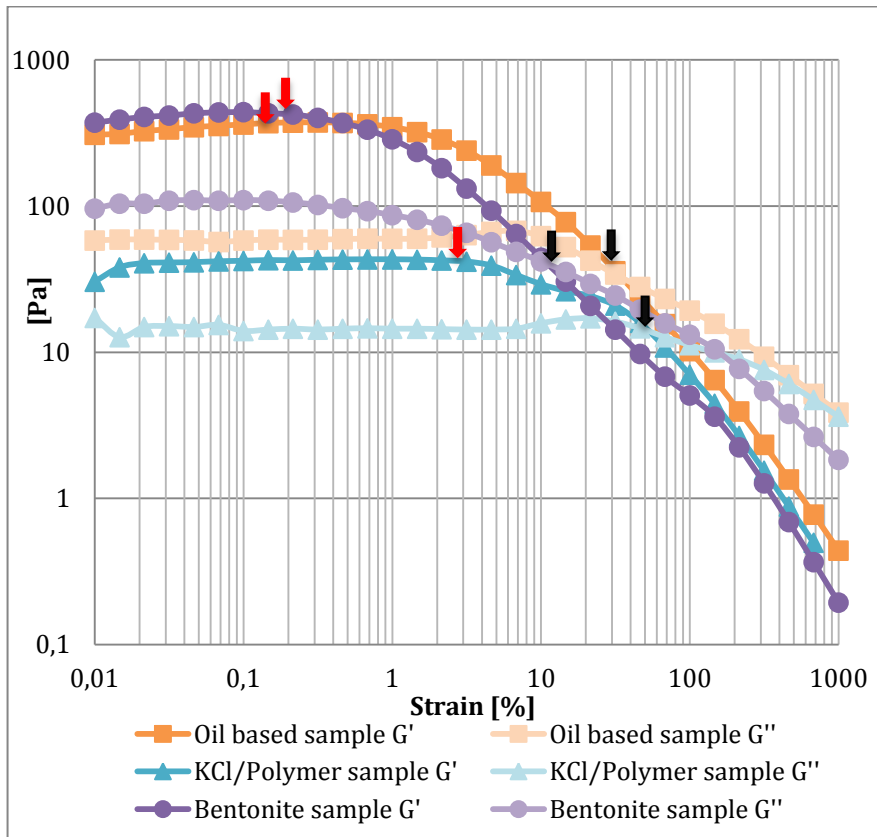


Figure 28: Plot showing amplitude sweep for all three samples at 20°C with a frequency of  $1s^{-1}$ . Storage modulus ( $G'$ ) and loss modulus ( $G''$ ) are plotted. Red arrows indicate the limit value of the LVE range. The black arrows point to the dynamic yield point.

## TEMPERATURE EFFECT

Fig. 27 and Fig. 28 illustrate amplitude sweeps performed at two 10°C and 20°C. When the amplitude sweeps performed at different temperatures were compared, the gel point was shifted. When the red and black arrows were evaluated, one could observe that the arrows mainly were shifted to the left and downwards when the temperature was increased to 20 °C. These changes were not large, and this might have been due to the slight increase in temperature of 10 °C. The value that limited the LVE range decreased for all samples. The increase in temperature affected the loss and storage modulus differently for the different samples. The value of the dynamic yield point for the different samples is illustrated in Fig. 29 and Table 2.

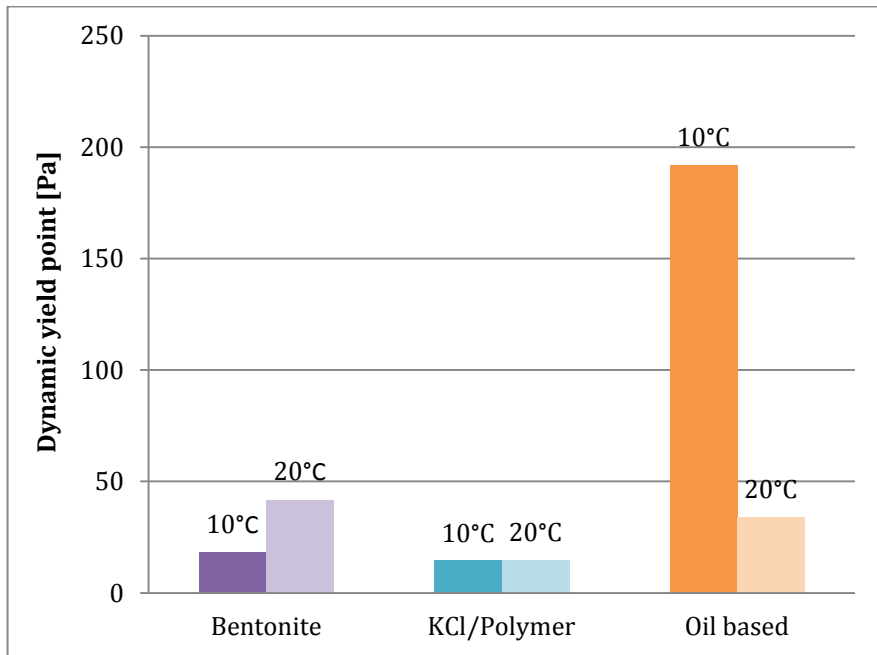


Figure 29: Change in dynamic yield point for all three samples for an increase in temperature from 10°C to 20°C, frequency of 1 s<sup>-1</sup>.

	T=10°C	T=20°C	Change
Bentonite sample [Pa]	18,2	41,9	23,7
KCl/Polymer sample [Pa]	14,5	14,6	0,1
Oil based sample [Pa]	192	34,1	-157,9

Table 2: Comparison of dynamic yield point found from amplitude sweeps performed at 10°C and 20°C, frequency of 1s<sup>-1</sup>.

The bentonite sample had a dynamic yield point of 18.2 Pa at 10 °C. The bentonite sample was the only sample that showed a significant increase in dynamic yield point for an increase in temperature. The dynamic yield point of the Bentonite sample at amplitude sweeps performed at a frequency of 10 s<sup>-1</sup> (Appendix C.1, Fig. 52, Fig. 53), more than doubled for an increase in temperature of 10°C. An increase in temperature leads to an increase in Brownian movements in the colloidal suspension, as described in subchapter 2.3.2. This could statistically lead the particles closer to each other, and might cause the face-to-edge electrostatic bond to increase.

The KCl/polymer sample showed close to zero change in dynamic yield point for the increase in temperature. When comparing this to the amplitude sweep performed at a frequency of 10 s<sup>-1</sup>, the sample showed a slight decrease in yield point for the increase in temperature. The KCl/polymer sample showed however very little sensitivity to temperature compared to the other two samples. Polymers are very different from colloidal suspensions and emulsions. The structure is not created by electrostatic bonds, and the particles

are much smaller with sizes around  $10^{-10}$  m. This might be the reason for the small effect of temperature increase seen on dynamic yield point for the KCl/Polymer sample.

The oil based sample showed a significant decrease in dynamic yield point for the increase in temperature. The dynamic yield point also decreased with over 100 Pa for the amplitude sweep performed at a frequency of  $10\text{ s}^{-1}$ . The size of the emulsion droplets is larger than the particles in the other two mixes, in the range of  $10^{-5}$  m. Brownian movements increase with an increase in temperature, but there is no difference in charge on the particles here such as for the bentonite sample. Brownian movements create a crystalline structure, however this might have been broken down by the strain the sample was exposed to causing a decrease in dynamic yield point.

The curves of the elastic and viscous modulus in Fig. 28 and Fig.29 were also influenced by temperature. For the bentonite sample, the value of  $G'$  and  $G''$  increased when the temperature increased. For the KCl/polymer sample, the value of  $G'$  and  $G''$  decreased when the temperature increased. For the oil based sample the values of  $G'$  and  $G''$  decreased with increasing temperature. The temperature difference of  $10\text{ }^{\circ}\text{C}$  might have been too small to draw any conclusions, but it was evident that the three samples did not show the same response to an increase in temperature. This corresponds to the findings regarding in change dynamic yield point.

Fig. 30 illustrates a time sweep performed on the oil based sample. The time test with constant shear of  $50\text{ s}^{-1}$  was performed to evaluate the effect of constant shear over time. When the oil based sample underwent constant deformation, the viscosity decreased. A decrease in temperature of  $10\text{ }^{\circ}\text{C}$  led to a significant increase in viscosity. This confirmed the observations made on the amplitude sweep tests with varying temperature performed on the oil based sample. The test also confirmed the thixotropy of the sample.



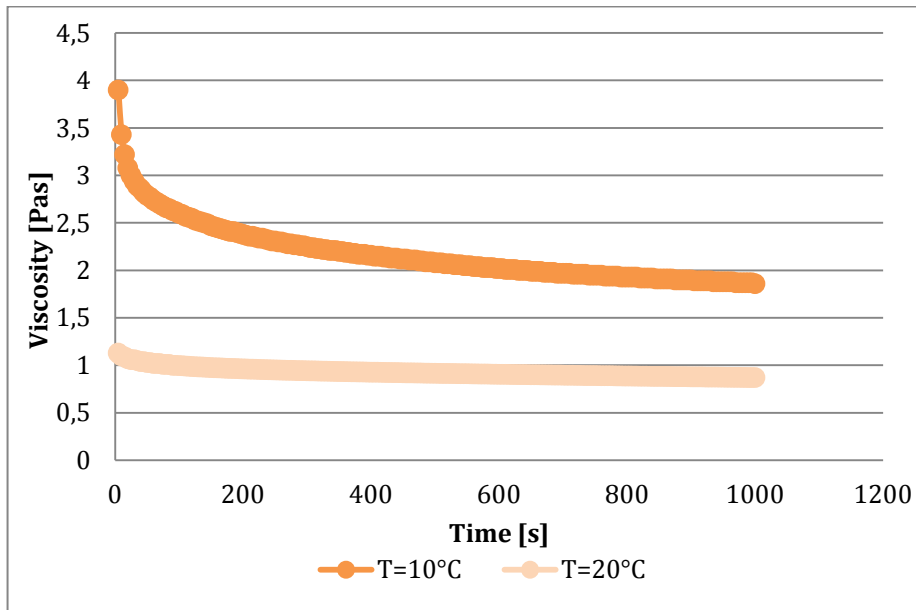


Figure 30: Time sweep with constant shear of  $50 \text{ s}^{-1}$  performed on the oil based sample with a temperature of  $10 \text{ }^\circ\text{C}$  and  $20 \text{ }^\circ\text{C}$ .

There were performed experiments at  $50 \text{ }^\circ\text{C}$  on the bentonite and KCl/polymer sample, and the result of an amplitude sweep is included in Appendix C.1 Fig. 56 to illustrate the poor results. The rest of the tests performed at  $50 \text{ }^\circ\text{C}$  are not included, because these tests were impossible to interpret and pointless to use, because the samples solidified during each sweep. The learning from these tests was that in order to produce good results at high temperatures, it was important to make sure that no evaporation occurred and to remember to check the sample after each test to make sure it was still liquid and that no solidification or vaporisation had occurred.

## FREQUENCY EFFECT

In addition to varying temperature of the amplitude sweeps, the frequency was varied. Fig. 31 shows the amplitude sweep performed at 10 °C with a frequency of 10 s<sup>-1</sup>. Fig. 32 shows the comparison between the dynamic yield point found by amplitude sweeps with a frequency of 1 s<sup>-1</sup> and 10 s<sup>-1</sup>.

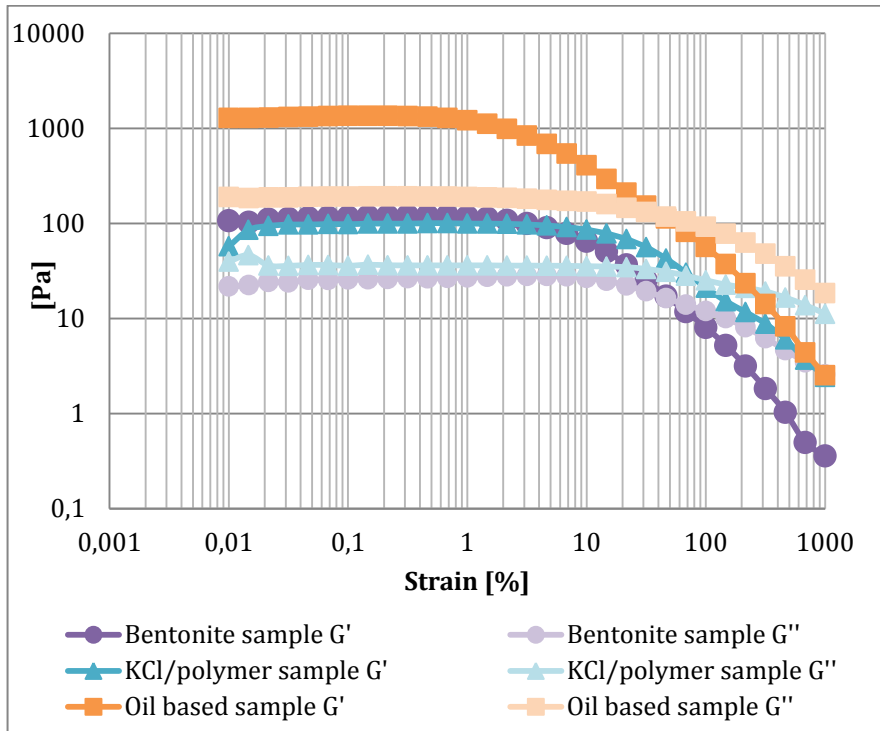


Figure 31: Plot showing amplitude sweep for all three samples at 10°C with a frequency of 10s<sup>-1</sup>.The storage modulus (G') and loss modulus (G'') is plotted.

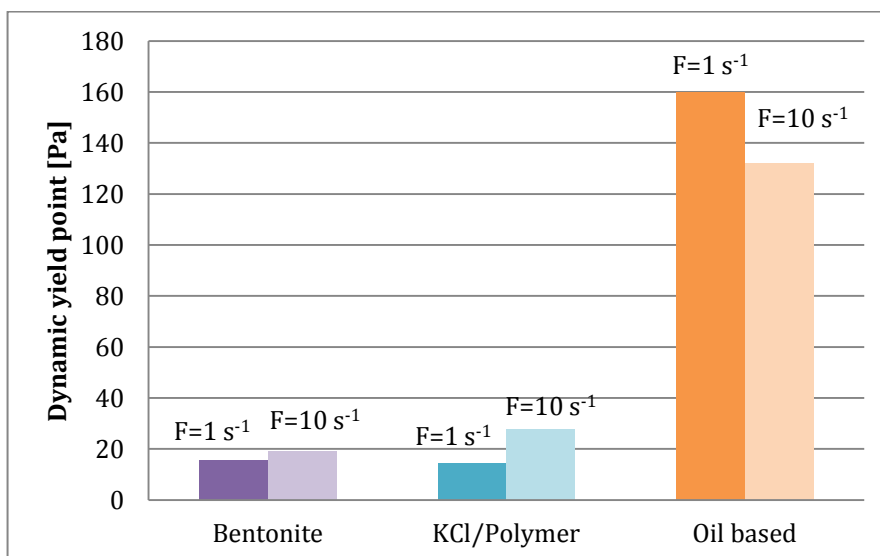


Figure 32: Comparison of dynamic yield point of amplitude sweep performed at 10 °C with a frequency of 1 s<sup>-1</sup> and 10 s<sup>-1</sup>.

Comparison of the results of the amplitude sweeps performed with the different frequencies showed that the point where the storage and loss modulus cross changed when the frequency was changed. This indicated that the cross point of  $G'$  and  $G''$  was frequency dependent. For the bentonite sample the dynamic yield point increased when the frequency was changed from  $1\text{ s}^{-1}$  to  $10\text{ s}^{-1}$ . The same trend was shown for both a temperature of  $10\text{ }^{\circ}\text{C}$  and  $20\text{ }^{\circ}\text{C}$ . For the KCl/Polymer sample the dynamic yield point increased significantly when the frequency was increased from  $1\text{ s}^{-1}$  to  $10\text{ s}^{-1}$ . The same trend was shown for both temperatures. For the oil based sample the dynamic yield point decreased when the frequency was increased from  $1\text{ s}^{-1}$  to  $10\text{ s}^{-1}$ . The same trend was shown for both temperatures. The decrease in dynamic yield point that occurred for the bentonite and oil based sample when the frequency was increased might have happened because the vibrations hindered the formation of a structure.

The amplitude sweeps performed at different frequencies suggests that frequency had an effect on dynamic yield point. When drilling a well, this means that to break the gel strength when resuming circulation, a slow increase in pump pressure would require a less increase of the pump pressure, if the drilling fluid displayed behaviour where the yield point decreased for an increase in frequency. The results were not conclusive regarding at which temperature the effect of frequency was largest or vice versa.

Amplitude sweeps with a frequency of  $100\text{ s}^{-1}$  were performed and the results are included in Appendix C.1. The curves were almost impossible to interpret, and this indicates that a frequency of  $100\text{ s}^{-1}$  was too high for the rheometer to give good results.

## 6.2.2 OSCILLATORY FREQUENCY SWEEP TEST

Frequency sweeps were performed on all three samples. The frequency sweeps were performed with a range of frequency from  $0.1 \text{ s}^{-1}$  to  $100 \text{ s}^{-1}$ , and with strains of 1 %, 5 %, and 10 %. All of these results are found in appendix C.2. The results of the experiments of a strain of 1 % is presented and discussed in Fig. 33, since this is within the LVE range. The frequency was ramped from  $100 \text{ s}^{-1}$  and down to  $0.1 \text{ s}^{-1}$ . The reason for starting at the high frequency was to avoid sag, or that the heavier components moved down and the lighter components stayed at the upper layer due to weak gel structures in the sample. The purpose of performing frequency sweeps was to investigate the time dependence of the deformation behaviour, since frequency is the inverse of time.

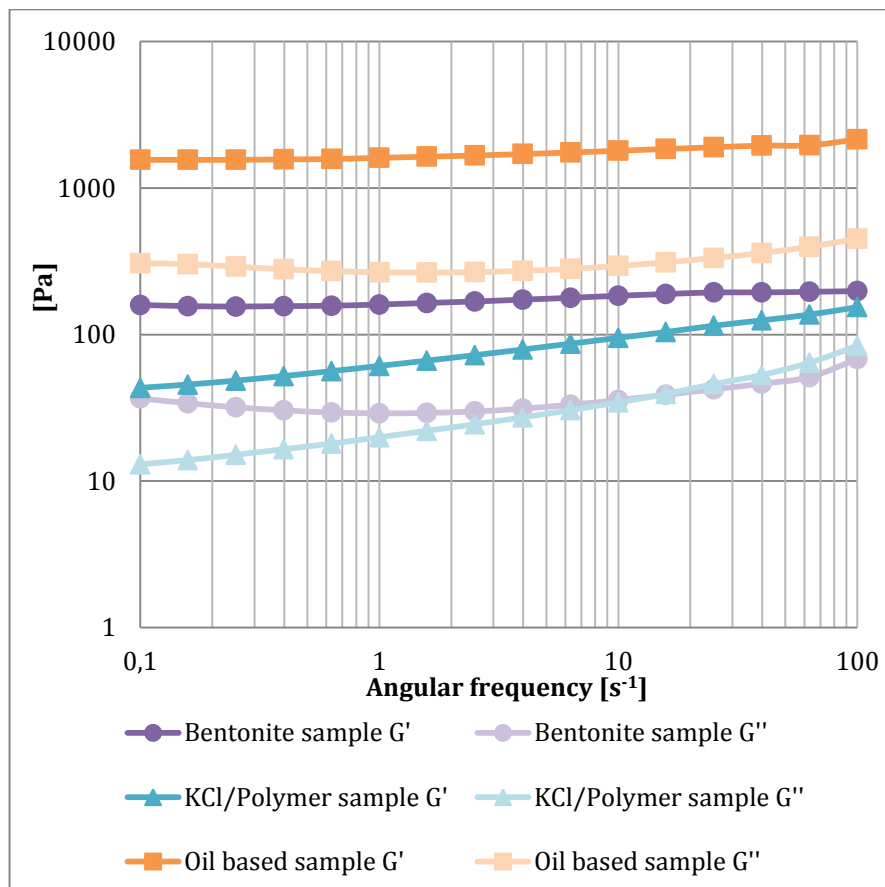


Figure 33: Frequency sweeps for all three samples at  $10 \text{ }^\circ\text{C}$  and strain of 1 %.

The plot of the frequency sweep with a constant strain of 1% showed that the value of  $G'$  was higher than  $G''$  for all three samples. This means that the elastic response dominated the viscous response for both when the sample was deformed slowly and abruptly. When  $G'$  dominates the  $G''$  for the whole range, it is not recommended to use

viscosity curves for practical use to describe the fluids behaviour in this region.

The frequency sweeps of the different samples resulted in different curves for  $G'$  and  $G''$ . The elastic portion for the oil based and bentonite based sample remained almost constant for the whole range of frequencies. For the KCl/polymer sample,  $G'$  increased with increasing frequency. This means that this sample was more sensitive to the rate of deformation. The curves for the KCl/polymer sample indicate that the sample consisted of cross-linked molecules (Mezger, 2011). The results for the bentonite sample might have been influenced by the low LVE range. The  $G''$  curve started to bend upwards when passing a frequency of  $10\text{s}^{-1}$ . Frequency sweep with a strain of 1% at a temperature of  $10^\circ\text{C}$  might have irreversibly deformed the fluid, and this might have been the reason for the bend on the  $G'$  and  $G''$  curves.

Fig. 34 illustrates that when the temperature was increased to  $20^\circ\text{C}$ , the  $G'$  and  $G''$  curves were less constant. All the curves had a bend upwards from around a frequency of  $40\text{s}^{-1}$  to  $100\text{s}^{-1}$ , and this was probably caused by the fact that the LVE range was exceeded. The temperature also influenced the values of  $G'$  and  $G''$ . For the bentonite sample  $G'$  and  $G''$  increased with increasing temperature. For the KCl/polymer sample  $G'$  and  $G''$  increased slightly with increasing temperature. For the oil based sample  $G'$  and  $G''$  decreased with increasing temperature. For both temperatures the KCl/polymer sample was the sample that was most affected by the frequency.

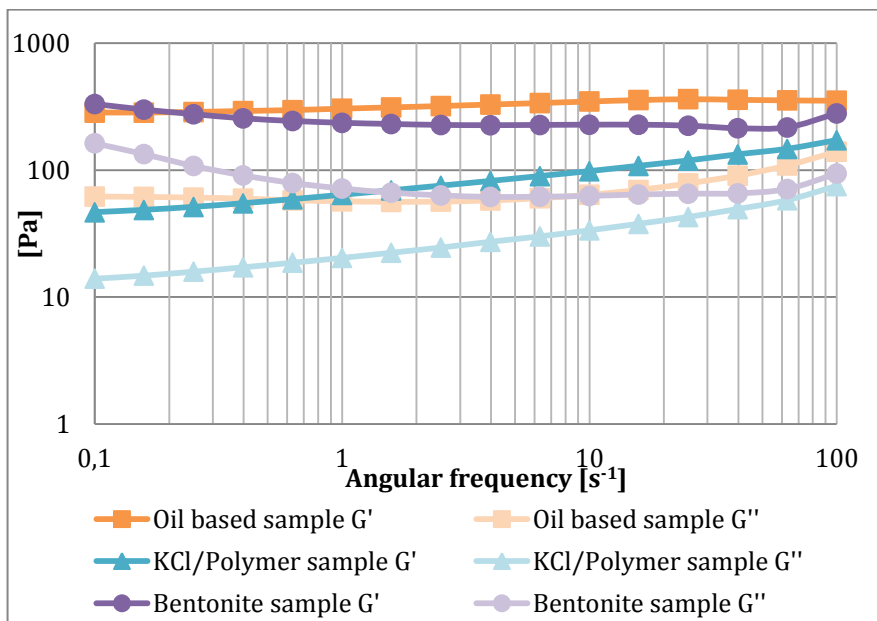


Figure 34: Frequency sweep for all three samples at  $20^\circ\text{C}$  with a strain of 1 %.

### 6.2.3 COMPARISON OF DYNAMIC YIELD POINT

By comparing the yield point found by the Herschel Bulkley model to the dynamic yield point found by amplitude sweeps it was evident that the yield point found by this model deviated from the dynamic yield point found from the amplitude sweep. The values are shown in Table 3. There was no correlation between the yield points found by the two different methods. The yield point found by the extrapolation of the Herschel Bulkley underestimated the yield point for all three samples, and this corresponds to findings in several previously discussed papers (Coussot et al., 2002), (Barnes & Walters, 1987), (Hertzhaf et al., 2006), (Masalova et al., 2008), (Maxey et al., 2008), (Jachnik, 2003).

	Bentonite	KCL/Polymer	Oil based
Yield point flow curve (HB) [Pa]	9	12	19
Yield point Amplitude sweep [Pa]	42	15	34

**Table 3: Comparison of yield point found from extrapolation of flow curve with the Herschel Bulkley model and the value of dynamic yield point found by amplitude sweep for all three samples at 20°C.**

By comparing the yield point found by the Bingham plastic models and the yield point found from the amplitude sweep there were large differences for all samples. The values are presented in Table 4. There was no correlation between the yield points found by the two different methods. This indicates that extrapolation of flow curves to determine yield point was a method that gave an incorrect value and that there is a need to develop different models to describe the low shear rheology of drilling fluids (Yap et al., 2011), (Tehrani, 2007), (Bui et al., 2012).

	Bentonite	KCL/Polymer	Oil based
Yield point (Bingham)[Pa]	21	45	48
Yield point Amplitude sweep [Pa]	42	15	34

**Table 4: Comparison of yield point found from extrapolation of flow curve with the Bingham plastic model and the value of dynamic yield point found by amplitude sweep for all three samples at 20°C.**

Fig. 35 illustrates a comparison of the flow curves found with Fann viscometer and flow curves found with Anton Paar rheometer. The flow curve of the bentonite sample is not included, because the measurement seemed incorrect (the curve is included in Appendix C.3). Possible gel effects might have been formed due to too long rest period. The other two samples seemed to give a higher shear stress values for the measurements performed with the rheometer than the viscometer. This tendency increased with increasing shear rate.

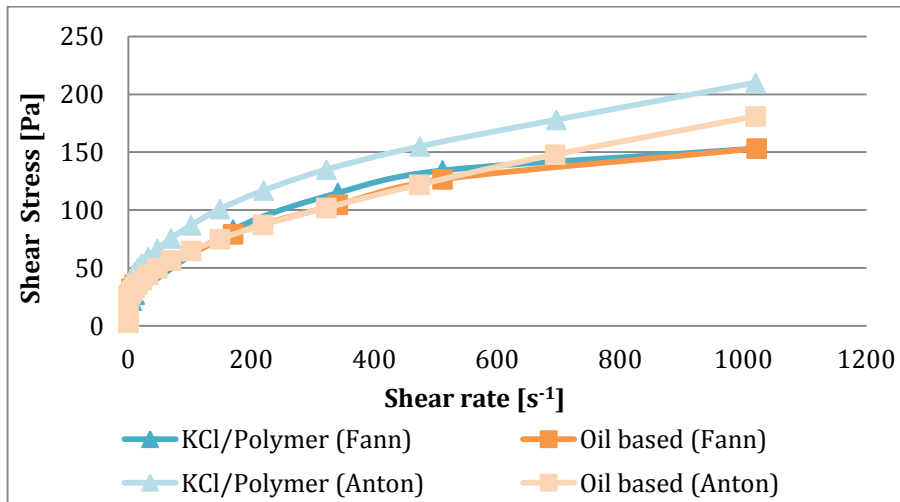


Figure 35: Comparison of flow curves for KCl/Polymer sample and oil based sample measured with Fann viscometer and Anton Paar rheometer.

Fig. 36 and Fig. 37 are plots of the very low shear rates measured with the rheometer. It was evident that the viscosity curves found with the Fann viscometer and the Bingham or Herschel Bulkley model gave a very simplified representation of the viscosity of low shear rates compared to these results.

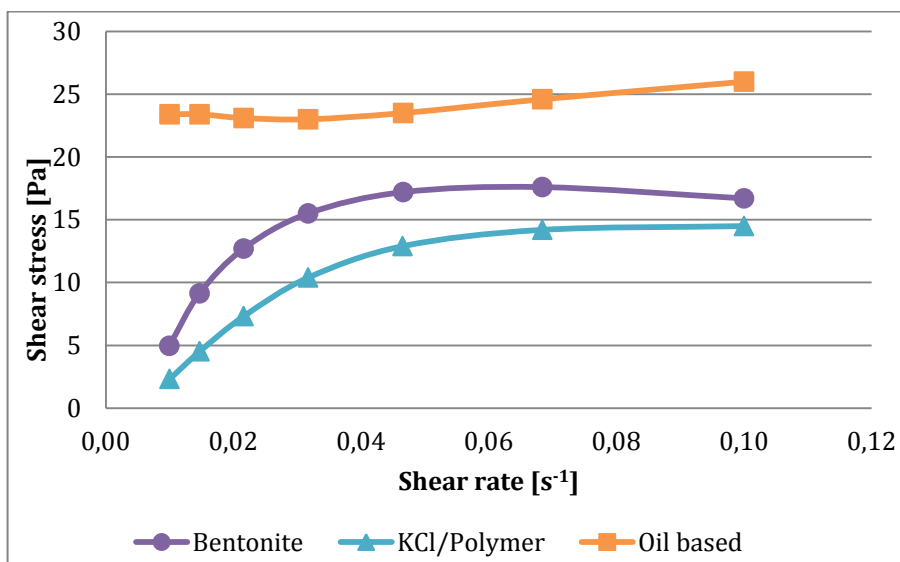


Figure 36: Low shear viscosity curves for all three samples measured with Anton Paar rheometer at T=10°C.

The oil based sample possibly displayed shear localization like behavior, with a sudden increase in viscosity for ultra low shear rates, such as pictured in Fig. 17.

Fig. 36 shows the plot of shear rates up to  $0.5s^{-1}$ . Here the deviation from a linear or a polynomial trendline became even more evident. A bump in the curves of the KCl/polymer and bentonite sample showed that the polynomial trendline, such as for the Herschel Bulkley model, gave a poor fit.

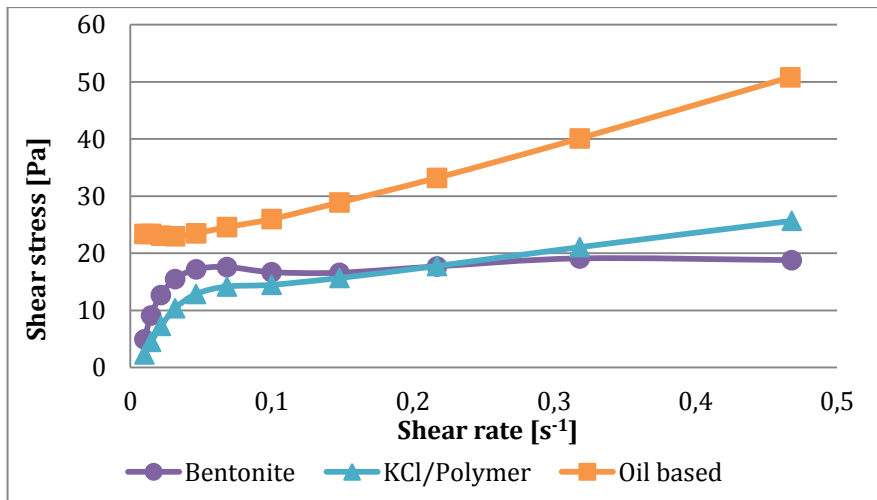


Figure 37: Low shear viscosity curves for all three samples measured with Anton Paar rheometer at  $T=10^{\circ}C$ .



### 6.3 A SPECIAL STUDY OF A WATER BASED DRILLING FLUID

Learning more about water based drilling fluids is a part of the process of increasing the understanding of the behaviour oil based drilling fluids. In cooperation with Sintef, several experiments were performed on a water based drilling fluid currently used in an experimental project on cuttings transport running at Sintef. A paper published on the rheological properties of this water based drilling fluid is included in Appendix E, where the details of content of the drilling fluid and the experimental set up for the project are included. The purpose of these experiments was to investigate the repeatability of the water based fluid during testing. The goal was to design a fluid that had little changes in properties throughout the experiment. The drilling fluid was a mixture of a synthetic clay and Xantham gum biopolymer. The drilling fluid was required to have yield strength, shear thinning and thixotropic properties. The experiments were performed on samples that were taken at different stages in the circulation process. Additionally, several experiments were performed on samples taken at the same time in the circulation process, but with a varying period of rest. This was done to see whether it was the time at rest or the time of circulation that lead to the largest changes in the drilling fluids properties.

#### 6.3.1 EXPERIMENTAL SET UP – ANTON PAAR RHEOMETER

- The experiments were conducted using the smooth parallel geometry, with a 1 mm gap. Plates with a diameter of 25mm, depicted in Fig. 27.
- The sample was pre-sheared at a rate of  $1000 \text{ s}^{-1}$  for two minutes and then allowed to rest for three minutes prior to testing.
- Amplitude sweep was performed with a strain from 0.01-1000 % and a frequency of  $10 \text{ s}^{-1}$ , temperature  $30 \text{ }^{\circ}\text{C}$ .
- Frequency sweep was performed with a frequency from 0.1-100  $\text{s}^{-1}$  and a strain of 1 %, temperature  $30 \text{ }^{\circ}\text{C}$ .
- Flow curve was found, temperature  $30 \text{ }^{\circ}\text{C}$ .
- Temperature sweep was performed with an increasing temperature from  $21.5 \text{ }^{\circ}\text{C}$  to  $50.1 \text{ }^{\circ}\text{C}$  with a shear rate of  $50 \text{ s}^{-1}$ .
- Four different samples were tested. The samples are named WBM 1 to WBM 4. Sample WBM 1 and WBM 2 were taken from the same batch, but at early (WBM 1) and late (WBM2) stages in the circulation process. To test the difference between two different batches, a new batch of the drilling fluid was mixes and prepared. WBM 3 and WBM 4 were taken from

this new batch. WBM 3 was taken from the new batch of drilling fluid, after two hours of circulation. WBM 4 was circulated two days longer.

- WMB 1: From first batch of drilling fluid. Circulated for one week.
  - WBM 2: From first batch of drilling fluid (same as WBM2). Circulated for two weeks.
  - WBM 3: From second batch of drilling fluid. Circulated for two hours.
  - WBM 4: From second batch of drilling fluid (same as WBM 3). Circulated for two days.
- The samples were also tested with varying time of rest to study the effect time of rest had on properties such as viscosity, loss and storage modulus and dynamic yield point.

### 6.3.2 EFFECT OF TIME OF REST

The repeatability of the samples was investigated. Sample WBM 3 and WBM 4 were tested two times consecutively to see if the results differed. The frequency sweep was chosen to illustrate the repeatability of WBM 3 and WBM 4. Fig. 38 and Fig. 39 illustrate the loss and storage modulus comparison for the two tests performed consecutively on WBM 3.

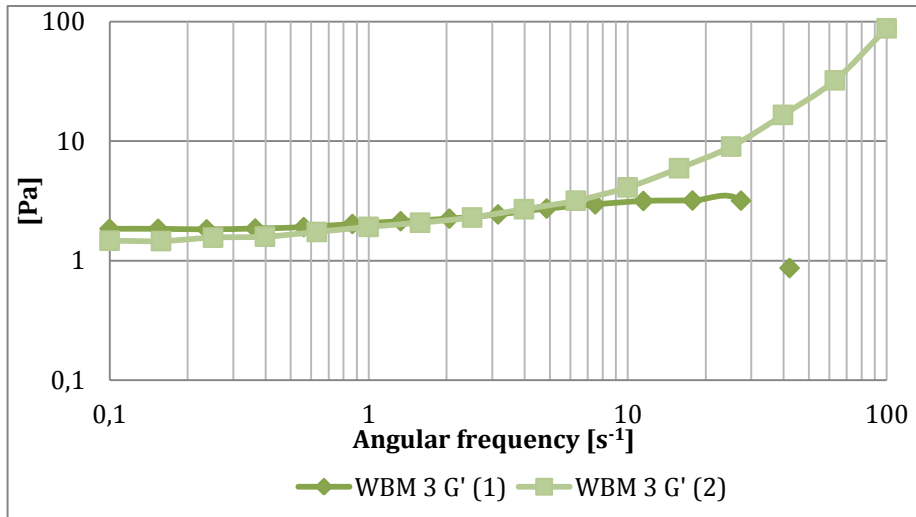


Figure 38: Storage modulus of two tests performed consecutively on WBM 3 at 30 °C and a strain of 1%.

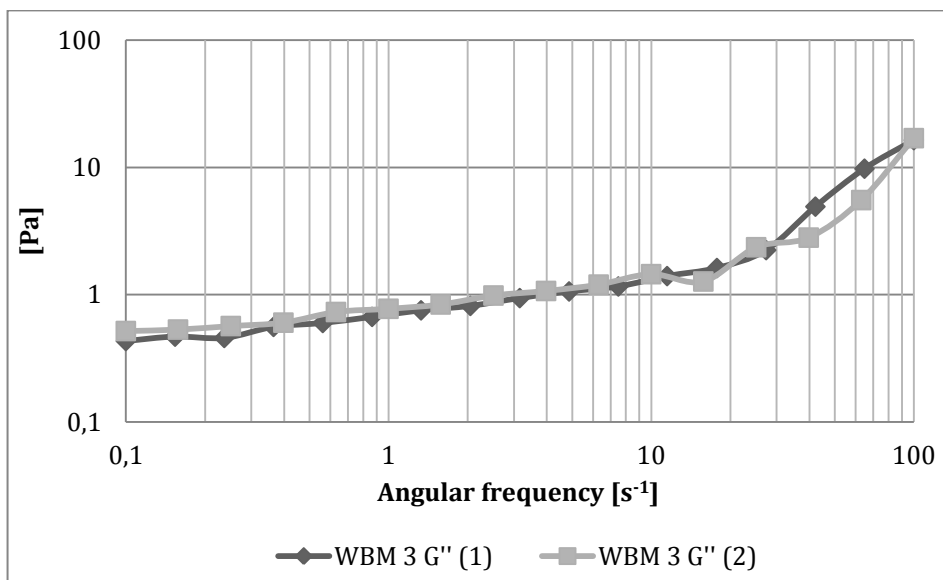


Figure 39: Loss modulus of two tests performed consecutively on WBM 3 at 30 °C and a strain of 1%.

Fig. 38 and Fig. 39 showed that the repeatability of WBM 3 was relatively good when the tests were performed consecutively. There

were very small differences for both moduli. This indicated that sample WBM 3 was homogeneous, and that the measurements were performed in a reproducible manner. The discrepancy that occurred for the high frequencies was most likely caused by measurement errors for the instrument that occurs when the frequency was too high. The results for the frequency sweep performed consecutively on WBM 4 are presented in Fig.40 and Fig. 41.

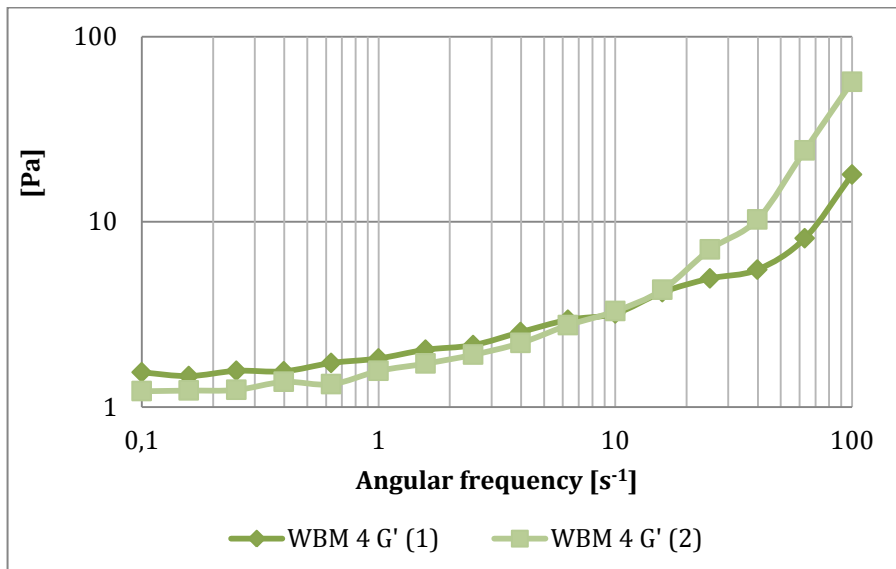


Figure 40: Storage modulus of two tests performed consecutively on WBM 4 at 30 °C and a strain of 1 %.

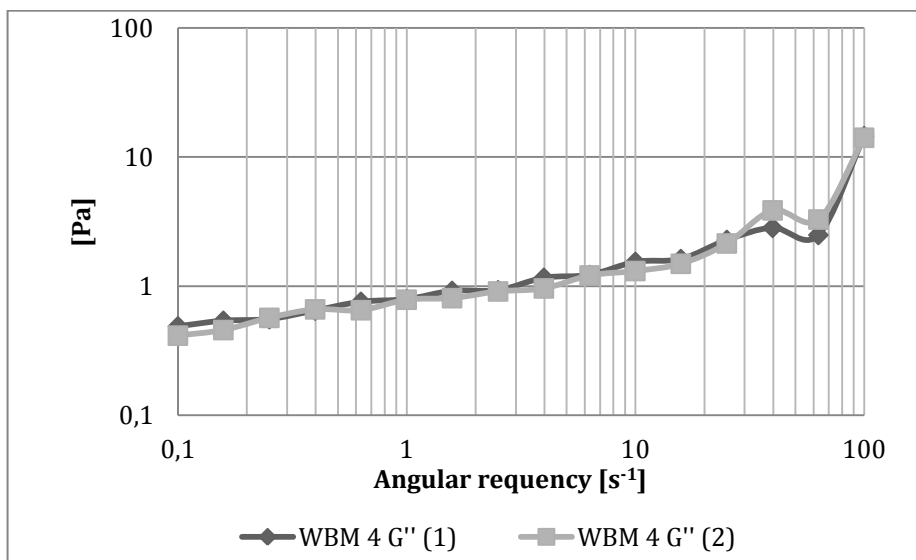


Figure 41: Loss modulus of two tests performed consecutively on WBM 4 at 30 °C and a strain of 1 %.

The frequency sweeps of sample WBM 4 showed the same as the ones for WBM 4. The repeatability was good, and there were very small

changes for the values of both the loss and storage modulus when the tests were performed consecutively.

Sample WBM 1 and WBM 2 were tested with a two week interval to see how a longer period of rest influenced the results. The mixes were not mixed or prepared in any way during these two weeks. Figure 42 and Fig. 43 show the frequency sweep for sample WBM 1 and WBM 2.

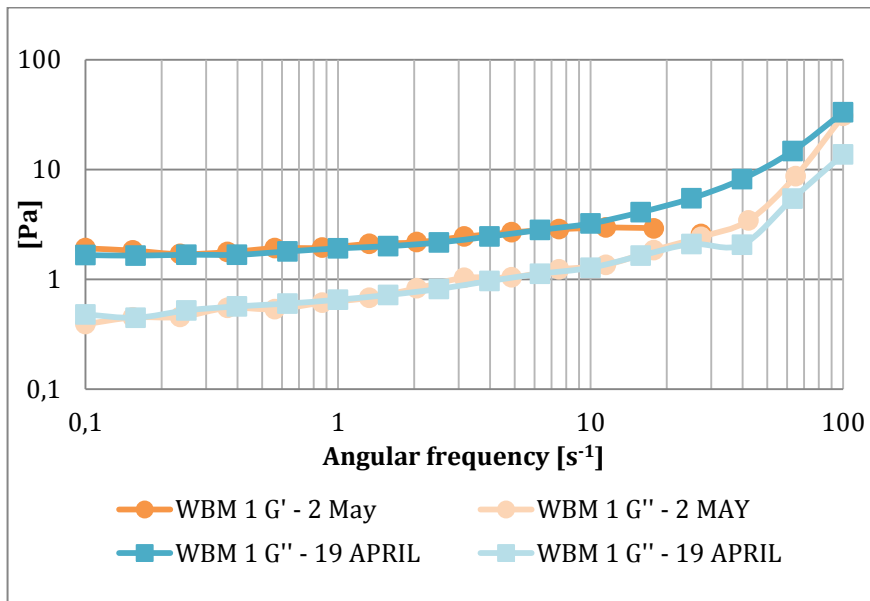


Figure 42: Frequency sweep performed on WBM 1 measured with a two week interval.

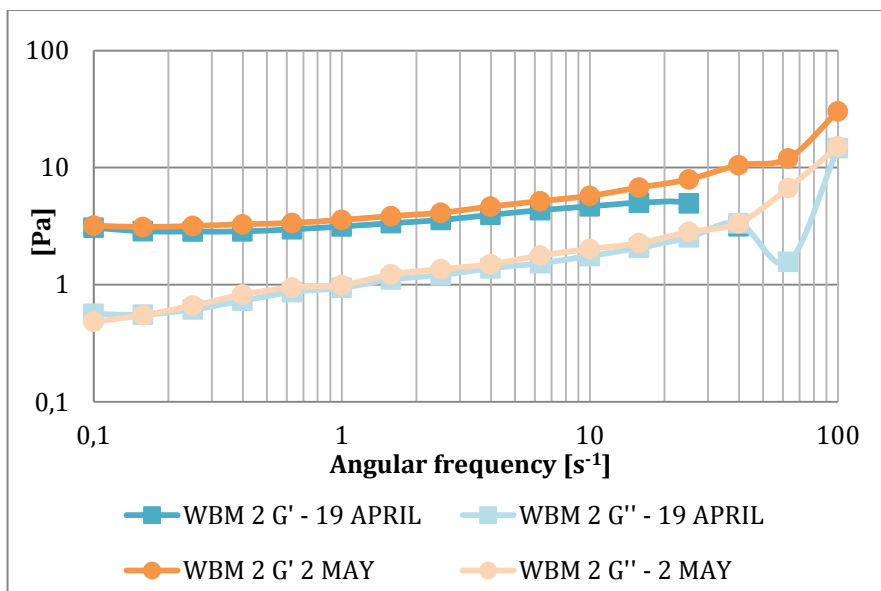


Figure 43: Frequency sweep performed on WBM 2 measured with a two week interval.

The plots of the frequency sweeps on both sample WBM 1 and WBM 2 showed that very little change had happened to the elastic and viscous modulus. The moduli were practically overlapping each other for almost all frequencies. By comparing the change in flow curves for the two samples, some change was observed. It seemed that the curve was shifted upwards, showing an increase in viscosity. The flow curves of all samples before and after rest showed that sample WBM 1, WBM 2, WBM 3 and WBM 4 all showed a slight increase in viscosity after a longer period of rest (Appendix D.1).

### 6.3.3 EFFECT OF TIME CIRCULATED

To investigate the effect of the time the fluid had spent being circulated in the system, samples were taken at different stages in the circulation loop. Sample WBM1 and WBM 2 were compared, and sample WBM 3 and WBM 4 were compared. The amplitude sweep and flow curve illustrate the effect of time circulated. Fig. 44 illustrates the amplitude sweep of sample WBM 1 and WBM 2

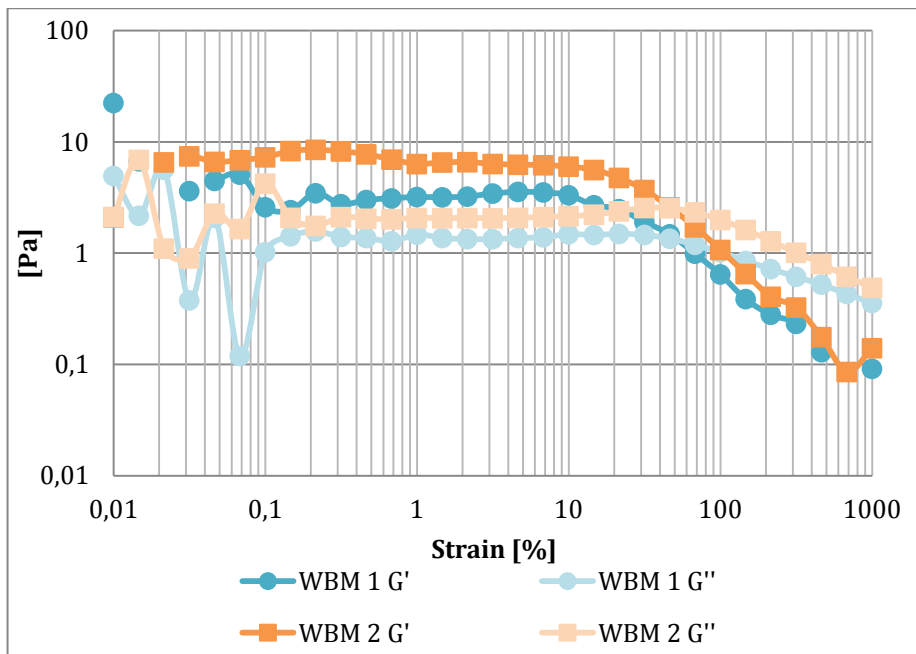


Figure 44: Plot showing amplitude sweep of sample WBM 1 and WBM 2 and the effect time of circulation have on the viscous and elastic modulus.

Sample WBM 2 had been circulated for two weeks, one week longer than sample WBM 1, and differences could now be observed in Fig. 44. The viscous and elastic modulus for WBM 2 had slightly higher values compared to WBM1. The dynamic yield point was located at almost the same strain, but the value was higher for WBM 2. This is shown in Fig. 45.

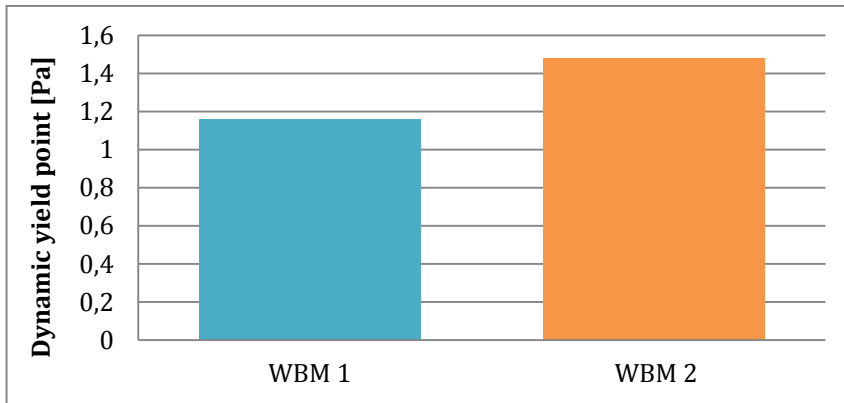


Figure 45: Difference in dynamic yield point between WBM 1 (circulated one week) and WBM 2 (circulated two weeks).

The viscosity curves for WBM 1 and WBM 2 illustrated in Fig. 46 indicated that a longer period of circulation lead to a slightly higher viscosity. The viscosity at low shear rate was 1.4 times higher for WBM 2.

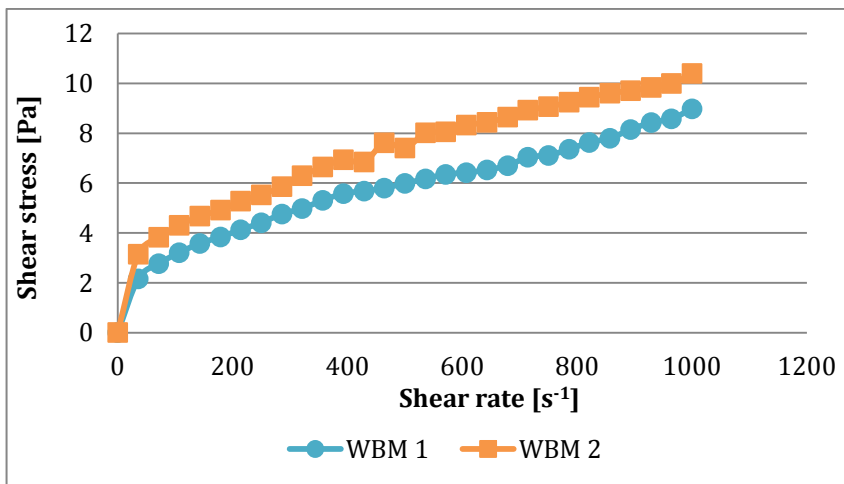


Figure 46: Flow curve for both WBM 1 (circulated one week) and WBM 2 (circulated two weeks) to illustrate the effect time of circulation have on the viscosity curve.

Fig. 47 of the shows an amplitude sweep comparison between WBM 3 and WBM 4, and the amplitude sweep showed less difference. These samples were taken with only two days interval, sample WBM 4 had been circulated for two days longer than sample WBM 3. Here, the same trend was showed, with an increase in dynamic yield point, and an increase in viscosity for a longer period of circulation is shown in Fig. 48.

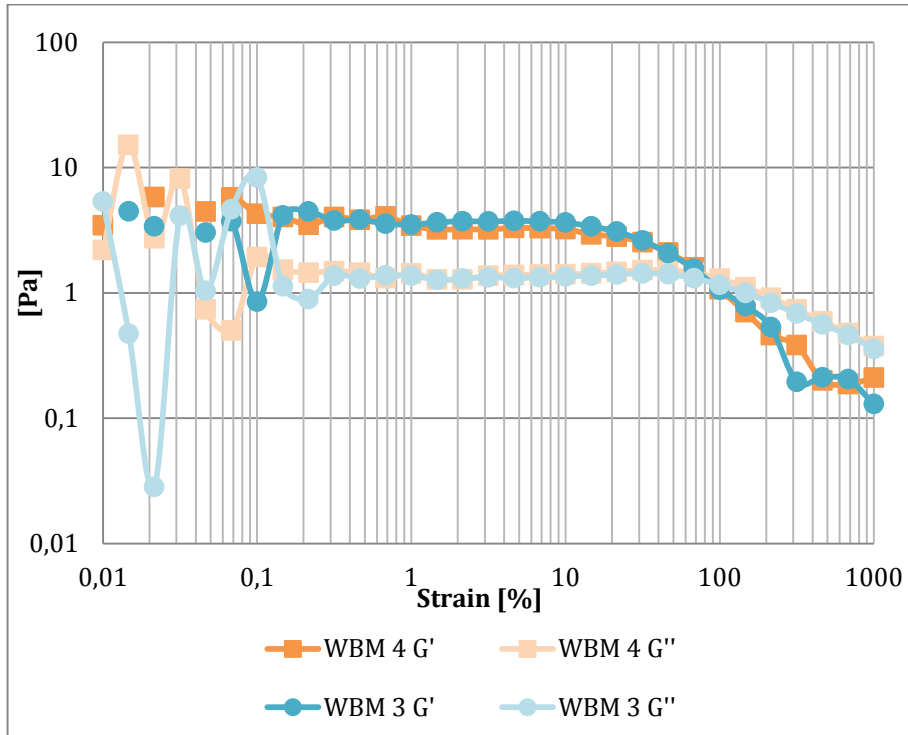


Figure 47: Amplitude sweep for WBM 3 (circulated two hours) and WBM 4 (circulated two days) illustrating the effect of two days longer circulation on the viscous and elastic modulus.

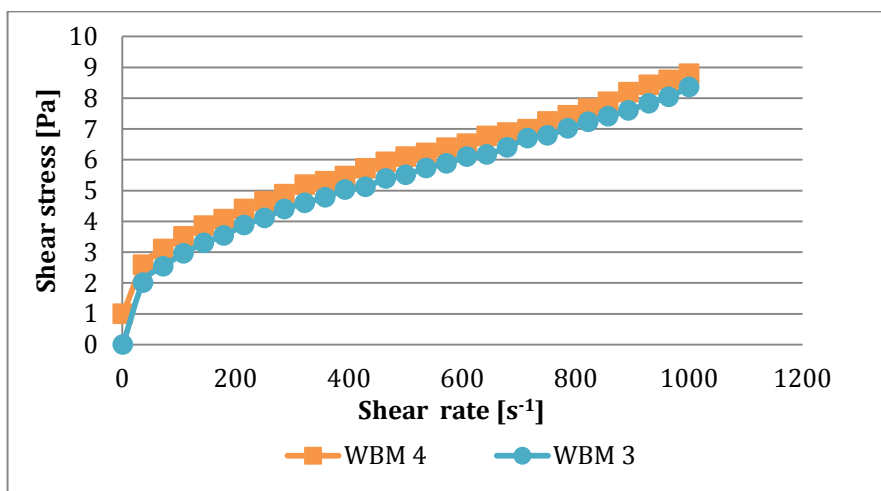


Figure 48: Flow curve for both WBM 3(circulated two hours) and WBM 4 (circulated two days) to illustrate the effect time of circulation have on the viscosity curve.



The difference in dynamic yield point was however larger between sample WBM 3 and WBM 4. The same tendency was observed, longer circulation time lead to an increase in dynamic yield point shown in Fig. 49.

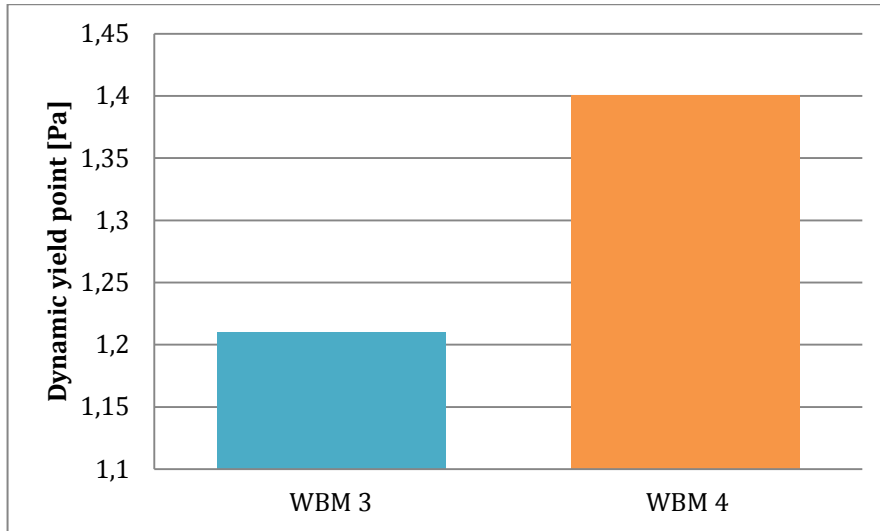


Figure 49: Difference in dynamic yield point between WBM 3 (circulated two hours) and WBM 4 (circulated two days).

Measurements showed that the repeatability of the experiments was good over short as well as long time. The measurements performed indicate that the time the fluid had been circulated was what had the largest impact on parameters such as dynamic yield point, viscosity and viscous and elastic modulus. This could have occurred for several reasons, for instance could particles from inside the pipe system have polluted the drilling fluid. Sand was injected into the test section to test how well it was transported through the system. These sand particles might have changed the properties of the drilling fluid. Grinded sand particles might have become a part of the drilling fluid. Dispersion of solids would make a drilling fluid more viscous. The time the fluid had been at rest seemed to have almost no impact on the samples, and hardly change the properties any of the measured of the drilling fluid.



## 7 DISCUSSION

Laboratory investigations demand accuracy in order to produce results that are repeatable. There are always many sources of error when performing measurements, readings and using different instruments. Time is a factor that limits the amount of work that can be done in a Master's Thesis, and there is often room for improvements and extended research. It is important to be critical of the results found, and to evaluate the quality of the results found.

### 7.1 WEAKNESSES AND LIMITATIONS

#### MIXING OF THE DRILLING FLUIDS

Mixing and preparing the drilling fluids was challenging because the aim was to design three different drilling fluids that had the same viscosity curve. The drilling fluids were delivered with a recipe that would give three similar viscosity curves. However, the mixes were found to have too low viscosity to give good results for measurements with the Anton Paar rheometer. The dual plate geometry demands a certain thickness of the fluid to keep the fluid stable between the two plates, avoiding the test fluid to flow off the plates and air to enter between the two plates. The mixes were therefore prepared a second time, this time increasing the amount of viscosifiers. After several attempts the result still was not three identical curves. Great care was taken in preparing the mixes, so that it would be possible to reproduce the results. During mixing it was important that the mixes did not exceed a maximum temperature. Since the Waring commercial blender used as mixer in this thesis was much more powerful than the Hamilton mixer, the mixes needed to be cooled down during mixing. Too much heat could have changed the properties of the mixes. Inaccuracy when measuring and weighing the ingredients could be a source of error.

#### MEASUREMENTS WITH FANN VISCOMETER

The experiments with the Fann viscometer were performed directly after mixing and cooling to room temperature. This was done to try to give the drilling fluids identical shear and resting time history. The results of the measurements were three viscosity curves that resembled both the Herschel Bulkley model and the Bingham plastic model. This was a reasonable result, drilling fluids have for many years been described using these two models. The disadvantage with three viscosity curve that did not resemble each other more is that it was harder to compare the three in the main experiments. Measuring the 30 minute gel strength would have been useful to determine how

progressive the oil based and bentonite sample were. Inaccurate readings, sag, different temperature of the mixes and wrong calibration of the Fann viscometer are factors that could lead to errors.

#### MEASUREMENTS WITH ANTON PAAR RHEOMETER

For the tests performed with the Anton Paar rheometer, the shear and temperature history of the drilling fluids was the factor that probably most influenced the results. The drilling fluids were not mixed in the hours previous to the experiment, because no mixer was available at the site of the rheometer. Leaving the samples at rest for too long might have caused heterogeneity in the sample. Settling of heavy particles and vaporisation might have occurred in the samples prior to testing, and this could have influenced the results. The focus was to try to set the same initial conditions for all samples. Because the fluids were prepared at a different location of the rheometer, some of the samples were allowed to rest for a longer period. The first fluid to be tested had the shortest rest period, and the last sample to be tested had the longest rest period. This might have led to more evaporation and settling of heavy particles in the last sample to be tested. This again might have led to a wrong interpretation of the results. The dual gap geometry was chosen because this geometry had the largest surface area, and would therefore give better results at low shear rates. The high frequency measurements might have been effected by the large inertia of the dual gap cylinder, and the results for high frequencies were therefore as mentioned in the result chapters often disregarded.

The results indicated that all three samples exhibit viscoelastic behaviour. Previous work referred to in this thesis has also concluded this, although drilling fluids have been characterized as purely viscous. Since all the different experiments indicated this without exception, it might be reasonable to assume that this was correct. The rest of the results indicated that the samples were influenced by temperature history, shear history and frequency. However, it was difficult to conclude how and why the samples were affected. This requires a more extensive study, with several series of experiments on large amounts of different drilling fluids. It is therefore only observed that these factors had an effect, and this gave an indication of how different drilling fluids could be affected by different external factors.

Although the title of this thesis is “Gel evolution in oil based drilling fluids”, there has also been focused on water based drilling fluids. A big part of this is due to the fact that one oil based drilling fluid sample was tested, whereas three water based samples were tested. However, the tests performed on water based drilling fluids were a good basis

for comparison and gel evolution in water based drilling fluid is a subject that is not fully explored. In retrospect, it might have been more balanced with regards to the title and description of the thesis, if more oil based drilling fluid samples were tested. Time was a limiting factor here. The next section therefore suggests extending the work to more oil based samples as a potential improvement.

## 7.2 POTENTIAL IMPROVEMENTS AND FURTHER WORK

In hindsight, the largest source of error probably lied in the preparation of the drilling fluids. Creating a set of initial conditions and preparing the samples as identically as possible would have led to more reproducible results. Decreasing the amount of time from preparation of the drilling fluids to performing the tests would lead to less alternation of the content of the drilling fluids. For the experiments performed on the Anton Paar rheometer, changing the sample after each sweep could have led to less vaporisation, less settling of heavy particles and less wear on the samples.

Future improvements of this work could also include extending the work on several different samples of oil-based drilling fluid. Performing the tests on different oil based drilling fluid samples would increase the basis for comparison. Also mixing drilling fluid samples of different composition to give the same viscosity curve would have made the comparison even better. Performing identical tests on all samples with varying time of rest could have told more about how time at rest influenced the three drilling fluids prepared for this thesis. Extending the test matrix to include time sweep and temperature sweep on all samples would give more information about the viscoelasticity of the samples.

## 8 CONCLUSION

The objective of this Master's thesis was to investigate the gel evolution in oil based drilling fluids. Literature study performed confirmed the need for more work on low shear rheological properties of drilling fluids in general. The models that exist today are not sufficient in describing dynamic yield point and low shear behaviour.

A short case study on a well that experienced problems due to gel effects, demonstrated the importance of thorough knowledge of the low shear rheology of drilling fluids. Temperature, the effect of influx from the formation that changes the oil water ratio and evaporation of lighter components of the oil portion of the drilling fluid were suggested external factor that might have changed the gel properties of the drilling fluid.

Three different drilling fluid samples have been prepared and tested. The water based drilling fluid samples were found to have flow curves that fitted the Herschel Bulkley and Bingham plastic model best. Amplitude sweeps showed that the linear viscoelastic range was approximately 1 % at 20 °C with a frequency of 1 s<sup>-1</sup>. The yield point of the KCl/polymer showed little dependence on temperature, while the bentonite sample showed a significant increase in dynamic yield point for an increase in temperature. The dynamic yield point of the KCl/Polymer sample showed more sensitivity to frequency than the bentonite sample. Frequency sweeps showed that the elastic modulus dominated the viscous modulus for both samples within the LVE range.

The oil based drilling fluid sample was found to fit the Herschel Bulkley model. Yield stress found by extrapolation of the flow curve of both the Bingham Plastic model and the Hershel Bulkley model differed from the dynamic yield point found from amplitude sweep test. The Herschel Bulkley model was found to strongly underestimate the yield stress for the oil based sample. The Bingham Plastic model was found to overestimate the value for the oil based sample.

Amplitude sweeps performed showed that the oil based sample exhibited viscoelastic properties, and that the linear viscoelastic range was approximately 1 % at 20 °C and frequency of 1 s<sup>-1</sup>. Linear viscoelastic range and dynamic yield stress was found to be influenced by temperature. The oil based sample showed a slight decrease in dynamic yield point when the frequency was increased from 1 s<sup>-1</sup> to 10 s<sup>-1</sup>.

Amplitude sweeps showed that the oil based sample showed a significant decrease in yield point for an increase in temperature from 10 °C to 20 °C. Explaining the response for an increase in temperature was difficult. Temperature had a much larger effect on the dynamic yield point of the oil based sample, compared to the water based samples. A time sweep exposing the oil based sample to constant shear over time showed that a slight decrease in temperature from 20 °C to 10 °C lead to a significant increase in viscosity.

Frequency sweeps showed that the elastic modulus dominated the viscous modulus within the LVE range for the oil based sample. This indicates that there existed a stable gel structure and that the samples in this range behaved as viscoelastic solids.

Experiments performed on a specific water based drilling fluid show that the repeatability of the experiments were good over short as well as long rest periods. Experiments performed consecutively indicated that the tests performed in this thesis should be fairly reproducible. Experiments performed with a varying time of rest indicate that it is possible to design a water based drilling fluid where little or no change occurs with time of rest.



## NOMENCLATURE

$\mu$	= viscosity
$\dot{\gamma}$	= shear rate
$\tau$	= shear stress
$\Omega$	= rounds per minute
$T_R$	= Truton ratio
$\eta_E$	= extensional viscosity
$\dot{\epsilon}$	= extensional rate
$\text{Tan}\delta$	= damping factor
$G'$	= storage modulus
$G''$	= loss modulus
$\tau_g$	= gel strength
$A_p$	= surface area of particle



## BIBLIOGRAPHY

Al-Mutairi, S.H., Nasr-El-Din, H.A. & Hill, A.D., 2009. Droplet Size Analysis of Emulsified Acid. In *2009 SPE Saudi Arabia Section Technical Symposium and Exhibition*. Al Khobar, Saudi Arabia, 2009.

Anon., 2010. *Nordic Rheology Society*. [Online] Available at: <http://www.sik.se/rheology/> [Accessed 8 September 2011].

Anon., 2011. *The Society of Rheology*. [Online] Available at: <http://www.rheology.org/sor/info/default.htm> [Accessed 5 September 2011].

Anon., 2012. *Anton Paar*. [Online] Available at: [http://www.anton-paar.com/Asphalt-Rheometer-SmartPave-SmartPave-Plus/Rheometer/60\\_Corporate\\_en?product\\_id=49#Accessories](http://www.anton-paar.com/Asphalt-Rheometer-SmartPave-SmartPave-Plus/Rheometer/60_Corporate_en?product_id=49#Accessories) [Accessed 20 February 2012].

Balhoff, M.T. et al., 2011. Rheological and Yield Stress Measurements of Non-Newtonian Fluids Using a Marsh Funnel. *Journal of Petroleum Science and Engineering*, 77(3-4), pp.393-402.

Barnes, H.A., Hutton, J.F. & Walters, K., 1989. *An Introduction to Rheology*. 1st ed. Amsterdam-Oxford-New York-Tokyo: Elsevier.

Barnes, H. & Walters, K., 1987. The Yield Stress Myth? *Rheological Acta*, 24(4), pp.323-26.

Bourgoyne, J.A.T., Millheim, H.K., Chenevert, M.E. & Young, J.F.S., 1984. *Applied Drilling Engineering*. SPE Textbook Series.

Bui, B. et al., 2012. Viscoelastic Properties of Oil Based Drilling Fluids. *Annual Transactions of the Nordic Rheology Society*, 20.

Coussot, P., Nguyen, Q.D., Huynh, H.T. & Bonn, D., 2002. Viscosity Bifurcation on Thixotropic Yielding fluids. *Journal of Rheology*, 46(3), pp.573-389.

Cruz, F.D., Chevoir, F., Bohn, D. & Coussot, P., 2002. Viscosity Bifurcation in Granular Materials, Foams and Emulsions. *Physical Review*, 66(5).

Det norske oljeselskap ASA, 2012. Mud report.

Han, C.D. & Charles, M., 1971. Entrance and Exit Correlations in Capillary Flow in Molten Polymers. *Transactions of the Society of Rheology*, 15(2), pp.371-84.

Hertzhaft, B., Ragouilliaux, A. & Coussot, P., 2006. How to Unify Low-Shear-Rate Rheology and Gel Properties of Drilling Muds; A Transient Rheological and Structural Model for Complex Well Applications. In *IADC/SPE 99080, Presented at the IADC/SPE Drilling Conference held in Miami, Florida*. Miami, 2006.

Herzhaft, B., 2003. Influence of Temperature and Clays/Emulsions Microstructure on Oil-Based Mud Low Shear Rate Rheology. *SPE Journal*, 8(3), pp.211-17.

Hodne, H., Galta, S. & Saasen, A., 2007. Rheological Modelling of Cementitious Materials Using the Quemada Model. *Cement and Concrete Research*, 37, pp.543-50.

Jachnik, J.P., 2003. Low Shear Rate Rheology of Drilling Fluids. *Annual Transactions of the Nordic Rheology Society*, 11, pp.21-27.

Kitchens, E., 2012. *Everything Kitchens*. [Online] Available at: <http://www.everythingkitchens.com/waring-commercial-food-blender-HGB150.html> [Accessed 20 February 2012].

Masalova, I., Malkin, A.Y. & Foudazi, R., 2008. Yield Stress of Emulsions as Measured in Steady Shearing and in Oscillations. *Applied Rheology*, 18(4), pp.44790-5000.

Maxey, J., 2010. A Rheological Approach to Differentiating Muds by Gel Structure. In *2010 AADE Fluids Conference and Exhibition held at the Hilton Houston North*. Texas, 2010.

Maxey, J., Ewoldt, R. & MKinley, G., 2008. Yield Stress: What is the "True Value"? In *AADE Fluids Conference and Exhibition held at the Windam Greenspoint Hotel*. Houston, 2008.

Mezger, T.G., 2011. *The Rheology Handbook*. Hanover: European Coating Tech Files.

Mørk, P.C., 1997. *Overflate og kolloidkjemi*. 5th ed. NTNU.

Nguyen, T. et al., 2011. Experimental Study of Dynamic Barite Sag Using a Modified Rotational Viscometer and a Flow Loop. *Journal of Petroleum Science and Engineering*, (78), pp.160-65.

Omland, T.H., 2009. *Particles Settling in Non-Newtonian Drilling Fluids*. PhD Thesis. UiS.

Ragouilliaux, A., Hertzhaft, B., Bertrand, F. & Coussot, P., 2006. Flow Instability and Shear Localization in a Drilling Mud. *Rheological Acta*, 46, pp.261-71.

Saasen, A., 2002. Sag of Weight Materials in Oil Based Drilling Fluids. In *IADC/SPE 77190 Asia Pacific Drilling Technology Conference*. Jakarta, 2002.

Sandvold, I., 2011. *Gel Evolution in Oil Based Drilling Fluids*. TPG 4520 Project report. Trondheim: Department of Petroleum Engineering and Applied Geophysics, Norwegian University of Science and Technology.

Skalle, P., 2012. *Drilling Fluid Engineering*. Trondheim: Ventus Publishing ApS.

Speers, R.A., Holme, K.R., Tung, M.A. & Williamson, W.T., 1987. Drilling Fluid Shear Stress Overshoot Behaviour. *Rheological Acta*, 26(5), pp.447-52.

Tehrani, A., 2007. Behaviour of Suspensions and Emulsions in Drilling Fluids. *Annual Transactions of the Nordic Rheology Society*, 15.

UiS, 2011. *Øvinger i Bore- og Brønnvæsker*. Stavanger: UiS.

Wikipedia, n.d. *Wikipedia*. [Online] Available at: <http://en.wikipedia.org/wiki/Rheology> [Accessed 10 September 2011].

Yap, J., Leong, Y.K. & Liu, J., 2011. Structural Recovery of Barite-Loaded Bentonite Drilling Muds. *Journal of Petroleum Science and Engineering*, 78(2), pp.552-58.



## APPENDICES

APPENDICES .....	83
APPENDIX A – CONTENTS DRILLING FLUID SAMPLES .....	85
<i>Included to inform the reader of what type of drilling fluid are tested, makes it possible to reproduce the same samples</i>	
APPENDIX A.1 - BENTONITE DRILLING FLUID .....	85
APPENDIX A.2 - KCL/POLYMER DRILLING FLUID .....	86
APPENDIX A.3 - OIL BASED DRILLING FLUID .....	87
APPENDIX C – MEASUREMENTS ANTON PAAR RHEOMETER .....	89
<i>The appendix C and D includes results that confirm the work which is mentioned and not shown with figures in the thesis, truly has been performed.</i>	
<i>All figures in the appendix C and D is included to confirm what is stated in the thesis but they have not been prioritized as a part of the thesis itself.</i>	
APPENDIX C.1 – AMPLITUDE SWEEPS .....	89
APPENDIX C.2 – FREQUENCY SWEEPS .....	93
APPENDIX C.3– FLOW CURVES ANTON PAAR RHEOMETER .....	96
APPENDIX D – MODEL WATER BASED DRILLING FLUID .....	97
APPENDIX D.1 – TIME OF REST AS VARIABLE .....	97
APPENDIX D.2 – TIME CIRCULATED AS VARIABLE .....	100
APPENDIX E – ARTICLE PUBLISHED ON SINTEF PROJECT .....	103
<i>This article is included to give the reader the opportunity to read more about the research project that is referred to in the thesis. The paper gives information on the content of the drilling fluid and the circulation system is referred to in the thesis</i>	





## APPENDIX A – CONTENTS DRILLING FLUID SAMPLES

### APPENDIX A.1 - BENTONITE DRILLING FLUID

<b>MIX 1</b>		<b>BENTONITE SAMPLE</b>	
<b>SPECIFICATONS</b>			
Mix Type	Mix Volume	KG/L	
Water based	1400 ml	1,6	
<b>MATERIALS</b>			
Material	Test Amount	Mixing Time	
Fresh water	558,6 g	0	
Sea water	558,6 g	0	
Bentonite	42 g	5	
Dextrid E	19,6 g	10	
BARAZAN	2,8 g	10	
Soda Ash	1,96 g	1	
Barite	1058,96 g	15	
SUM	2242,52 g	41	

APPENDIX A.2 - KCL/POLYMER DRILLING FLUID

<b>MIX 2</b>	<b>KCl/POLYMER SAMPLE</b>	
<b>SPECIFICATONS</b>		
Mix Type	Mix Volume	KG/L
Water based	1400ml	1,3
<b>MATERIALS</b>		
Material	Test Amount	Mixing Time
KCl Brine SG:1,073	1188,24 g	0
Dextrid E	35 g	0
PAC-LE	8,4 g	10
BARAZAN	0,98 g	10
KOH, Salt	15,68 g	2
Barite	825,15 g	15
BARACARB® 50	91 g	0
BARACARB® 50	91 g	0
SUM	2255,45 g	37

APPENDIX A.3 - OIL BASED DRILLING FLUID

<b>MIX 3</b>		<b>OIL BASED SAMPLE</b>	
<b>SPECIFICATONS</b>			
Mix Type	Mix Volume	KG/L	
Water based	1400 ml	1,6	
<b>MATERIALS</b>			
Material	Test Amount	Mixing Time	
EDC 95/11	610,83 g	0	
EZ MUL® NS	35,98 g	10	
GELTONE® II	21 g	0	
DURATONE E	35,98 g	10	
Lime	28 g	5	
CaCl, Brine SG: 1,145	317,39 g	15	
Barite	1176,3 g	10	
SUM	2225,48 g	50	



## APPENDIX C – MEASUREMENTS ANTON PAAR RHEOMETER

### APPENDIX C.1 – AMPLITUDE SWEEPS

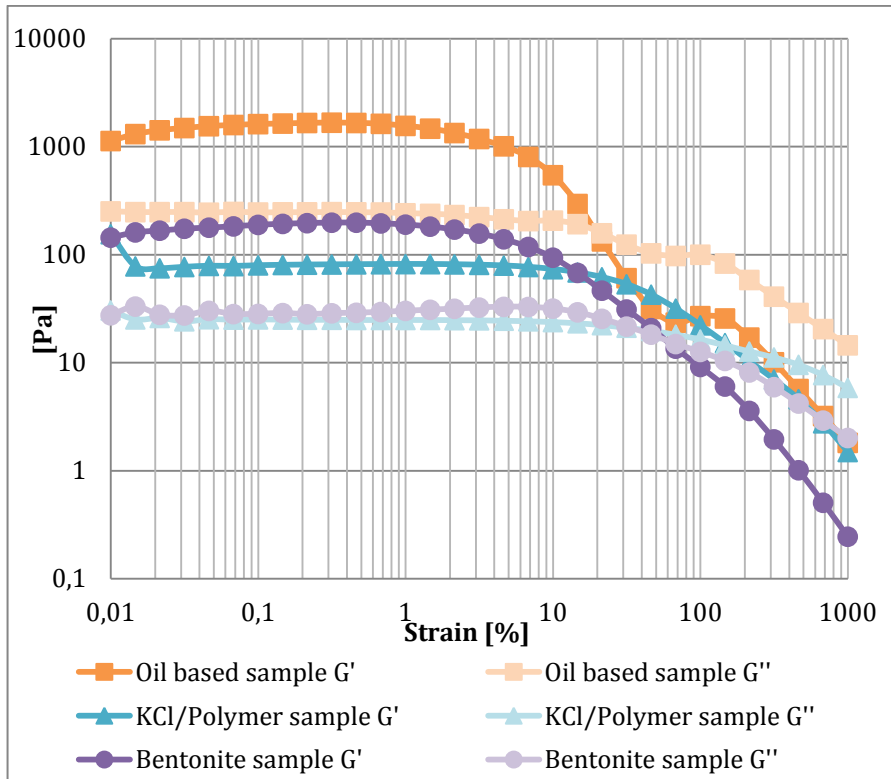


Figure 50: Plot showing amplitude sweep for all three samples at 10°C with a frequency of 1 s<sup>-1</sup>.

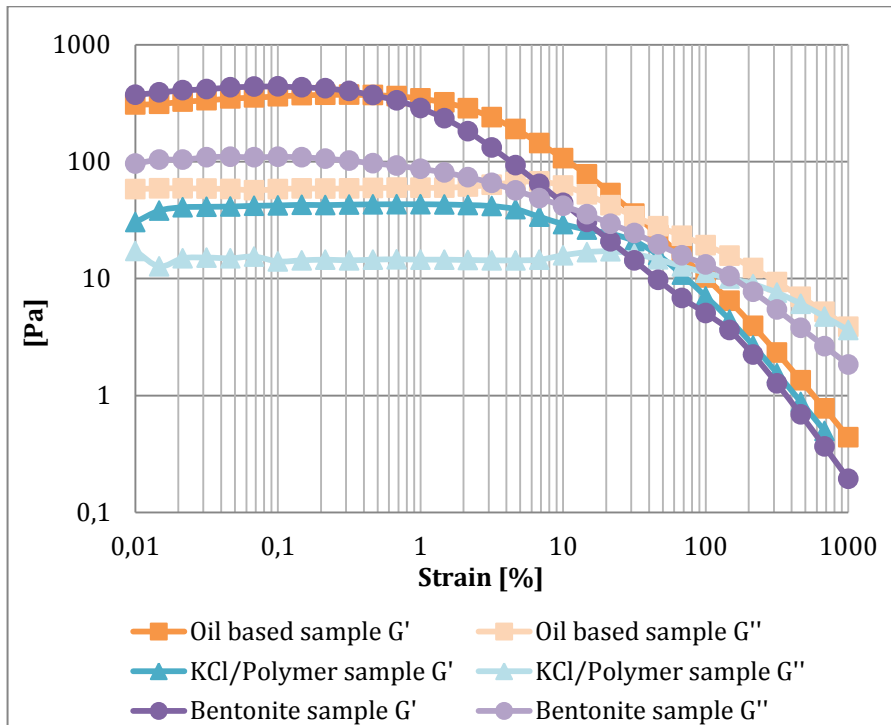


Figure 51: Plot showing amplitude sweep for all three samples at 20°C with a frequency of 1 s<sup>-1</sup>.

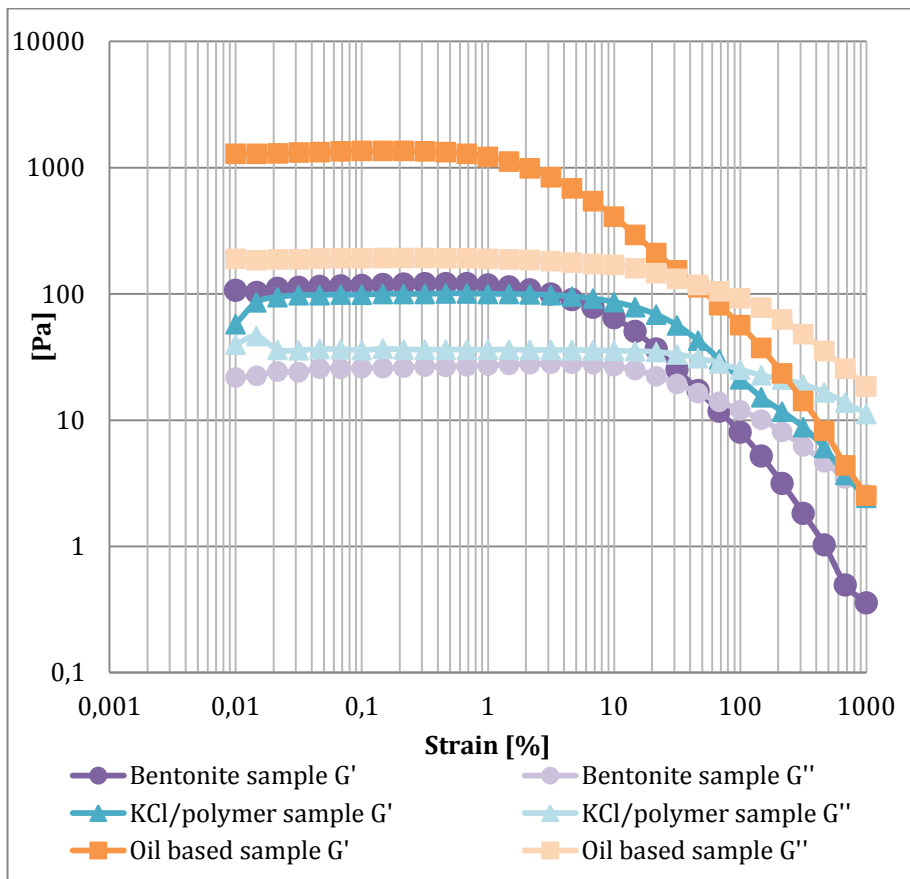


Figure 52: Plot showing amplitude sweep for all three samples at 10°C with a frequency of  $10\text{s}^{-1}$ .

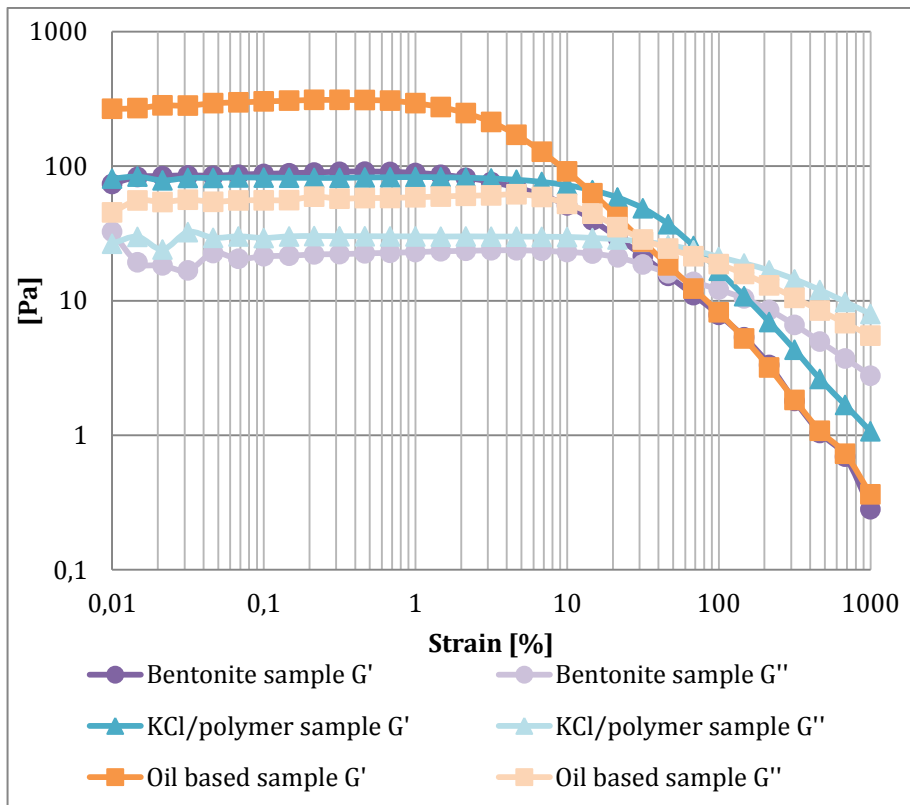


Figure 53: Plot showing amplitude sweep for all three samples at 20°C with a frequency of  $10\text{s}^{-1}$ .

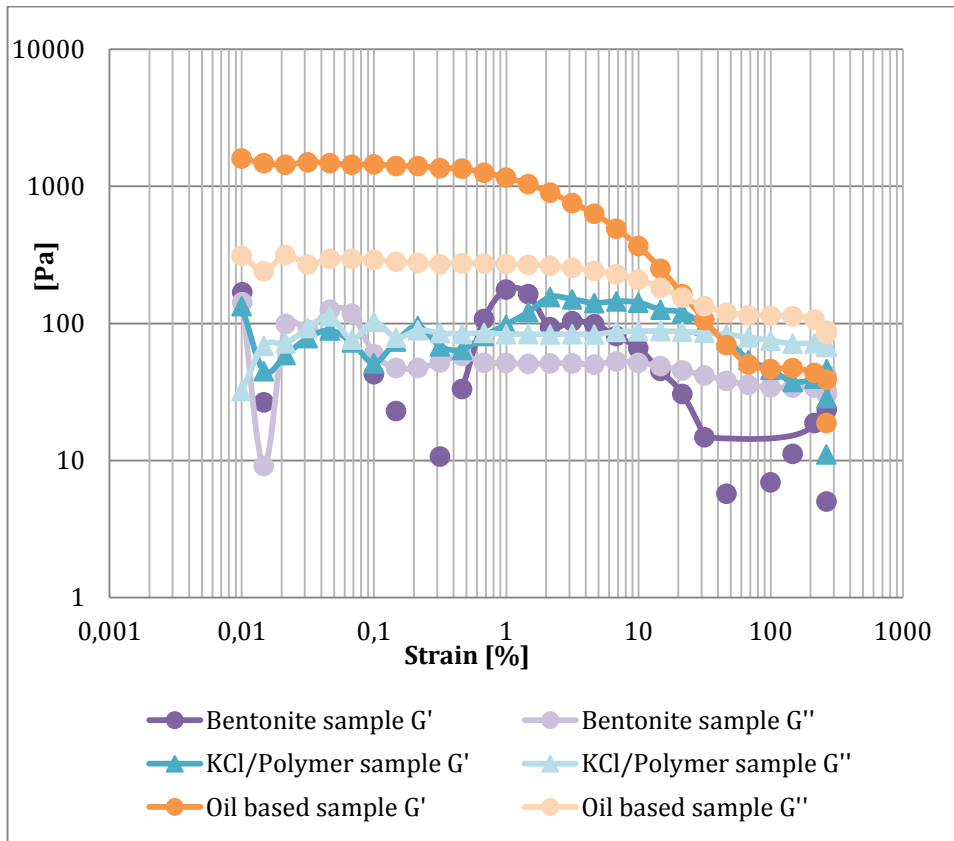


Figure 54: Plot showing amplitude sweep for all three samples at 10°C with a frequency of 100s<sup>-1</sup>.

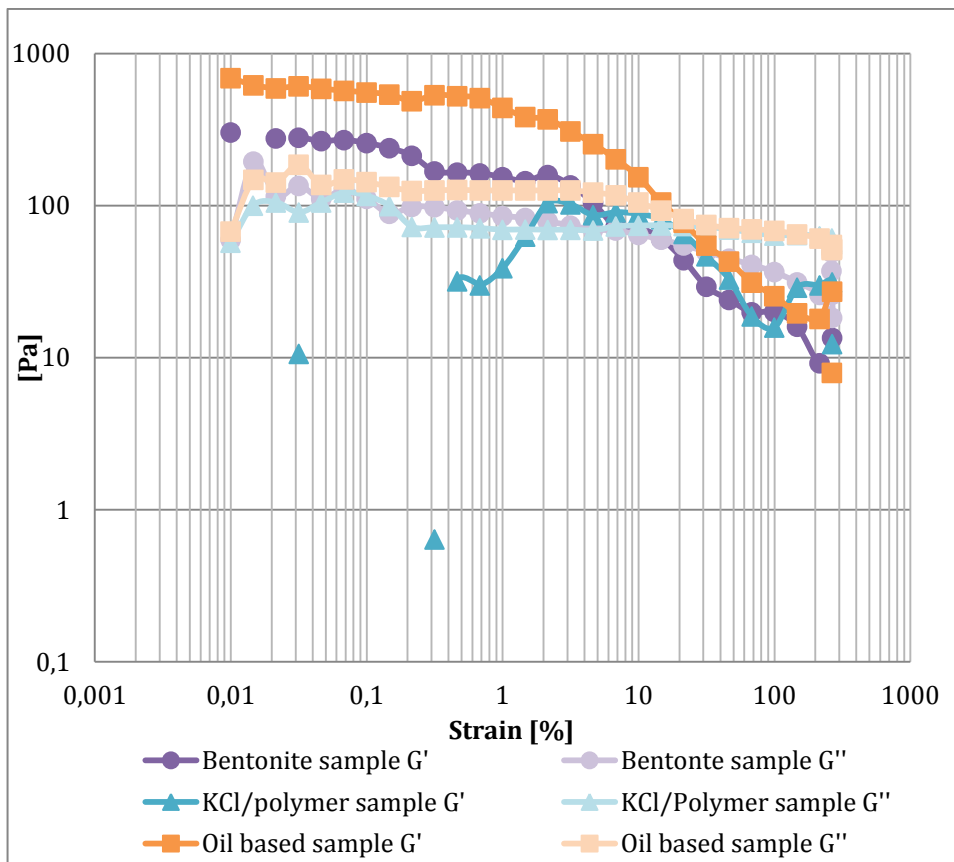


Figure 55: Plot showing amplitude sweep for all three samples at 20°C with a frequency of 100s<sup>-1</sup>.

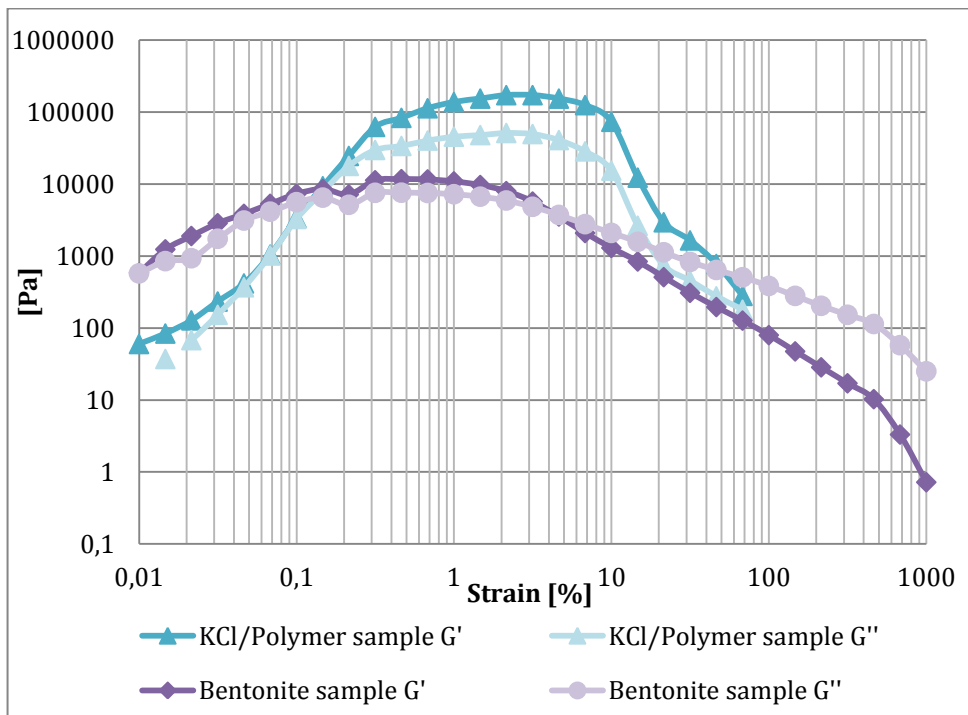


Figure 56: Plot showing frequency sweep for the Bentonite and KCl/Polymer sample at 50°C at a frequency of  $1s^{-1}$ .



APPENDIX C.2 – FREQUENCY SWEEPS

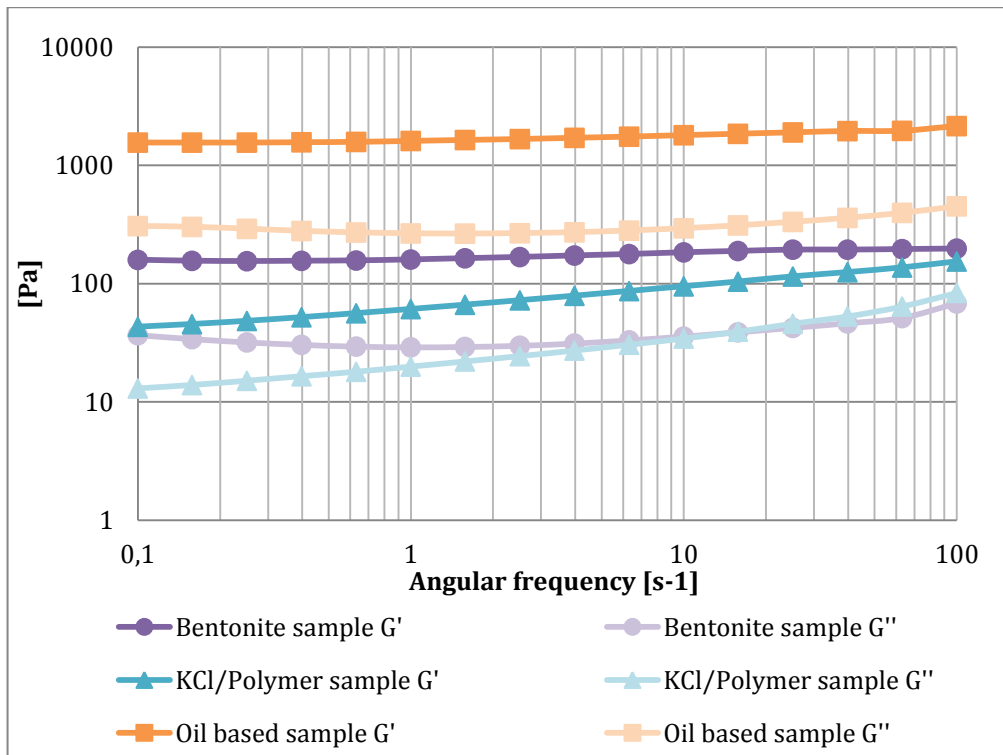


Figure 57: Plot showing frequency sweep for all three samples at 10°C with a strain of 1%.

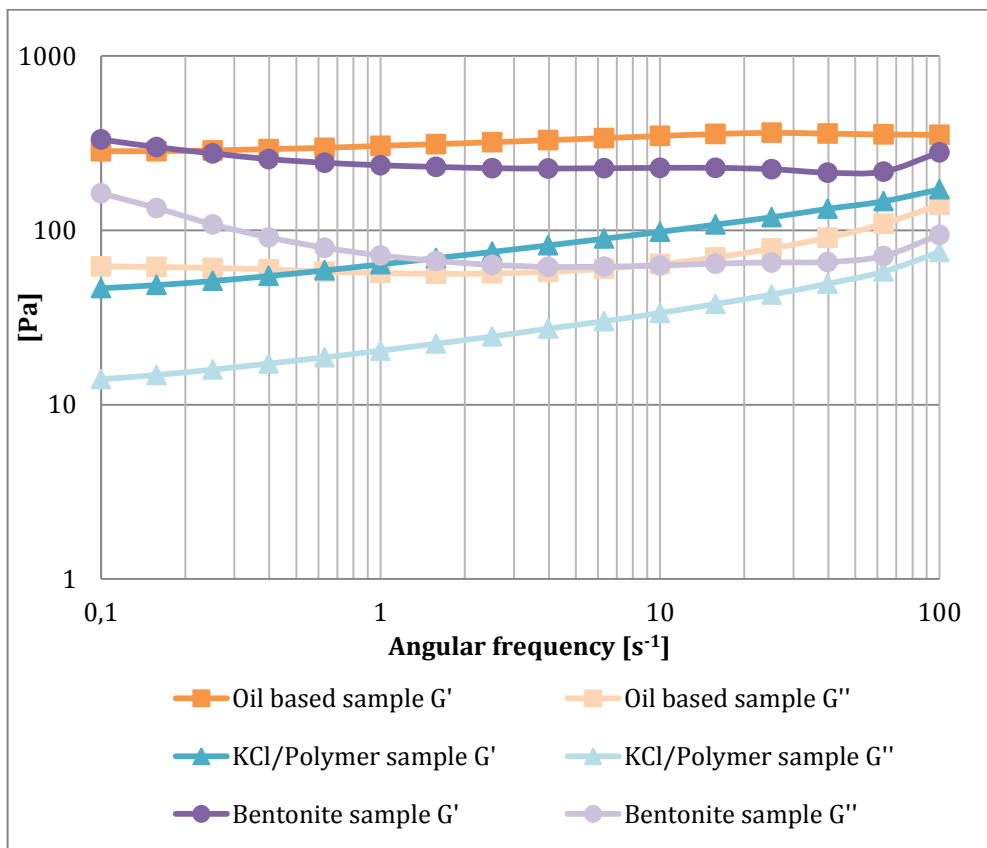


Figure 58: Plot showing frequency sweep for all three samples at 20°C with a strain of 1%.

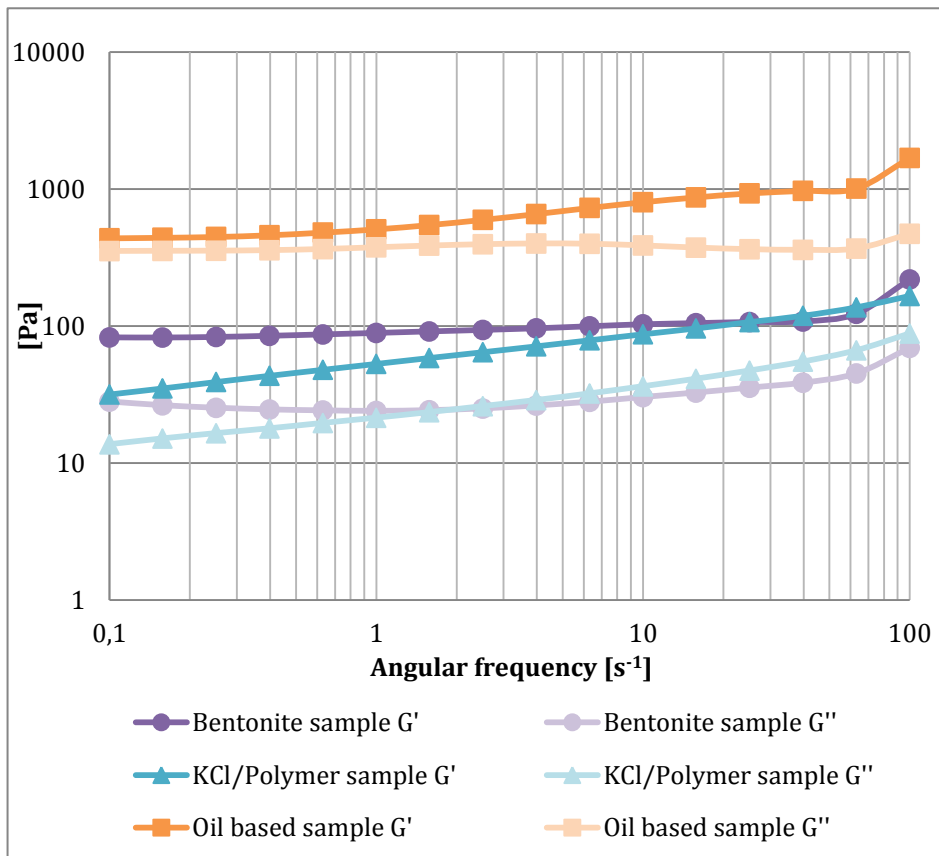


Figure 59: Plot showing frequency sweep for all three samples at 10°C with a strain of 5%.

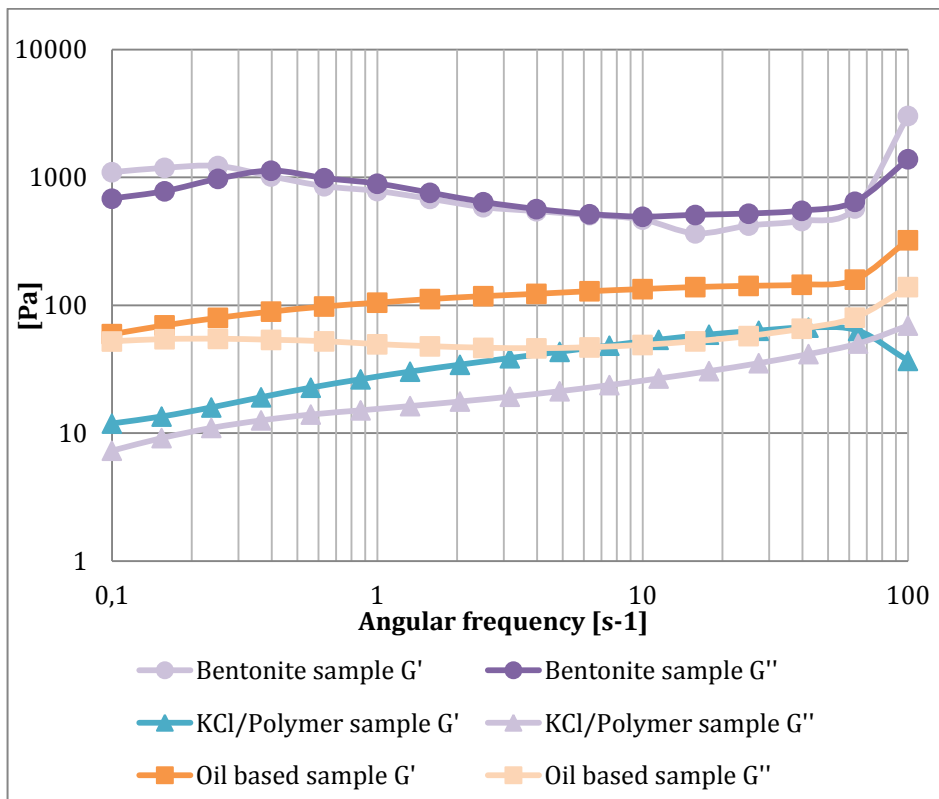


Figure 60: Plot showing frequency sweep for all three samples at 20°C with a strain of 5%.

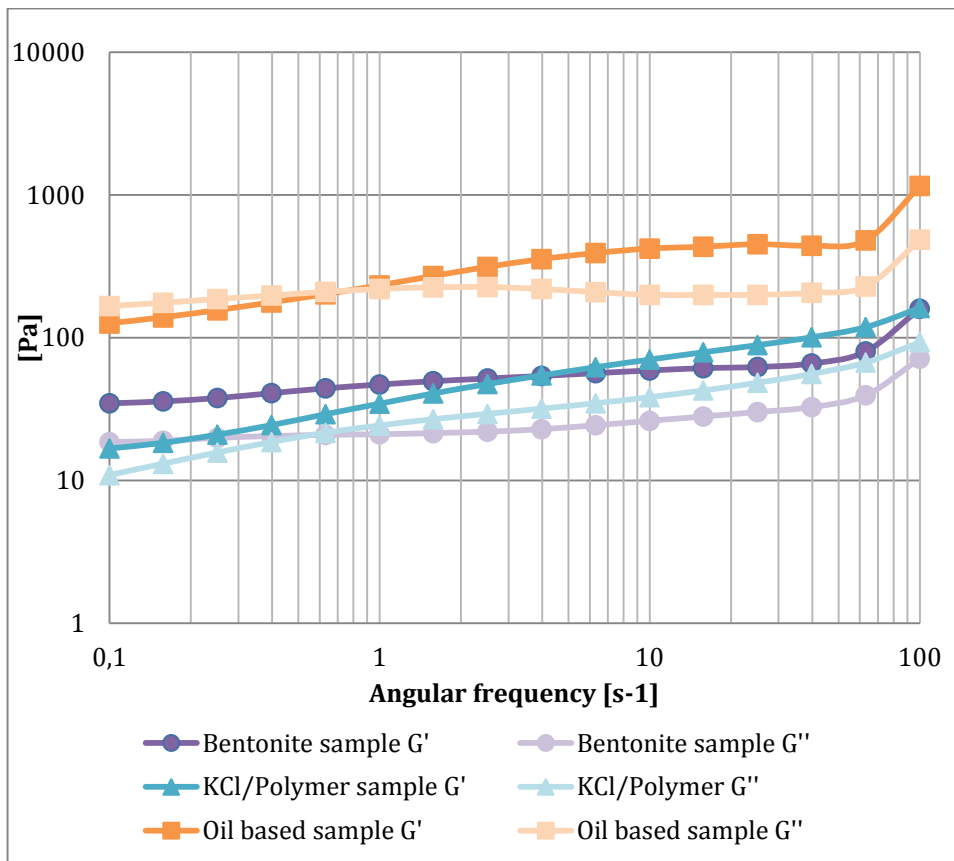


Figure 61: Plot showing frequency sweep for all three samples at 10°C with a strain of 10%.

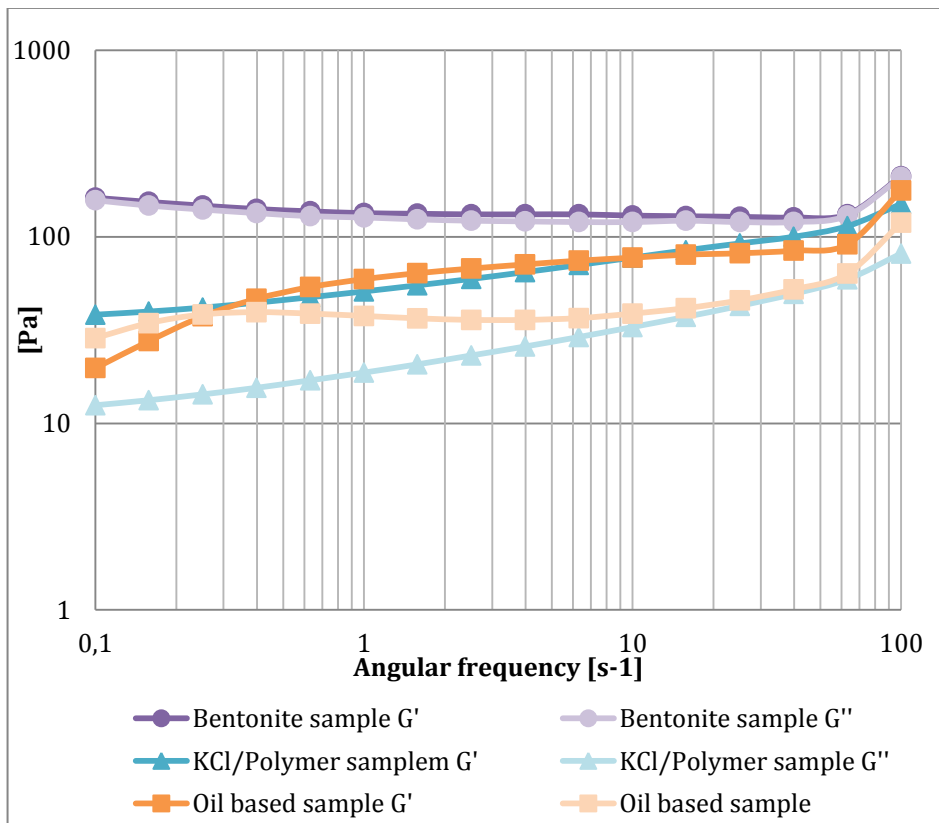


Figure 62: Plot showing frequency sweep for all three samples at 20°C with a strain of 10%.

APPENDIX C.3- FLOW CURVES ANTON PAAR RHEOMETER

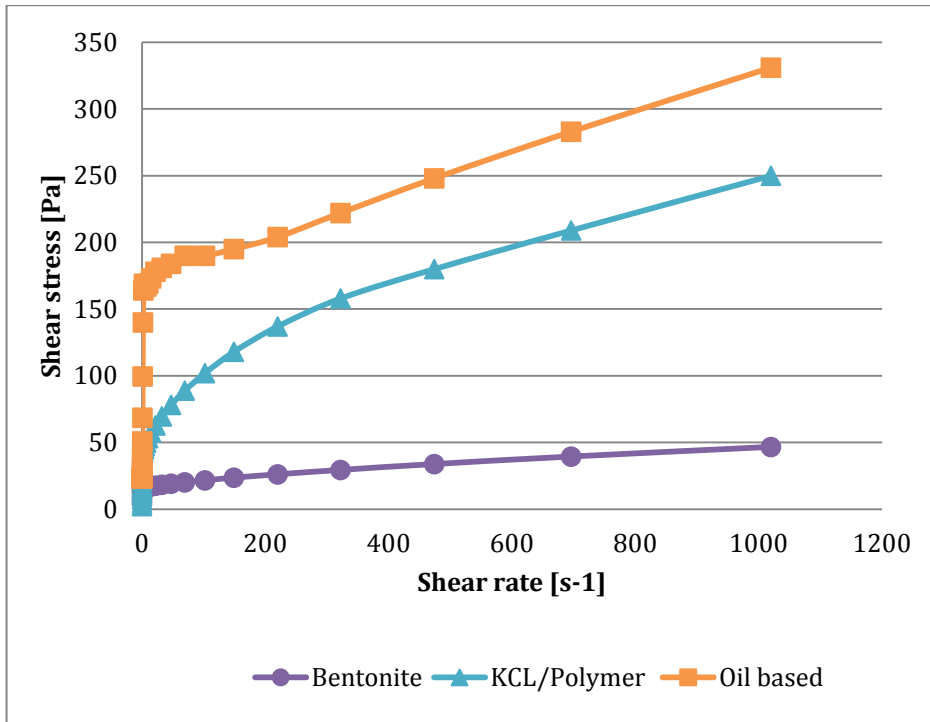


Figure 63: Plot showing flow curves for all three samples at T=10°C performed measured with the Anton Paar rheometer.

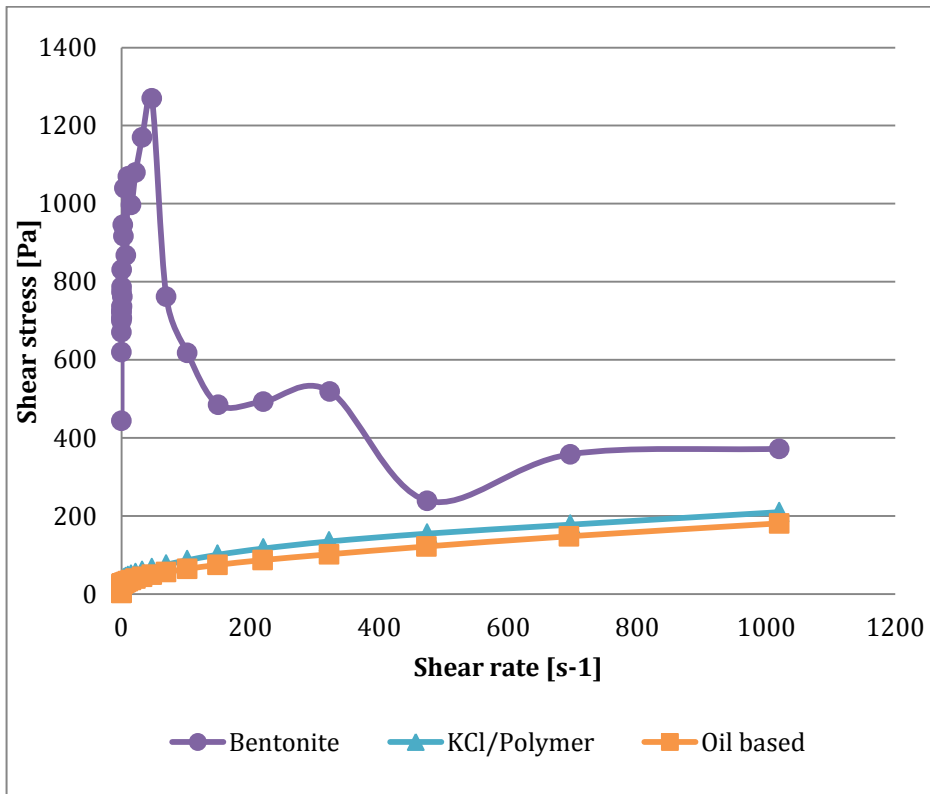


Figure 64: Plot showing flow curves for all three samples at T=20°C performed measured with the Anton Paar rheometer.

## APPENDIX D –MODEL WATER BASED DRILLING FLUID

### APPENDIX D.1 – TIME OF REST AS VARIABLE

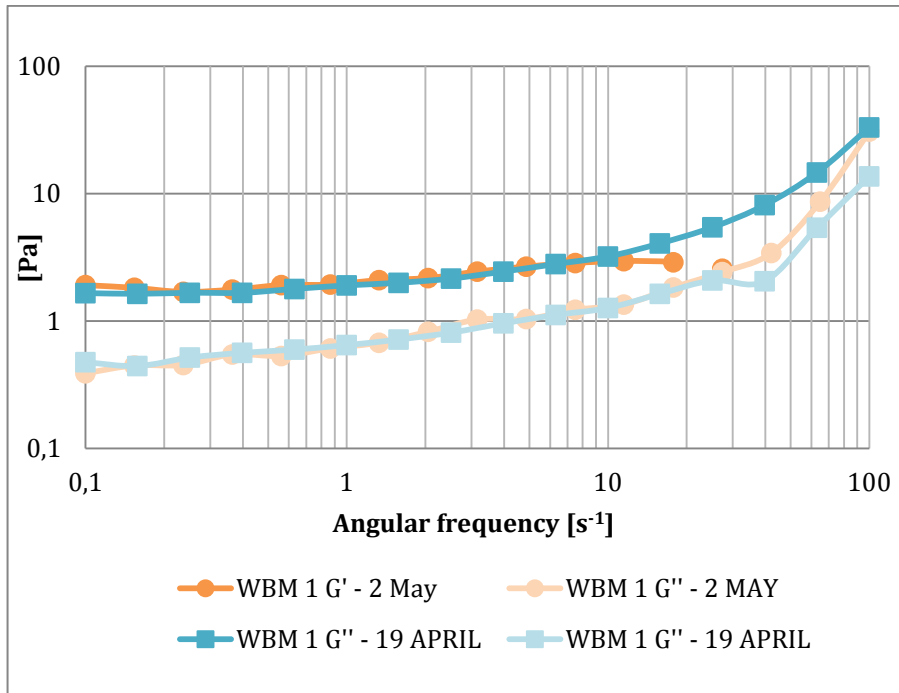


Figure 65: Frequency sweep performed on WBM 1 measured with a two week interval.

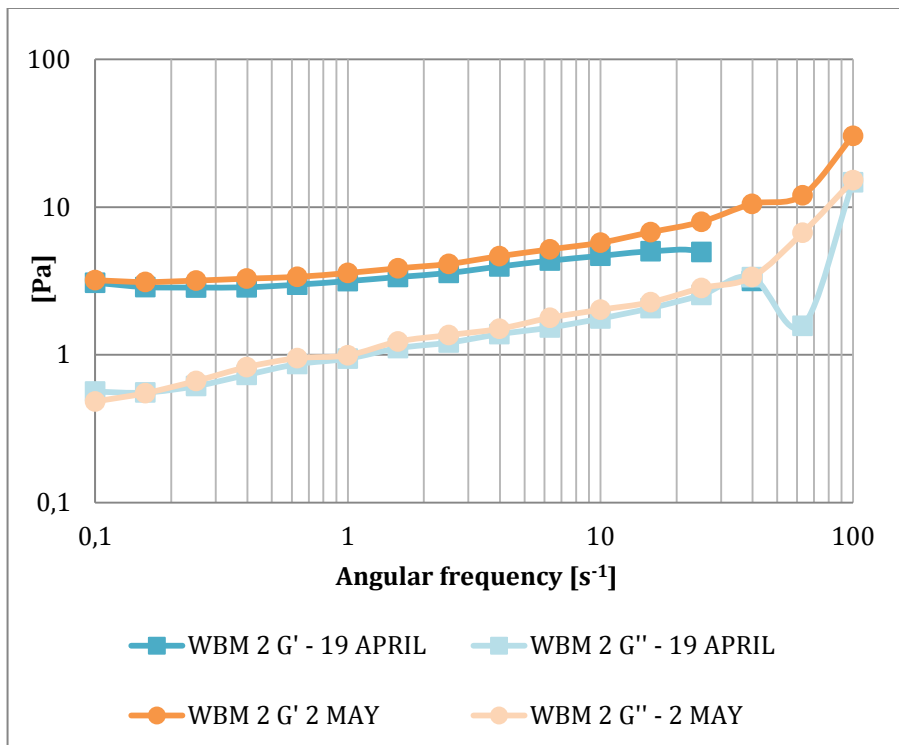


Figure 66: Frequency sweep performed on WBM 2 measured with a two week interval.

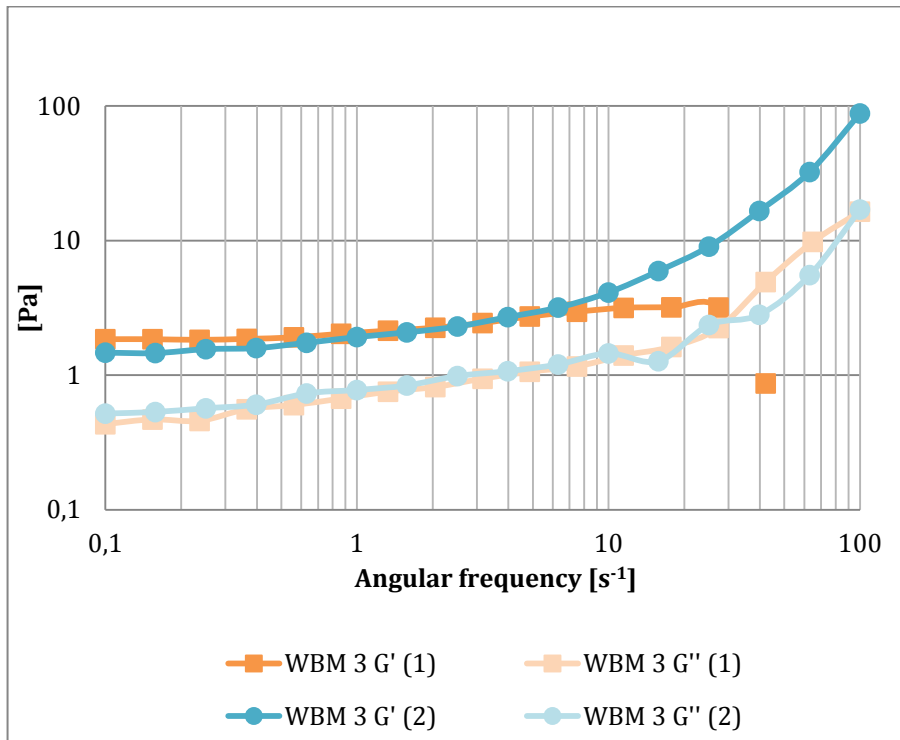


Figure 67: Frequency sweep performed consecutively on sample WBM 3.

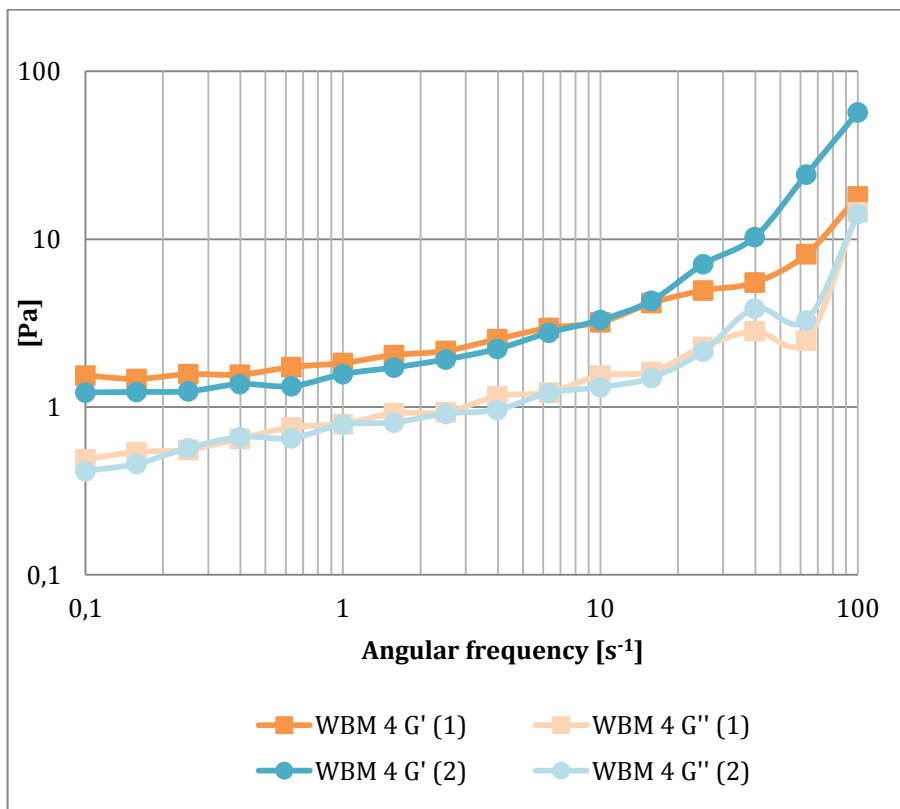


Figure 68: Frequency sweep performed consecutively on sample WBM 4.

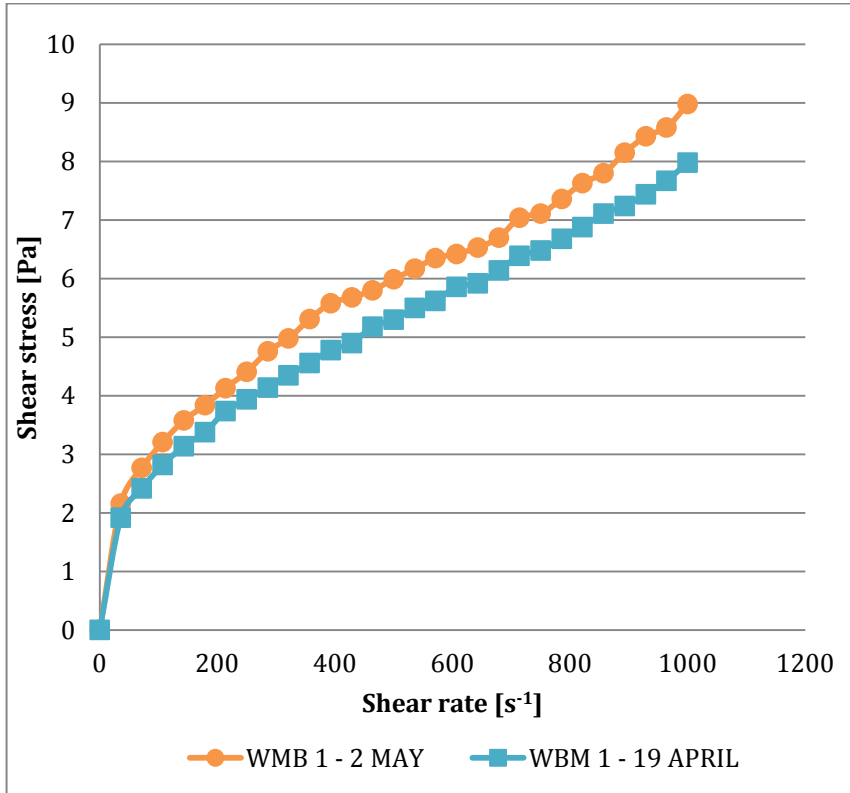


Figure 69: Flow curves of WBM1 before and after a two week period of rest.

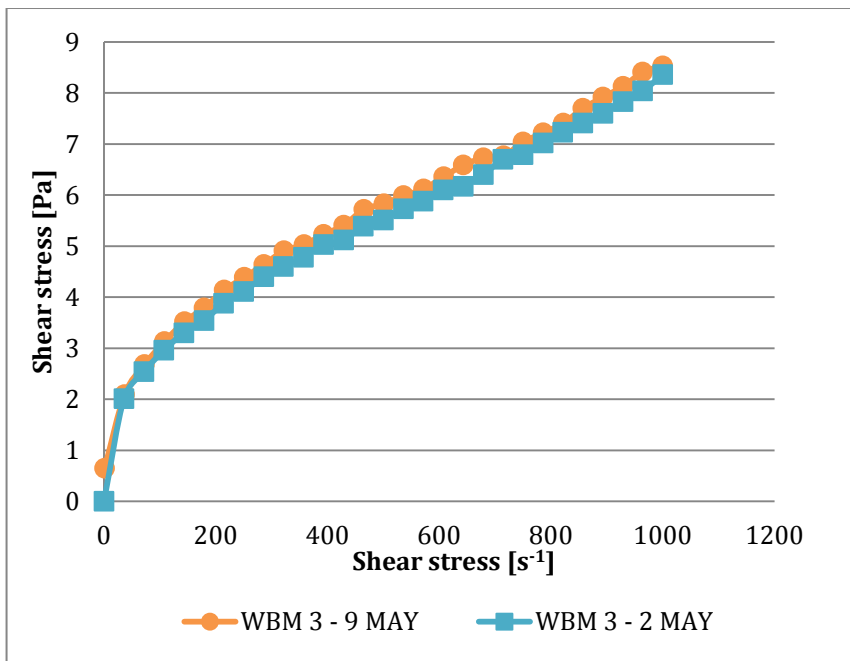


Figure 70: Flow curves for sample WBM 3 before and after one week rest.

APPENDIX D.2 – TIME CIRCULATED AS VARIABLE

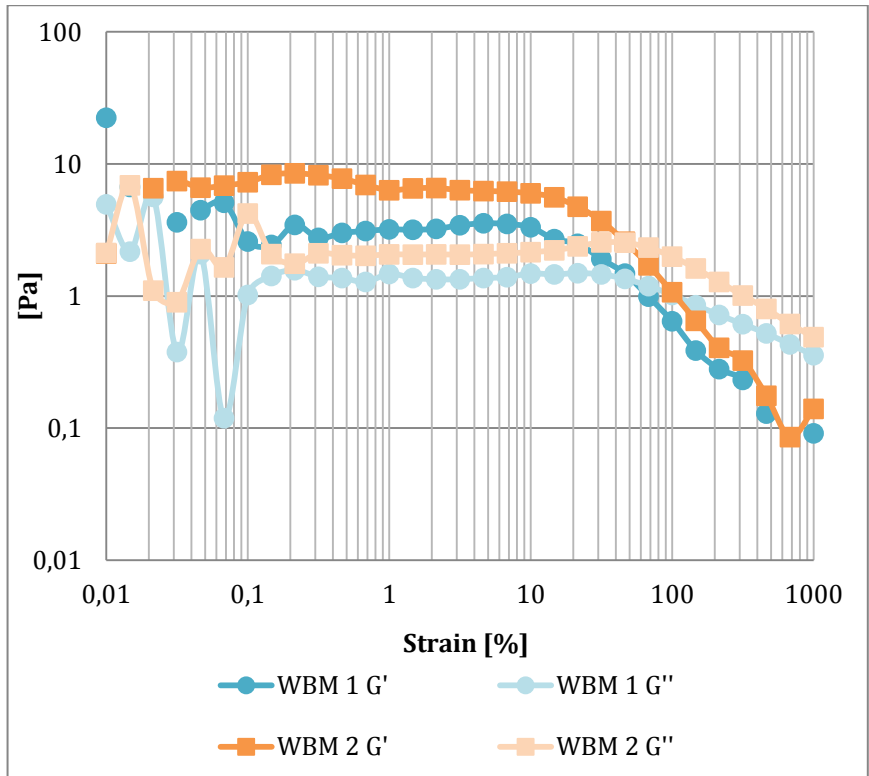


Figure 71: Amplitude sweep of sample WBM 1 and WBM 2 and the effect time of circulation have on the viscous and elastic modulus.

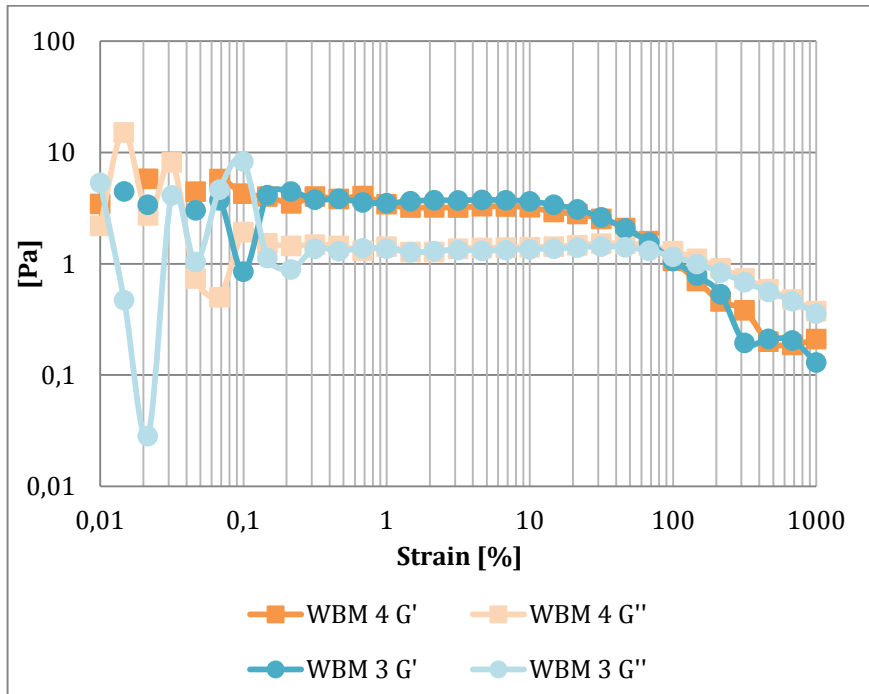


Figure 72: Amplitude sweep of sample WBM 3 and WBM 4 illustrating the effect of two days longer circulation on the viscous and elastic modulus.



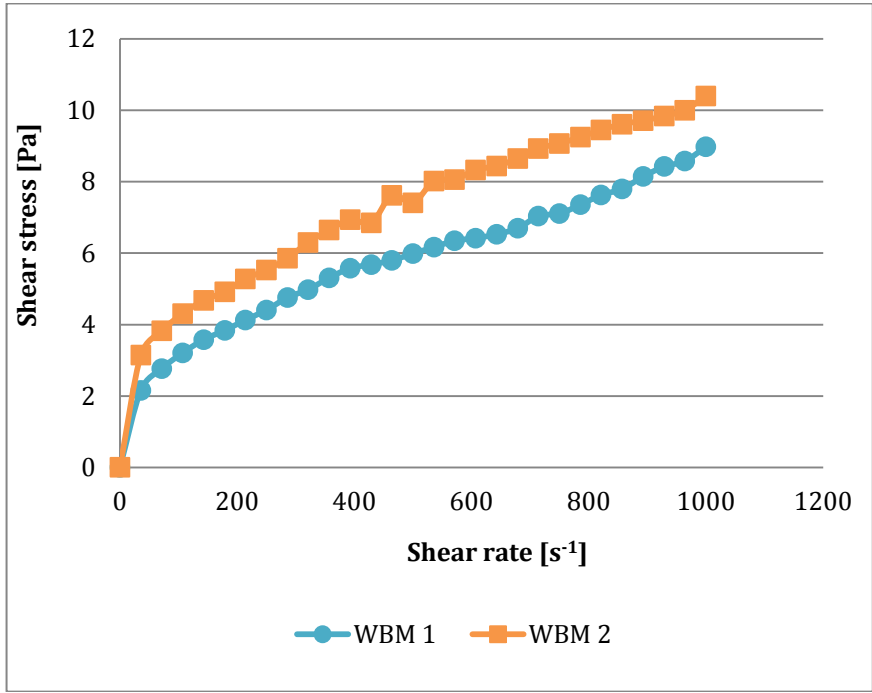


Figure 73: Flow curve for WBM 1 and WBM 2 to illustrate the effect time of circulation have on the viscosity curve.

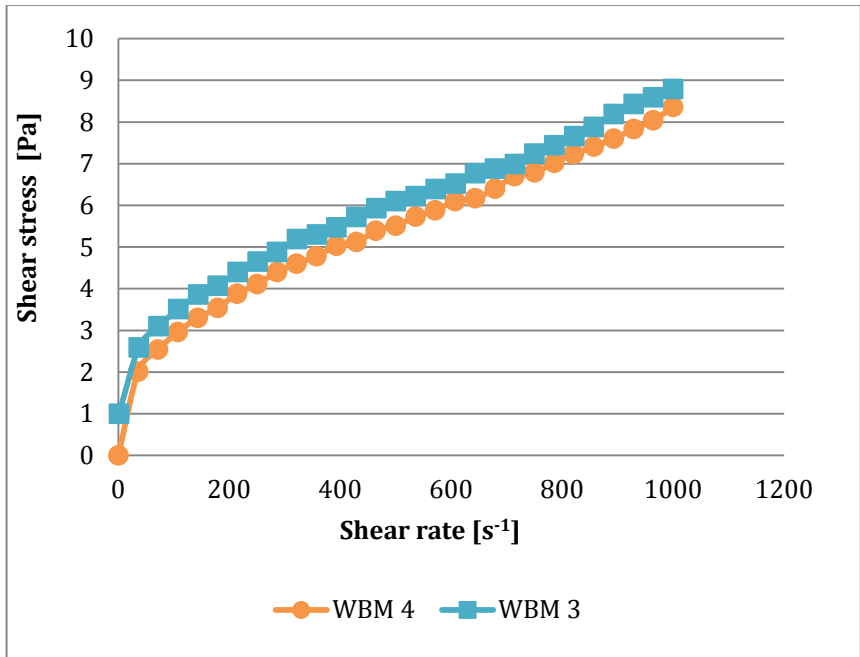


Figure 74: Flow curve for both WBM 3 and WBM 4 to illustrate the effect time of circulation have on the viscosity curve



**APPENDIX E – ARTICLE PUBLISHED ON SINTEF PROJECT**

## Experimental study of rheological properties of model drilling fluids

Ali Taghipour,<sup>1</sup> Bjørnar Lund,<sup>1</sup> Ida Sandvold,<sup>2,3</sup> Nils Opedal,<sup>1</sup> Inge Carlsen,<sup>1</sup> Torbjørn Vrålstad,<sup>1</sup> Jan David Ytrehus,<sup>1</sup> Pål Skalle,<sup>2</sup> Arild Saasen<sup>3,4</sup>

<sup>1</sup> SINTEF Petroleum Research

<sup>2</sup> Norwegian University of Science and Technology (NTNU)

<sup>3</sup> Det Norske Oljeselskap ASA

<sup>4</sup> University of Stavanger (UiS)

### ABSTRACT

We report the design, use and characterization of a model drilling fluid used in a series of laboratory flow loop experiments with hydraulic transportation of sand. The experiments are part of a project with the purpose of studying noncircular wellbore geometries for drilling applications, and in particular helical grooves.

The main objective of the work reported here was to design, characterize and tune a model drilling fluid for a series of flow loop experiments. The fluid should have realistic properties relative to field applications, while also being practical for the specific flow loop experiments. The characterization and tuning should ensure consistent experimental conditions with respect to rheological properties using different batches of chemicals, different fluid batches and during the experiments.

The main tool used for fluid characterization was the Fann viscometer, which is a de facto standard method for rheology characterization in the oil industry.

A water-based drilling fluid using laponite and Xanthan polymer was designed, and the fluid characterization allowed us to detect changes in fluid rheological properties due to aging and experimental use. Further, we were able to adjust the formulation to maintain the rheological properties with different chemical batches.

Transient flow loop experiments with presheared and rested fluid respectively showed some differences which could be due to gelling

effects. Further experiments are needed to conclude on this.

### INTRODUCTION

Oil well drilling fluids are complex fluids which are designed to serve several purposes; maintaining integrity of the formation, cooling and lubrication of the drill bit, as well as transportation of the rock particles (cuttings) which are cut loose by the bit. The challenge of the latter has increased with the introduction of long inclined and horizontal well. Modelling and simulation of this transport problem is an equally challenging problem as it should account for

- Non-Newtonian fluid rheology
- Annular flow geometry
- Eccentric pipe position
- Pipe rotation
- Lateral pipe movement
- Particle-laden fluid

Most of the literature on this topic, both experimental and theoretical, take into account only a subset of these conditions. In particular the lateral pipe movement is often overlooked in this context. In the experimental setup of the present work all of these characteristics are considered.

The effect of non-Newtonian viscosity on cuttings transport properties was summarized by Nazari et al.<sup>1</sup>

Typically, the drilling fluid viscosities are characterized by a yield strength  $\tau_y$ , a flow behaviour index  $n$ , and a plastic viscosity (or consistency index)  $K$ . The Herschel-Bulkley model is

$$\tau = \tau_y + K\dot{\gamma}^n \quad (1)$$

where the case  $n = 1$  reduces to the Bingham model and the case  $\tau_y = 0$  to the power-law model.

Escudier et al.<sup>2</sup> reported experiments with Newtonian and non-Newtonian fluids in a concentric annulus. One of the fluid systems was made from 1.5% Laponite and 0.05 % CMC in water. The Herschel-Bulkley model parameters were  $\tau_y = 1$  Pa,  $n = 0.41$  and  $K = 0.988$  Pa\*s<sup>n</sup>.

An unconventional non-circular wellbore design has recently been developed<sup>3</sup>. The main idea of this design is to create a wellbore with spiral-shaped grooves along the borehole wall in order to enhance cuttings transport and reduce mechanical friction between drillstring and wellbore.

The idea of using pipe geometries which encourage swirl in order to enhance particle transport in fluids is more than 100 years old, as described by Raylor et al.<sup>4</sup>. In a more recent SPE paper Surendra et al.<sup>5</sup> discuss the use of swirl flow in oil and gas production systems and present results from CFD simulations. The work presented in this paper is the first to apply this principle to drilling applications, accounting for annular flow geometry and non-Newtonian fluids.

We have previously tested this principle in a flow loop with circular and non-circular wellbores produced from plastic and using fresh water as flowing medium and with quartz sand representing the cuttings. Hydraulic pressure losses and sand bed height were recorded during both steady state and transient conditions. Results showed that the non-circular geometry performed favourably compared to the circular geometry.

The paper is organized as follows. We first describe the design of the model drilling fluid.

Next we briefly describe the experimental setup and present some flow loop results.

We then discuss the fluid management conducted during and in parallel with the experiments. This involved fluid characterization as well as tuning by adjusting the composition to maintain the desired rheological properties.

We conclude by discussing the choice of fluids, their rheological properties with respect to the objectives of the project, as well as the methods used for fluids characterization.

## EXPERIMENTAL

### Drilling Fluid Design

The objective of the drilling fluid design was to obtain a formulation of a water based fluid with distinct non-Newtonian properties, including yield strength, shear thinning, and thixotropy. Due to the particle separator unit of the flow loop, the yield strength of the fluid should not too large such that particles become suspended in still fluid. The fluid should also be transparent for visual observation and video recording.

It was therefore decided to use a synthetic clay (laponite) in combination with a Xanthan gum biopolymer.

Laponite is a layered silicate colloid (lithium magnesium sodium silicate) consisting of extremely small platelets of 1 nm thickness and 25 nm diameter. It is used as a rheology modifier and will impart thixotropic, shear sensitive viscosity and improve stability and syneresis control. The rheological properties of Laponite suspensions are influenced greatly by solvent ionic strength and shear history<sup>6</sup>.

Hydrated laponite produces a completely transparent fluid due to the small clay particle size. The laponite particles will further counteract the drag reducing effect of the polymer.

Xanthan gum was chosen for the polymer due to its high resistance to mechanical degradation. It has lower resistance to biological degradation, but this can be compensated by adding a biocide.

A defoamer was added to some of the fluid batches used, in order to minimize the concentration of air bubbles.

Fresh water from the municipal supply was used. The water quality was not analysed for this project. However, according to information from Trondheim kommune<sup>7</sup>, the water is soft (hardness = 3

dH), pH = 8.1 with electrical conductivity = 12.1 mS/m.

The chemicals added to the water were thus

- Laponite RD (synthetic clay powder)
- Duotec NS (Xanthan gum powder)
- Soda Ash (powder)
- SafeCide (liquid biocide)
- Defoamer

Soda Ash was added for pH stabilization, and has a significant impact on the rheological properties of laponite.

Laponite RD produced by Rockwood Additives was purchased from Andreas Jennow A/S, whereas the other chemicals were provided free of charge courtesy of MI-Swaco.

The concentrations chosen for the active rheological components (laponite and Xanthan gum) were determined from a compromise between the field-realistic drilling fluid rheology, and the practical aspects of operating the loop, mainly in terms of sand handling and separation.

Figure 75 below illustrates the optical properties of water with laponite only (left), and with some polymer added (right). Sand particles used in the experiments at the bottom of 3 cm liquid layer.

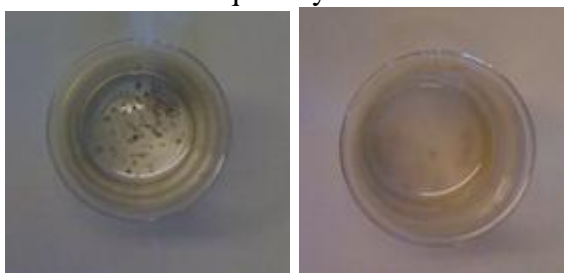


Figure 75. Optical properties of water + 5g/l Laponite RD (Figure 1a, left) and with 5 g/l Laponite + 0.25 g/l Xanthan Gum (Figure 1b, right).

Based on recommendations and preliminary Fann viscometer tests conducted by MI-Swaco, we initially decided to use the following default formulation for the flow loop experiments:

0.46 % Laponite RD  
0.1% Duotec NS

0.1% Soda Ash  
0.025% SafeCide

where all percentages are by weight.

#### Fluid Characterization

Fluid samples were prepared and characterized using a Fann Viscometer Model 35SA. A Fann viscometer is a Couette coaxial cylinder rotational viscometer, and is a de-facto standard rheometer used in the oil industry. The test fluid is contained in the annular space (shear gap) between an outer cylinder and a bob.

Samples of drilling fluid were analyzed during the flow loop experiments to characterize the rheological properties.

The primary purpose of this characterization was to ensure consistent experimental conditions during flow loop experiments with circular and non-circular wellbore geometries. The main tool for characterization was the Fann viscometer measurements and consequently consistency was determined in terms of the Fann viscometer readings. The fluid characterization is necessary for several reasons:

a) The chemical composition of the Xanthan gum (Duotec NS) viscosifier used in fluid batches in latter experiments (in year 2012) differed from the composition used in experiments in 2011.

b) differences in concentrations between fluid batches due to inaccuracies and human errors during fluid preparations

c) fluid aging

d) fluid contamination

#### Flow Loop

The experimental flow loop has a 12 m long test section with an annular flow geometry with a steel pipe inside a wellbore consisting of replaceable concrete wellbore sections confined within a steel housing, with a transparent section in the middle.

The test section is inclinable and experiments were conducted with horizontal and 30° inclination.

Process equipment included fluid pump and sand injection and separation units. A motor connected to the steel pipe allowed this to rotate freely inside as a real drill pipe. Pressures (absolute and differential) as well as flow rate and temperature were measured and logged.

The fluid is pumped from a main tank together with sand which is injected from a dry sand feeder, through the test section and returned to the same tank. The fluid is recirculated, whereas the sand is separated out in a basket and disposed of.

In order to test and compare circular and non-circular flow geometries, two sets of concrete pipes have been produced, each consisting of short segments for easy assembly and disassembly. The non-circular geometry is constructed with a spiral shaped pattern in the inner wall as shown in Figure 76. Both geometries have a drift diameter (diameter of largest inscribed circle) of 10 cm, and the inner rod has a diameter of 5 cm.

The sand injected with the fluid (see Figure 75) is Dansand nr. 3 (0.9-1.6 mm diameter) from Dansand A/S. This is a nearly pure natural quartz sand from a marine deposition. The sand size range was chosen as a fairly realistic cuttings size range.

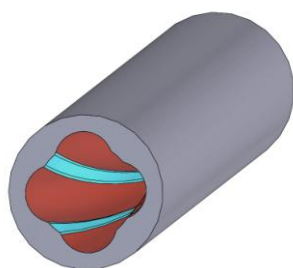


Figure 76. Noncircular wellbore geometry used in flow loop experiments.

Fluid Preparation

Laponite was mixed with water only, as recommended, and allowed to hydrate for at

least 12 hours, at weight concentration of 5.5%. This produced a clear gel. The hydrated laponite was then diluted with more water.

The other chemicals were then mixed separately with some water to produce a high concentration viscosifier mixture which was then added to the diluted laponite.

**RESULTS**

Fluid Characterization

Figure 77 shows measured Fann data from initial fluid batch and manually matched model data.

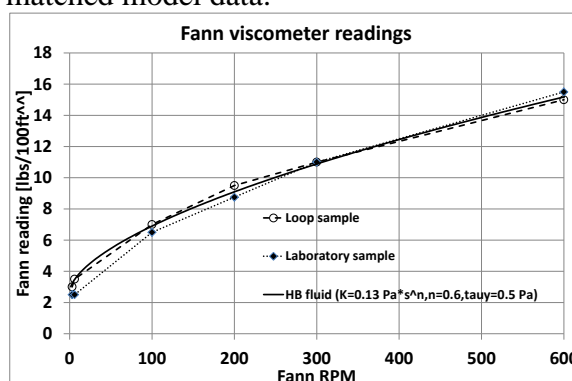


Figure 77. Fann viscometer data from laboratory and loop samples using default formulation, and matched Herschel-Bulkley model.

Fann viscosimeter readings showed that the Xanthan gum polymer used for experiments in 2012 gave higher viscosity than was obtained in experiments conducted in 2011. Consequently, the target fluid composition was changed relative to the original composition as shown in Table 5 and in Fig. 4.

Table 5. Mass fractions of Laponite and Xanthan used in different formulations.

Formulation	Mass fraction	
	Laponite	Xanthan
1	0.0040	0.00051
2	0.0038	0.00074
3	0.0038	0.00081
4	0.0042	0.00088
5	0.0041	0.00096

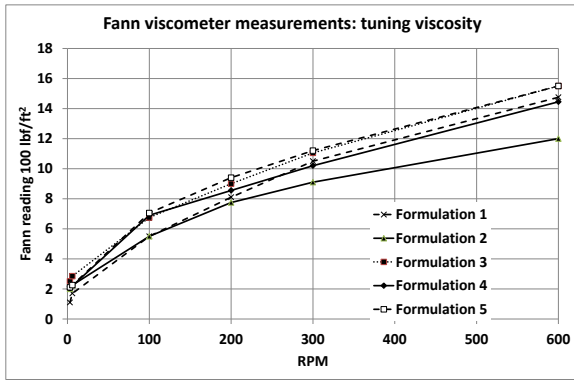


Figure 78. Fann viscometer measurements of different formulations, measured with new fluid.

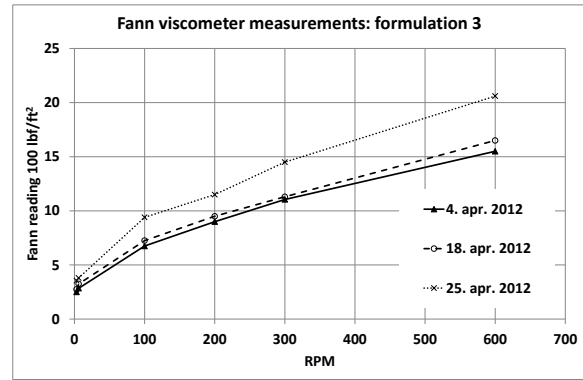


Figure 79. Fann viscometer reading of three fluid samples from loop fluid; taken when new (4.apr.2012), during the experiments (18.apr.2012) and after the final experiment (25.apr.2012).

Fluid contamination was mainly caused by erosion of sand particles and of the concrete wellbore walls.

The general trend observed was an increase in the Fann viscometer readings (i.e. shear stress) versus time. This increase is due to a combination of pure aging and deterioration due to fluid wear and contamination with particles. However, as seen in Figure 79, this process is very nonlinear.

We observed that the fluid became contaminated with fine particles as more experiments are conducted. This could be a more important factor than aging in terms of changed rheology. Thus, the Fann readings of the used fluid in Figure 79 shows larger values than the aged fluid in Figure 80.

The latter figure shows the pure effect of aging of a single fluid sample.

Samples taken from the flow loop at different times but measured at the same time show significant differences due to use, see Figure 81. This will be a combination of the stress loading of the fluid (e.g. in the pump) and contamination by particles.

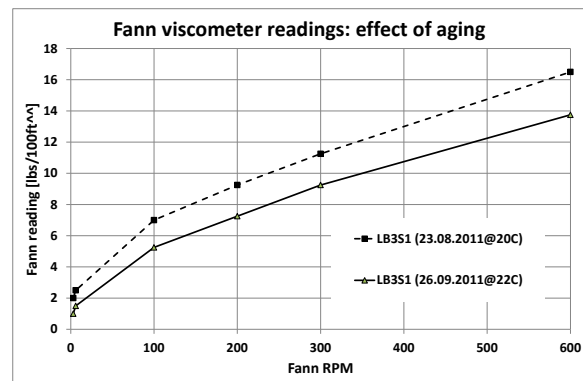


Figure 80. Fann viscometer reading of fluid sample at two different times.



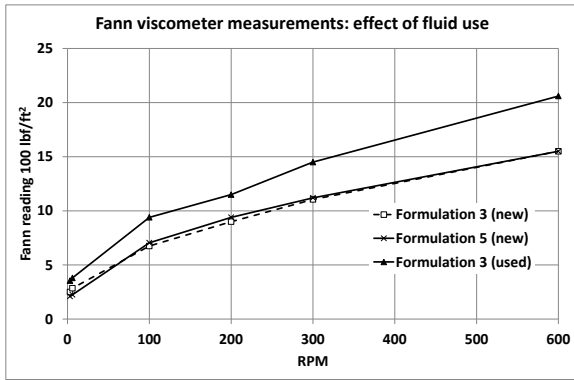


Figure 81. Fann viscometer reading showing effect of use of formulation 3.

We can relate the difference in Fann viscometer readings to a corresponding difference in flow loop measurements. A flow loop experiment conducted for the circular geometry and with horizontal test section, using fluid formulation 3 (see Table 5) was repeated using fluid formulation 5. These formulations have similar Fann viscometer characteristics when new, but experiment 1 was conducted with formulation 3 (used), see Figure 81. The measured pressure drop in the test section for these two experiments is shown in Figure 82. The difference seen can be explained qualitatively by the difference in Fann viscometer characteristics.

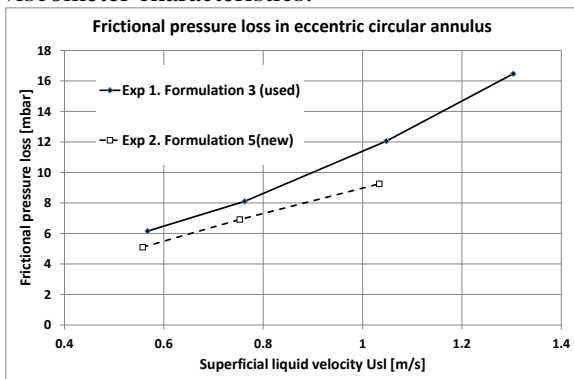


Figure 82. Repeated flow loop experiment, showing effect of different fluid properties due to use.

In addition to the fluid characterization reported above, measuring the steady state shear stress response to a given strain rate, we also noticed a distinct thixotropic effect during the Fann viscometer measurements. Typically we observed that the Fann viscometer readings at the highest shear rate (600 RPM) would decrease by 10-20 % over a period of ca 5

minutes when starting with a nonsheared fluid. The Fann viscometer results reported above are generally for a sheared fluid.

#### Other methods of fluid characterization

We also characterized the fluid using a Marsh funnel viscometer and using an Anton Paar rheometer. The former is a very simple device for oil field use, measuring the time required for a given amount of fluid to drain through a funnel. The geometric shape may make this a useful tool for measuring fluids with a significant extensional viscosity. For the fluids used here the viscosity was so low, however, that the measurement was dominated by the pure inviscid hydrodynamic effects.

Two samples of formulation 3, measured at the same time, but taken at different times and thus exposed to different use, were characterized using an Anton Paar rheometer. The steady state viscosity measurements confirmed qualitatively the aging effects observed in the Fann viscometer measurements.

#### Flow Loop Results

We here present results showing the effect of drillpipe rotation on frictional pressure losses during steady state flow with 60 g/s sand in inclined pipe. The sand mass rate is so large that a sand bed is formed. Pressure loss is measured over a 4 m long distance in the test section.

Notice that without drillstring rotation, there is a minimum in the pressure drop versus flow rate.

This minimum can be explained as follows. At very low flow rates there is a thick sand bed and thus a small effective flow area which creates a large flow resistance. As the flow rate increases, more sand is being entrained from the bed into the flow. The flow area increases and the pressure drop decreases. As the sand bed vanishes the flow area cannot increase anymore, and the pressure drop increases due to increased wall shear stress. The location and magnitude of this minimum depends on operational parameters such as drillstring rotation which affects the effective Reynolds number, but also on the viscosity of the fluid. At a high rotational

drillstring speed, the effect described above is completely masked.

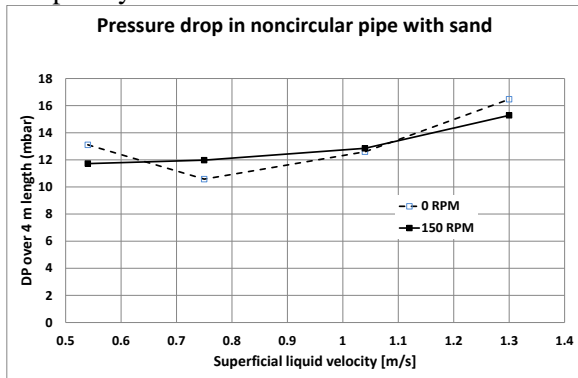


Figure 83. Effect of string rotation on frictional pressure loss in sand-laden liquid flow with noncircular wellbore geometry.

We have noticed a small gelling tendency of the fluid when left to rest for some time. To check whether this could have any impact on hydraulics and sand cleanout capacity we conducted a pair of cleanout tests with circular wellbore in horizontal position. We first prepared a sand bed in the test section by injecting sand with fluid, see Figure 84. Then we allowed the sand bed and fluid to rest overnight. We then turned on pumping with a preset flow rate  $U_{sl} = 0.75$  m/s without sand injection. A gradual reduction in the pressure gradient in the test section will be seen as the bed is eroded until a new steady state bed height is reached. This flow rate is not sufficient to clean the test section. We then cleaned the test section, prepared a sand bed again and repeated the cleanout test without allowing the fluid to rest. The resulting pressure transients over a 4 m length in the test section are shown in Figure 85.

We do not observe any significant differences in the pressure transients. However, there is a difference in the transient sand bed height. This could be due to gelling effects. However, further experiments are needed to confirm this.

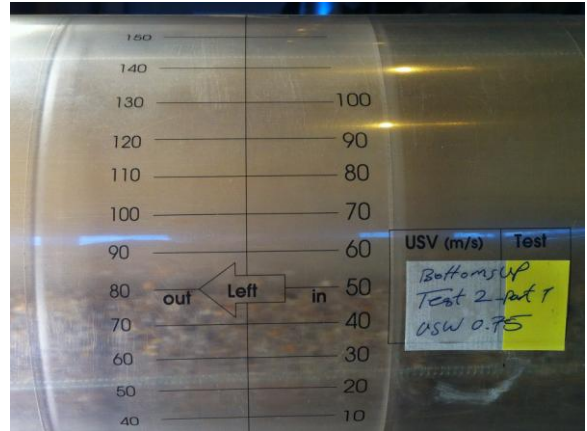


Figure 84. Initial sand bed before cleanout operation.

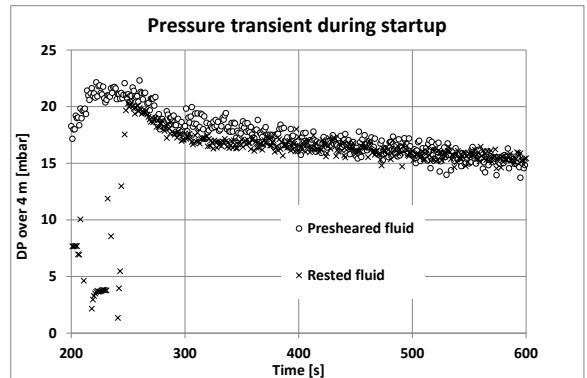


Figure 85. Measured differential pressure versus time during sand cleanout operation: comparing tests with presheared and rested fluid.

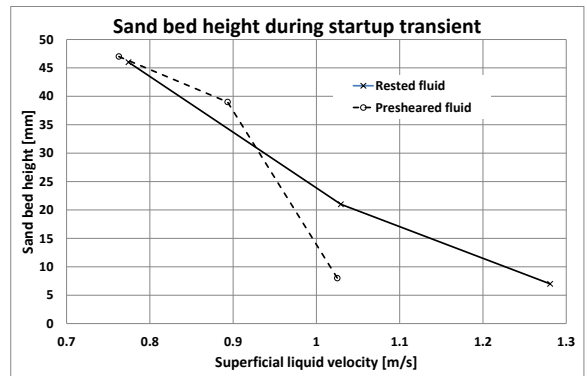


Figure 86. Measured sand bed height versus flow rate during sand cleanout operation: comparing tests with presheared and rested fluid.

## DISCUSSION

We have used the Fann viscometer as our primary tool for characterizing the rheological properties of the drilling fluid used, to ensure and, if necessary, tune the fluid formulation. The Fann viscometer readings are found to be quite repeatable, and differences can be explained by aging and use of fluid. We also have some data showing sensitivity of flow loop results to rheological properties as measured with the Fann viscometer. Thus, it appears that the Fann viscometer is a suitable tool for the characterization of the fluid used here, as the Fann viscometer exposes the fluid to a pure shear strain rate. This will be quite representative to the situation in an annulus as in the present experiments, with a combined cylindrical Couette and Poiseuille flow. The steel rod used in the present experiments does not have any tool joints with increased diameter. A real drillstring with tool joints may cause extensional viscosity effects and time dependent effects to be more important.

## CONCLUSION

We have used a Fann viscometer for characterizing a model drilling fluid for flow loop experiments with a drillpipe inside.

We find that the Fann viscometer can be used to measure the most relevant rheological properties of the fluid used in the present experiments with a non-Newtonian model drilling fluid.

Some effects of fluid history on sand transport properties were found. These could be due to fluid gelling effects. However, further studies are recommended to investigate this.

## ACKNOWLEDGMENTS

We acknowledge the financial support from BG Group, Det Norske, Dong Energy, Statoil, and from the Research Council of Norway. We also appreciate the technical assistance provided from MI-Swaco.

## REFERENCES

1. Nazari, T., Hareland, G., and Azar, J. J., "Review of cuttings transport in directional well drilling: systematic approach", Society of Petroleum Engineers paper no. SPE SPE 132372.

2. Escudier, M. P., Gouldson, I. W., Jones, D. M., "Flow of shear-thinning fluids in a concentric annulus", *Experiments in Fluids* **18** (1995) 225-238.

3. Taghipour, A., "Experimental study of cuttings transport in non-circular wellbores", to be published.

4. Raylor, B., Jones, T. F., Miles, N. J., (1999) "Helically formed pipes improve the efficient transportation of particle-laden fluids", BHR Group 1999 Hydrotransport 14.

5. Surendra, M., Falcone, G., Teodoriu, C., (2009) "Investigation of swirl flows applied to the oil and gas industry", Society of Petroleum Engineers paper no. SPE 115938, SPE Projects, Facilities & Construction. March 2009.

6. van Olphen, H., "An Introduction to Clay Colloid Chemistry", John Wiley & Sons, New York 1977. ISBN 0-471-01463-X

7. <http://www.trondheim.kommune.no/drikkevannskvalitet2011/>